Natural Resources Canada | Ressources naturelles Canada

GEOLOGICAL SURVEY OF CANADA
OPEN FILE 8943

Swiftsure Bank water column survey SO294, offshore British Columbia

Version 1.0

J. Kehew, K. Douglas, M. Riedel, I. Klaucke, T. Norgard, C. Du Preez, Z. Li, and C. Stacey

2023

Canada

GEOLOGICAL SURVEY OF CANADA
OPEN FILE 8943

Swiftsure Bank water column survey SO294, offshore British Columbia

Version 1.0

J. Kehew[1], K. Douglas[2], M. Riedel[3], I. Klaucke[3], T. Norgard[4], C. Du Preez[4], Z. Li[2], and C. Stacey[2]

[1]Department of Earth and Environmental Sciences, University of Ottawa, 75 Laurier Ave. E, Ottawa, Ontario
[2]Geological Survey of Canada, Pacific Geoscience Centre, 9860 West Saanich Road, Sidney, British Columbia
[3]GEOMAR Helmholtz Centre for Ocean Research Kiel, Wischhofstraße 1-3, 24148 Kiel, Germany
[4]Fisheries and Oceans Canada, Institute of Ocean Sciences, 9860 West Saanich Road Sidney, British Columbia

2023

Permanent link: https://doi.org/10.4095/331402

This publication is available for free download through GEOSCAN (http://geoscan.nrcan.gc.ca/).

Recommended citation

Kehew, J., Douglas, K., Riedel, M., Klaucke, I., Norgard, T., Du Preez, C., Li, Z., and Stacey, C., 2023. Swiftsure Bank water column survey SO294, offshore British Columbia; Geological Survey of Canada, Open File 8943 (ver. 1.0), 1 .zip file. https://doi.org/10.4095/331402

Publications in this series have not been edited; they are released as submitted by the author.

ISSN 2816-7155
ISBN 978-0-660-47365-9
Catalogue No. M183-2/8943E-PDF

TABLE OF CONTENTS **Page**

Abstract

A water column survey at Swiftsure Bank shows evidence of venting from the seabed across a 47.8 km transect with 109 individual plumes identified (Figure 1). The RV Sonne SO294 CLOCKS expedition, from September 12-October 27, 2022, provided opportunity for a multibeam echosounder survey at Swiftsure Bank on behalf of Fisheries and Oceans Canada (DFO) and Natural Resources Canada (NRCan) while transiting on September 17, 2022. The data and results are presented here. Cold seeps are relevant to marine spatial planning as they are ecologically and biologically significant areas (EBSAs), providing unique habitat for chemosynthetic organisms.

Un relevé de la colonne d'eau effectué au banc Swiftsure montre des signes d'exhalaison depuis le fond marin le long d'un transect de 47,8 km, où 109 panaches distincts ont été recensés (Figure 1). L'expédition SO294 CLOCKS du RV Sonne, menée du 12 septembre au 27 octobre 2022, a donné l'occasion d'effectuer un levé par échosondeur multifaisceaux sur le banc Swiftsure en cours de transit le 17 septembre 2022 au nom de Pêches et Océans Canada (MPO) et de Ressources naturelles Canada (RNCan). Les données et les résultats sont présentés ici. Les suintements froids présentent un intérêt pour la planification spatiale marine, car ils constituent des zones d'importance écologique et biologique (ZIEB) qui fournissent un habitat unique pour les organismes chimiotrophes.

Introduction

The German Research Vessel (RV) Sonne SO294 CLOCKS expedition led by GEOMAR conducted a multibeam water column survey across Swiftsure Bank on September 17, 2022 Pacific Standard Time (PST) on an opportunistic transit. The survey was conducted on behalf of Fisheries and Oceans Canada (DFO) and Natural Resources Canada (NRCan) to map the presence of plumes in the water column, possibly attributed to hydrocarbon seeps. Limited previous work in this area suggested that plumes were present but only single beam echosounder surveys had been possible. Single beam echosounders capture a narrow view of the water column. Multibeam echosounders provide full swath coverage, providing better estimates of plume height and presence.

SETTING

Outside of Juan de Fuca Strait, Swiftsure Bank sits on the Carmanah and Prometheus sub-basins of the larger Tofino Basin (Johns et al., 2012, p825). The Tofino Basin is characterized by unconformities, faulted mudstones and siltstones that were folded during the Pleistocene and are lacking or sparse in overlying sediments (Yorath, 1980, p.763). A 2011 expedition collected large pieces of mudstone containing gas, confirming the substrate as mudstone without much or any overlying sediment (Personal Communication V. Barrie, Chief Scientist Expedition 2011002PGC, 2022). A collocated fault, known as the Tofino Fault, runs WNW-ESE through the bank (Johns et al, 2012). Luternauer et al. (1986) assessed adjacent Amphitrite Bank geology to the Northwest of Swiftsure Bank for its sedimentology. The substrate was found to be predominantly gravel-size sediment at the seafloor with the exception of the troughs and lower slopes that were predominantly covered with sand and mud. Cobbles, boulders, and depressions were also present with varying levels of sediment mobility indicators on the bank (Luternauer et al., 1986, p. 112).

The recently collected RV Sonne CLOCKS expedition (SO294) multibeam bathymetry data at Swiftsure Bank show possible fault blocks, scoured hard substrate, steep-sided banks, and potential cold seep bioherms amongst their morphology (Figure 2). The possible fault blocks (Figure 2A) are identified solely from the multibeam bathymetry as block-like morphological structures. Future subbottom data would help determine if these are indeed fault blocks if there is presence of displaced reflectors at the boundary edges. Coring and carbon dating of overlying sediment would additionally help determine the age of these features. Cold seeps can generate hydrocarbon-derived carbonate chimneys, which may account for the potential bioherm morphology seen in Figure 2D (Diaz-del-Rio et al., 2003). The irregular morphology was seen in the bathymetry dataset at 48.557564° N, 125.037919° W.

Riedel et al. (2018) mapped and characterized acoustic signatures of venting along the continental shelf and slope from available water column data. There are numerous seeps in Tofino Basin in that dataset, but few data were available at the time from Swiftsure Bank for

assessment. An April 2022 survey on the CCGS Franklin mapped some gas flares at Swiftsure Bank using an EK60 single beam system (Personal Communication C. Stacey, Chief Scientist Expedition 2022002PGC, 2022). Those observations are provided in Appendix A. The survey route used in this report covers some of the existing identified locations as well as some new.

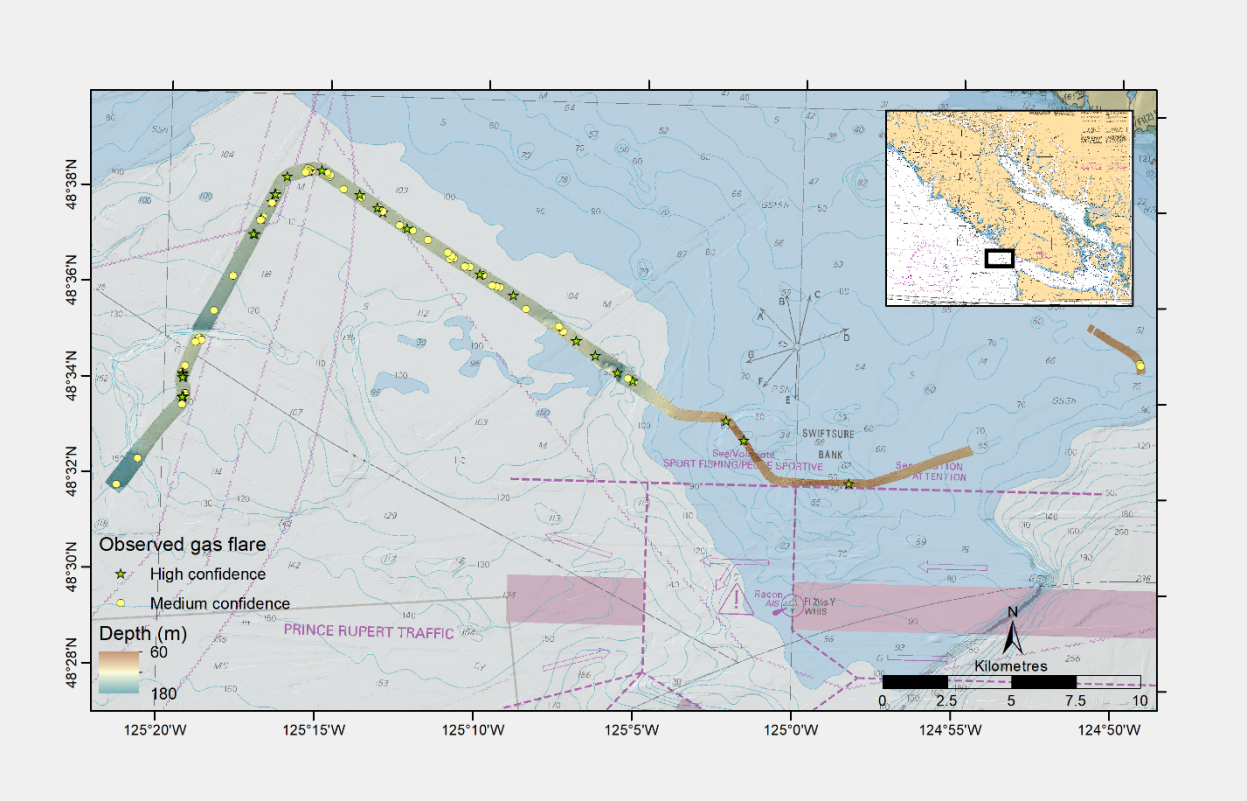

Figure 1. Observed gas plumes identified during survey with medium or high confidence levels overlaid on bathymetry collected at Swiftsure Bank. Inset shows location of survey in proximity to Vancouver Island, British Columbia.

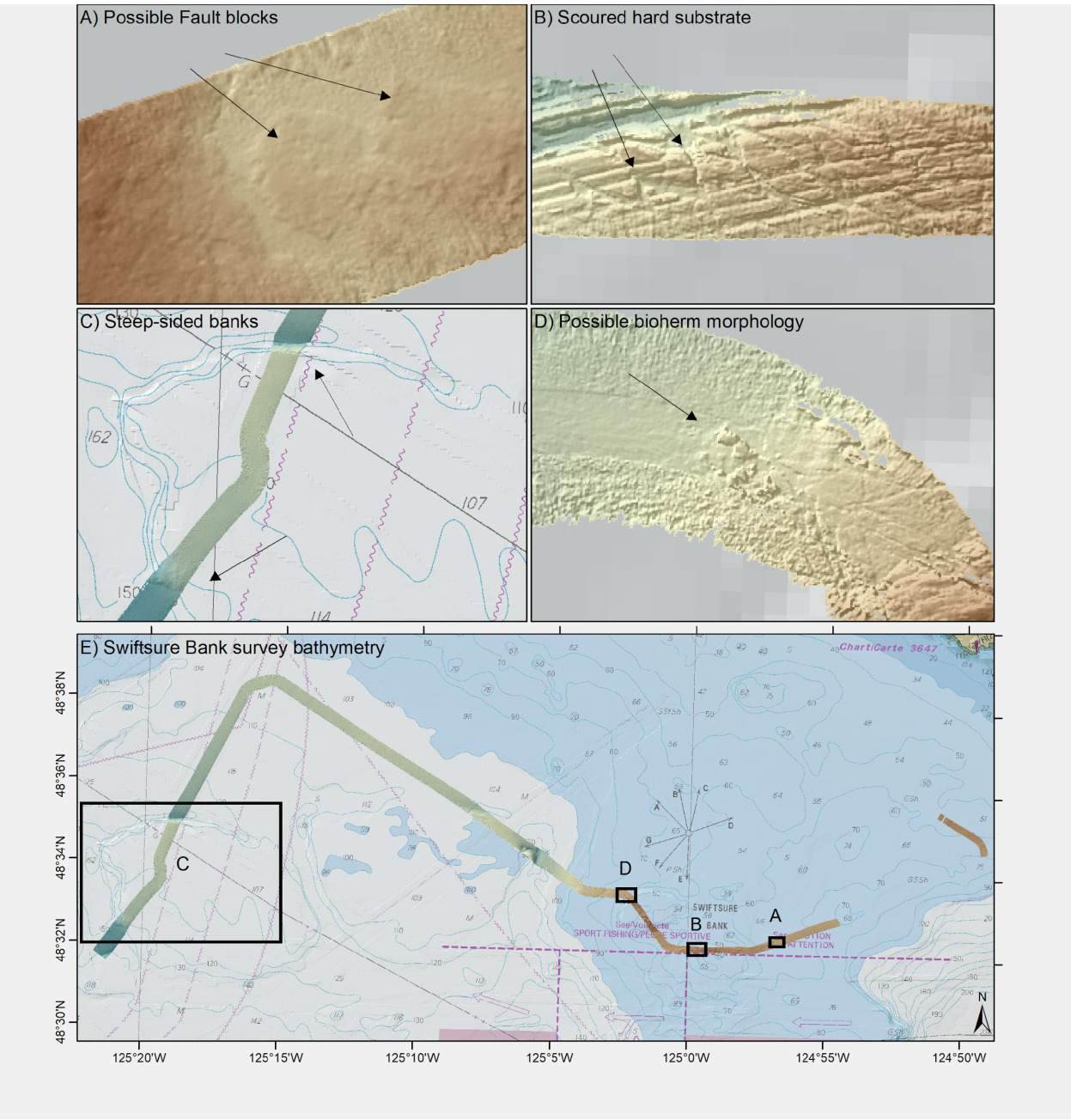

Figure 2. A) Possible fault blocks, B) scoured hard substrate, C) steep banks, and D) possible cold seep bioherms seen in E) Swiftsure Bank bathymetry, collected during the survey.

MOTIVATION

The Government of Canada has agreed to a suite of international biodiversity conservation goals and targets (the Convention on Biological Diversity 2011-2020 Strategic Plan for Biodiversity's Aichi Targets) and adopted complementary domestic 2025 Biodiversity Goals and Targets for Canada. Both international and domestic targets (Aichi Target 11 and Canada's Target 1) call for the conservation of 25% of coastal and marine areas by 2025 (and 30% by 2030). The

designation of new Marine Protected Areas (MPAs) in Canadian waters has been identified as one part of the national strategy to meet these targets.

DFO Science has been tasked to collect science data and provide science advice in support of the designation of marine conservation areas, where the identification of ecologically and biologically significant areas (EBSAs) is an important step. At the present time many of the EBSAs that are being reviewed for marine protection are in Canada's offshore waters and currently the Government of Canada has no means to map these areas. By working with international partners, we can begin to collect some seafloor and water column mapping data in areas of interest for marine protection to be used in our ecological assessments. The water column mapping herein will be used to help identify cold seeps, areas on the ocean floor where the leaking of hydrocarbon-rich fluid occurs. Hydrocarbon-rich fluids such as methane and hydrogen sulfide can support chemosynthetic communities (DFO, 2018). In 2018, cold seeps were classified as EBSAs, notable for their geomorphological characteristics, creating habitats upon which several endemic species depend; their rarity relative to other continental margin features; the vulnerability of long-lived habitat-forming species (tubeworms) to human disturbance; and high rates of biological productivity, especially compared with other regions in the deep sea (DFO 2018). There are a limited number of known cold seep locations (approximately six main sites within Pacific Canada) but it is anticipated focused offshore research and mapping will lead to the discovery of hundreds to thousands (DFO 2018).

Methods and Results

DATA ACQUISITION AND PROCESSING

The Kongsberg EM710 (SN236) system was used to acquire the multibeam echosounder water column data using Kongsberg SIS acquisition software. The output is pairs of .wcd and .all files. This system is a 0.5° x 1.0° array with 140° max swath and 400 beams. A 140° swath width was used to maximize the swath area for this survey thus allowing for potential sighting of acoustic anomalies (gas plumes or "so-called flares") in the outermost beams.

Data were collected in equidistant beam spacing. Instrument sampling rate varies by depth and values are recorded in the .all files (up to 30 Hz). The frequency of the sounding signal ranges between 40 and 100 kHz. A predicted 95% geographic accuracy for the navigation fixes is provided for the system with a horizontal accuracy of <20 m. Datum used is WGS84. The navigation system used is Glonass/GPS.

Qimera 2.4.5 post-processing software was used to merge the bathymetry data seen in Figure 1 into a grid, apply sound velocity corrections, apply tides, and flag potential outliers. As marine mammal mitigation measures required the use of the passive acoustic monitoring system and the starting point was near the shipping lanes, a sound velocity profile could only reasonably be acquired after the survey. A sound velocity profile obtained from Fisheries and Oceans Canada

collected along Swiftsure Bank earlier in the year provided an initial sound velocity file for the acquisition software and the one following the survey was applied in post-processing.

The survey coordinates sit approximately halfway between Port Renfrew and Bamfield tide stations. Tides were applied from Port Renfrew, but further processing could be done with a merged file between both stations. As this survey is currently the only multibeam bathymetry in the area, there was no need to merge with existing data and this one tide station was deemed sufficient for our purposes.

As Swiftsure Bank is a protected area for Southern Resident Killer Whales, strict marine mammal mitigation measures were followed for all marine mammals as outlined by Fisheries and Oceans Canada. A passive acoustic monitoring system was run by Jasco Applied Sciences starting 30 minutes prior to and at all times while surveying, as well as constant marine mammal observation by LGL Consulting. Any observation within the exclusion zone resulted in a shut down of all echosounders. This was applied shortly after the start of the survey accounting for a gap in the data. Data acquisition resumed following clearance of the exclusion zone for the required period of time.

Quality Positioning Services (QPS) FMMidwater software was used to process the .wcd files along with the corresponding .all navigation files. The raw sonar .wcd files were processed to create a .gwc (Generic Water Column) file which enables the data to be viewed in the software. The data were viewed in both the fan and the R-stack view options. Fan view is an along-track view that shows the signal strength along each beam during a single ping. R-Stacked (Range Stacked) shows an oblique view of the water column, created by collapsing all of the beams into a single signal, displaying the maximum level for each range of values (QPS, 2018). Each ping is stacked along the ship track in this way to produce a view of the water column through time which facilitates the identification of large gas flares.

During water column interpretation, the entire survey was viewed in fan view to locate the gas flares, which were then recorded using the Geo-Pick tool. The vertical display was maximized to optimize the view, and a 1:1 horizontal display was maintained. The colour range was kept constant for each survey for consistency in flare identification.

Gas flares were identified by their characteristic shape and high strength signal. Two main shapes are characteristic of gas flares: tall, thin streamers and short, teardrop-shaped clouds (Figure 3). Gas flares also must have a point of contact with the seafloor. In some circumstances flares were still recorded if the anomaly was distinctively flare shaped but no point of contact was visible. Since ocean currents can displace the flare plumes away from their source, it is possible that the plume is visible in the water column data, but the source is not. For the shorter, tear-drop shaped anomalies, the absence of contact with the seafloor helped to distinguish flares from fish and marine mammals which can be easily mistaken for flares if they are close to the

seafloor (Figure 4a). If strong signals are present along a set of beams and do not cross obliquely into other beams, they are considered noise (Figure 4b).

For each flare we recorded the coordinates, time stamp, and water depth of the base of the flare. We also recorded the position of the flare in fan view (port, centre, starboard), flare height and the level of confidence of the identification (low, medium, high). The level of confidence scale is qualitative and subjective, but helps to distinguish tall, obvious gas flares from small gas flares that could be misinterpreted noise or fish. Flares assigned low confidence are strong anomalies that lack the characteristic flare shape, may lack contact with the seafloor, and/or are heavily distorted by noise. Medium confidence was assigned to anomalies have the characteristic flare shape but cannot be assigned a high degree of confidence due to noise distortion or absence of seafloor contact. This confidence level was also assigned to flares with along-track variability that decreased confidence in the flare identification (e.g., had a characteristic gas flare shape in one ping, but had a different shape a few pings later). High confidence was assigned to flares with a distinct flare shape in the centre beams where the seafloor contact was visible and there was minimal noise distortion.

Ambient water column noise as well as noise caused by other echo sounders on board and marine life results in a degree of subjectivity when distinguishing gas flares from noise. The subjective nature of gas flare identification will inevitably result in their occasional misidentification. The side beams have a higher degree of noise that leads to the distortion of the gas flare shape and diffuses the outer boundaries, so off-track gas flares have a higher chance of being misidentified as noise.

Römer et al. (2016) found that gas flares are impacted by the change in pressure caused by tides. As tides fall, gas emissions from the seeps increase due to the decrease in water pressure. If the multibeam data were collected as the tide rose, it is possible that there are flares that were unidentifiable in this study.

Lastly, the SO294 survey identified flares were plotted alongside the flares identified by Riedel et al. (2018) and those identified during the 2022 CCGS Franklin expedition. Given the uncertainty of positioning, a buffer was used to look for collocated flares using the swath width of the multibeam sonar as a function of water depth. Using the “select by location” tool in ArcGIS 10.7 with the given search radius of the multibeam sonar swath halfwidth, Table 13 indicates which flares identified in the SO294 survey overlap with a flare identified during either of the other expeditions within the footprint of the multibeam sonar. This is intended to be used as an indicator of flare activity persistence. There are 44 flares with overlap within this footprint.

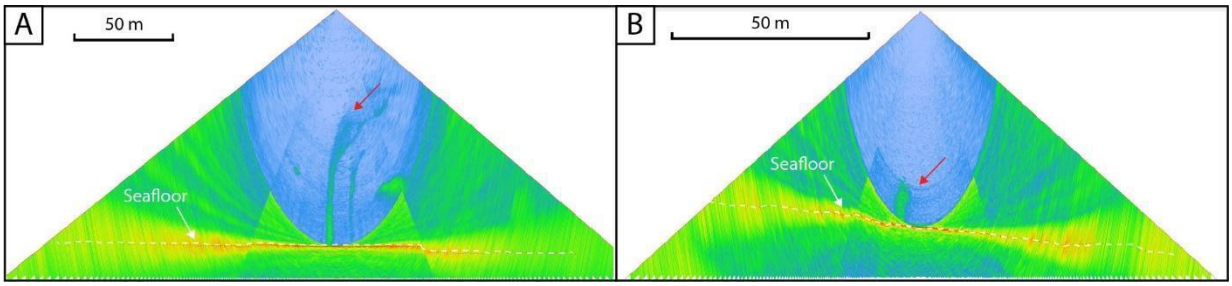

Figure 3. Examples of the two characteristic gas flare shapes shown in fan view. a) Tall, thin, streamer shaped gas flare; b) Short, teardrop shaped gas flare.

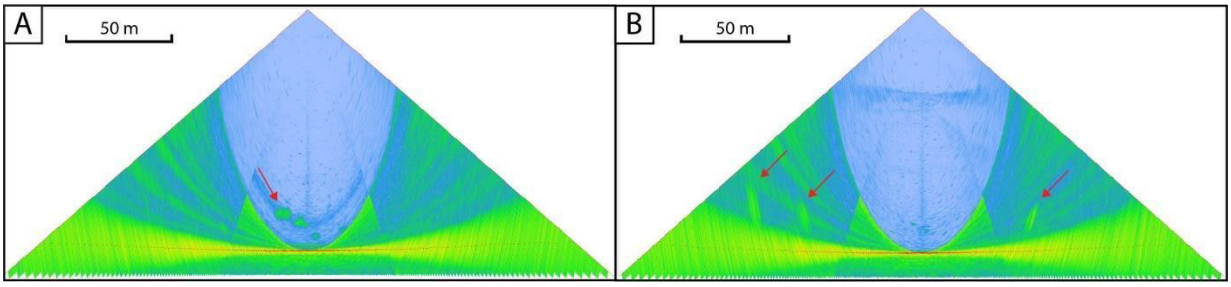

Figure 4. Examples of noise in a) centre beams and b) side beams. In both a) and b) the high strength anomalies do not touch the seafloor, and in b) they are contained within a group of beams that do not cross obliquely into other beams.

RESULTS

The results of the water column survey are presented here in Tables 1-11 with screenshots of the flares (Figures 6-87) and are organized by multibeam track number. The tables include the ID number assigned to each flare, coordinates in decimal degrees, water depth at the flare location, the height of the flare and the confidence level of the flare identification. The time stamp indicates when the flare was recorded and can be used to find the flares quickly in FMMidwater. The position column indicates if the flare was located in the centre beams or in the side beams on port (left) or starboard (right) side.

The figures present the flares in fan view (right side) and R-stacked view (left side) and include a time stamp. The gas flares are indicated by red arrows. The figures do not include a scale, as the scale changes with depth at each ping. The heights of the gas flares are in both the table and the figure caption and can be used as a scale. As the fan view is set to a 1:1 ratio, there is no vertical exaggeration. Screenshots of gas flares assigned medium and high confidence levels are included in this report, but low confidence flare data are only included in the tables. Additionally, we identified some non-flare water column anomalies (potentially fish, marine mammals, plankton) and have included Table 12 with their coordinates. Figure 4 shows two representative examples of these anomalies.

Tracks 0016 to 0021 have a higher concentration of high strength anomalies than tracks 0011 to 0015 (Figure 5). Tracks 0016 to 0021 also have significantly more gas flares than tracks 0011 to 0015. The anomalies are near the seafloor but do not have a point of contact, so they could be related to marine organisms and communities (e.g., schools of fish, marine mammals, kelp forests).

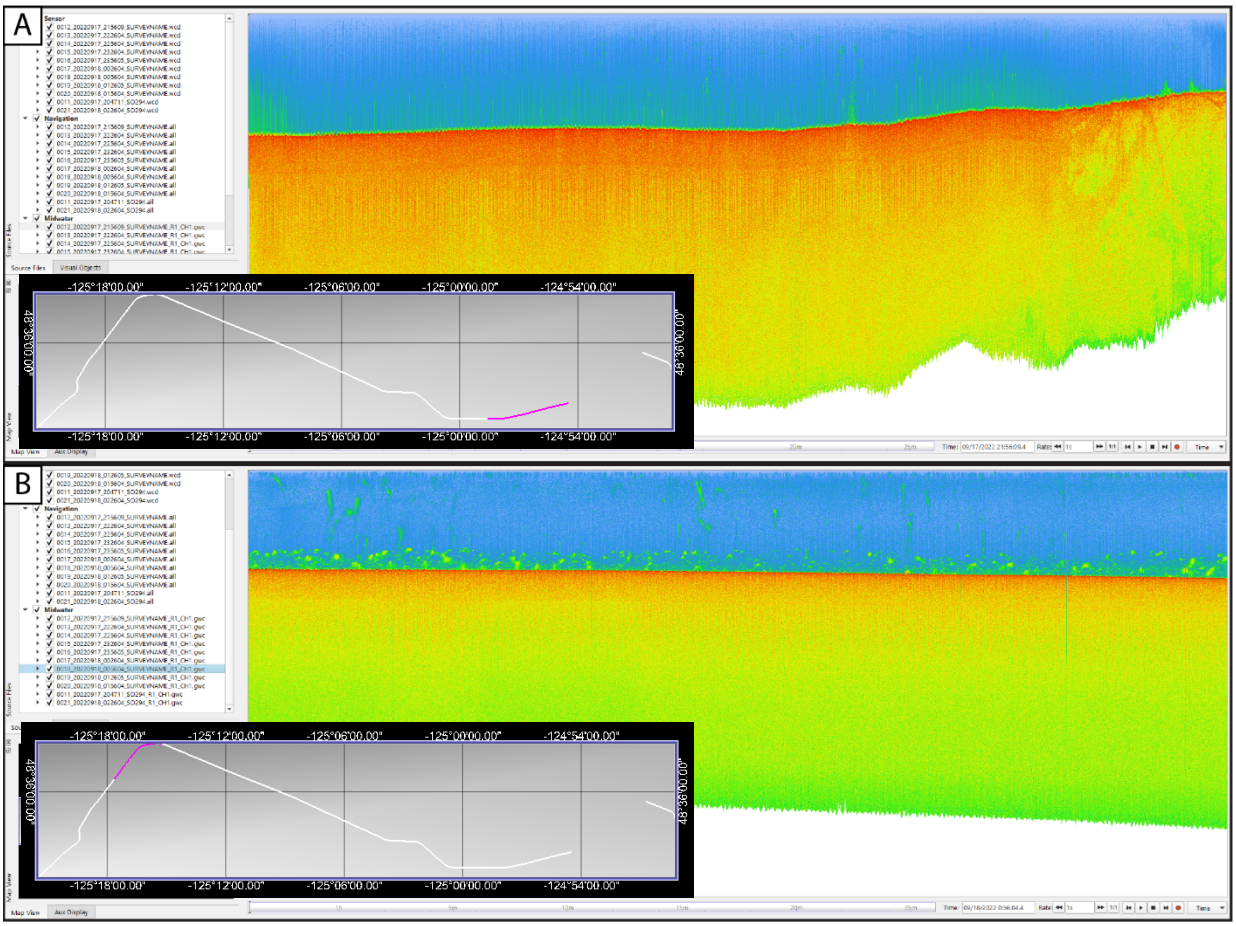

Figure 5. R-Stack views of tracks a) 0012 and b) 0018. Track locations are highlighted in pink in the bottom left corner. Near the seafloor, there are few high strength anomalies in a) and many in b).

Track 0011

Table 1. Gas flares from track 0011 (track ID 0011_20220917_204711).

Flare ID	Latitude	Longitude	Depth (m)	Height (m)	Time (UTC)	Position	Confidence
0011_1	48.58065795	-124.82115990	68.65	11.1	2022-09-17 21:04:51	centre	medium
0011_2	48.57977217	-124.82076078	69.03	8.6	2022-09-17 21:05:38	centre	medium

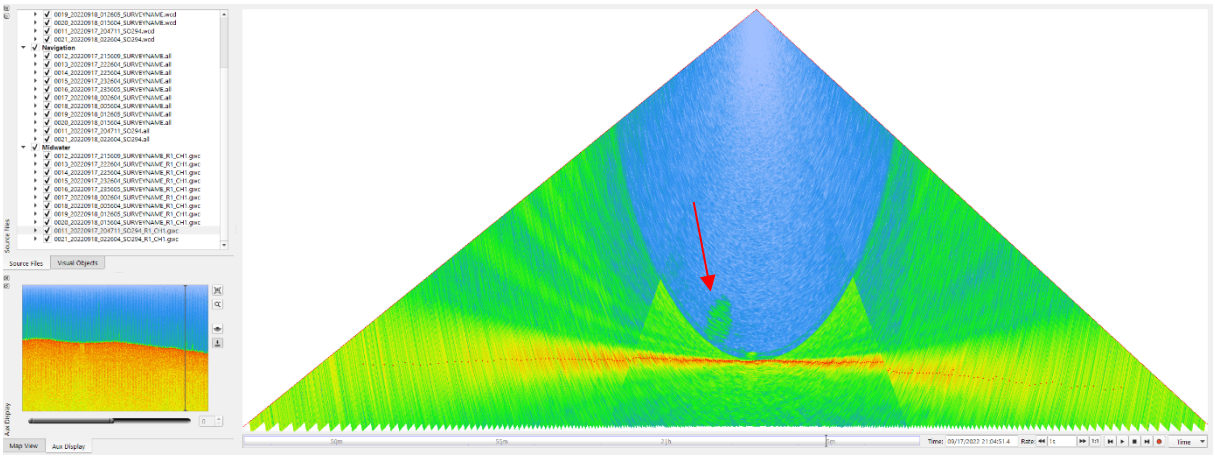

Figure 6. Gas flare 0011_1, 11.1 m high, medium confidence.

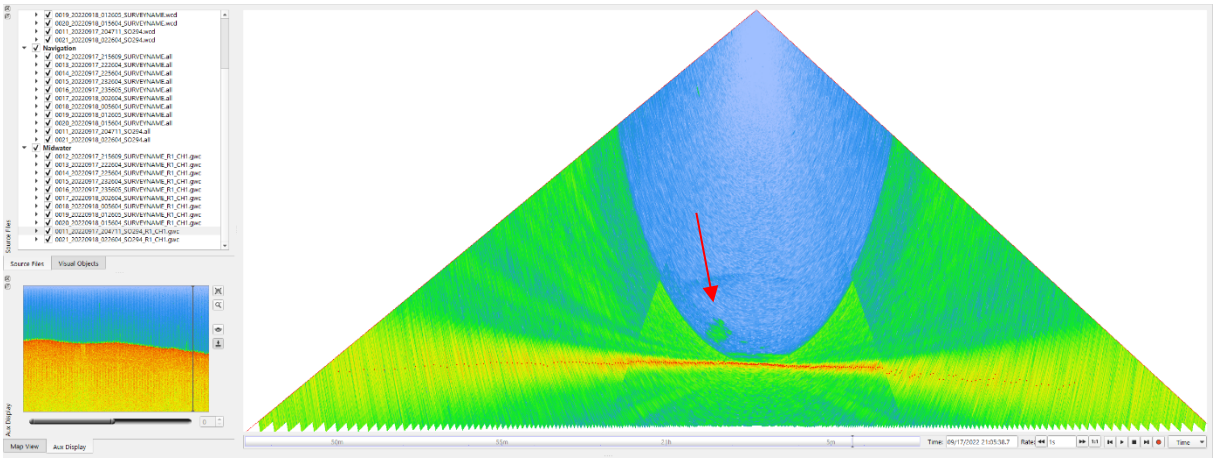

Figure 7. Gas flare 0011_2, 8.6 m high, medium confidence.

Track 0012

Table 2. Gas flares from track 0012 (track ID 0012_20220917_215609).

Flare ID	Latitude	Longitude	Depth (m)	Height (m)	Time (UTC)	Position	Confidence
0012_1	48.53680278	-124.96977296	56.49	7.5	2022-09-17 22:23:23	centre	low
0012_2	48.53653887	-124.97066768	55.61	3.4	2022-09-17 22:23:46	centre	low
0012_3	48.53649803	-124.97258452	53.29	10.5	2022-09-17 22:24:33	centre	high

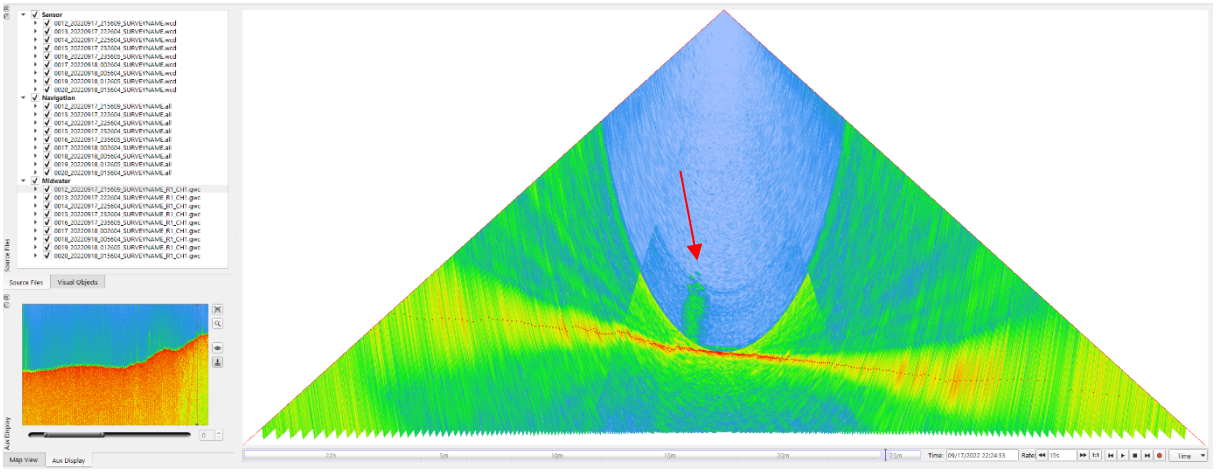

Figure 8. Gas flare 0012_3, 10.5 m high, high confidence.

Track 0013

Table 3. Gas flares from track 0013 (track ID 0013_20220917_222604).

Flare ID	Latitude	Longitude	Depth (m)	Height (m)	Time (UTC)	Position	Confidence
0013_1	48.54612054	-125.02363561	45.99	6.8	2022-09-17 22:49:39	centre	low
0013_2	48.55061599	-125.02828456	59.45	6.2	2022-09-17 22:52:58	centre	high
00 13_3	48.55378671	-125.03211960	54.15	5.7	2022-09-17 22:55:17	centre	low

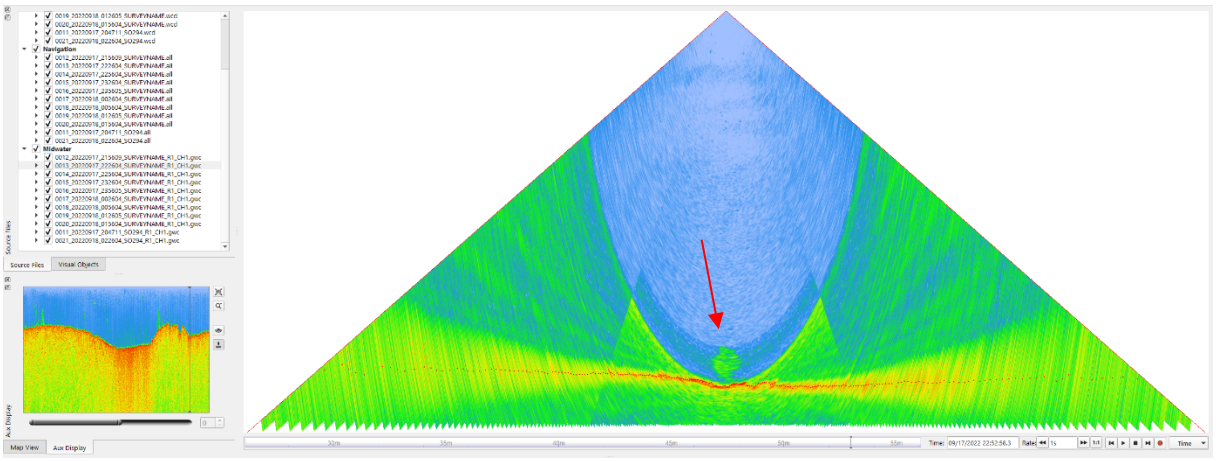

Figure 9. Gas flare 0013_2, 6.2 m high, high confidence.

Track 0014

Table 4. Gas flares from track 0014 (track ID 0014_20220917_225604).

Flare ID	Latitude	Longitude	Depth (m)	Height (m)	Time (UTC)	Position	Confidence
0014_1	48.55723056	-125.03784167	70.98	23.0	2022-09-17 22:58:19	centre	high
0014_2	48.56768338	-125.08350089	114.54	16.4	2022-09-17 23:20:46	centre	low
0014_3	48.56985119	-125.08678959	118.46	34.5	2022-09-17 23:22:48	centre	medium
0014_4	48.57023946	-125.08729549	120.64	66.1	2022-09-17 23:23:08	centre	high
0014_5	48.57105103	-125.08994933	126.55	69.9	2022-09-17 23:24:25	centre	medium

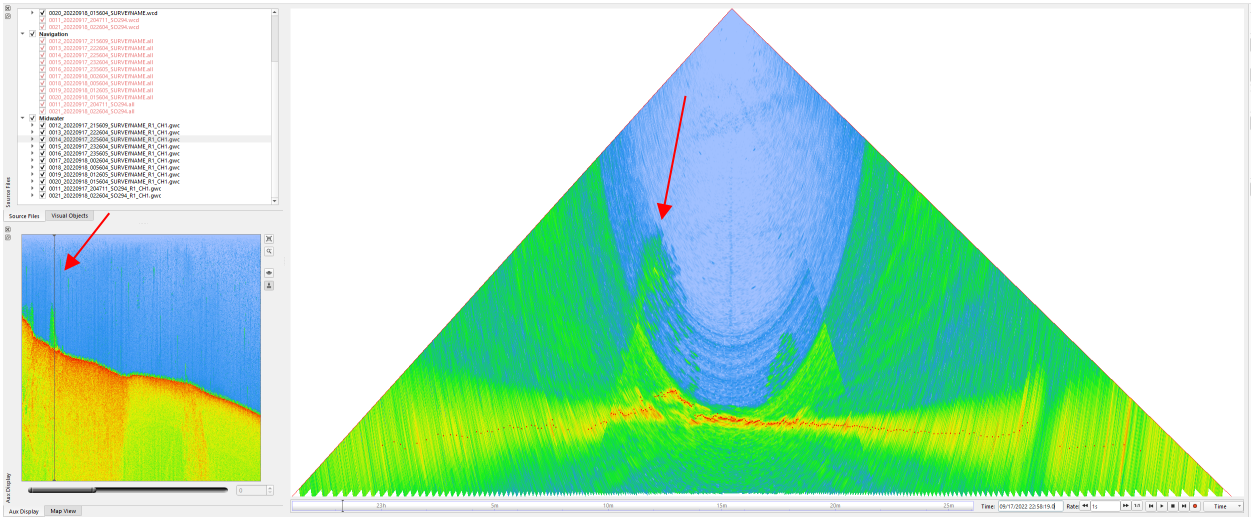

Figure 10. Gas flare 0014_1, 23 m high, high confidence based on R-stack anomaly.

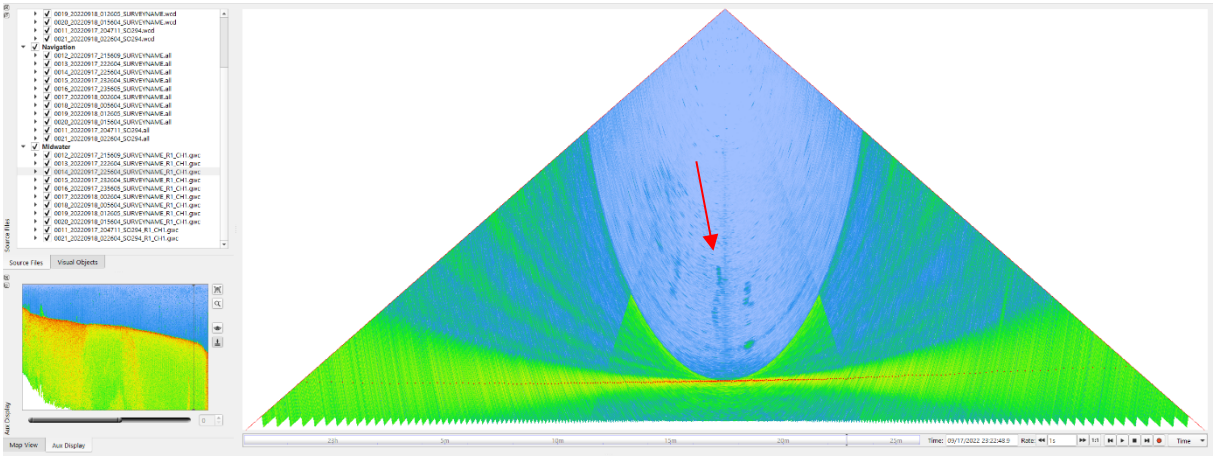

Figure 11. Gas flare 0014_3, 34.5 m high, medium confidence.

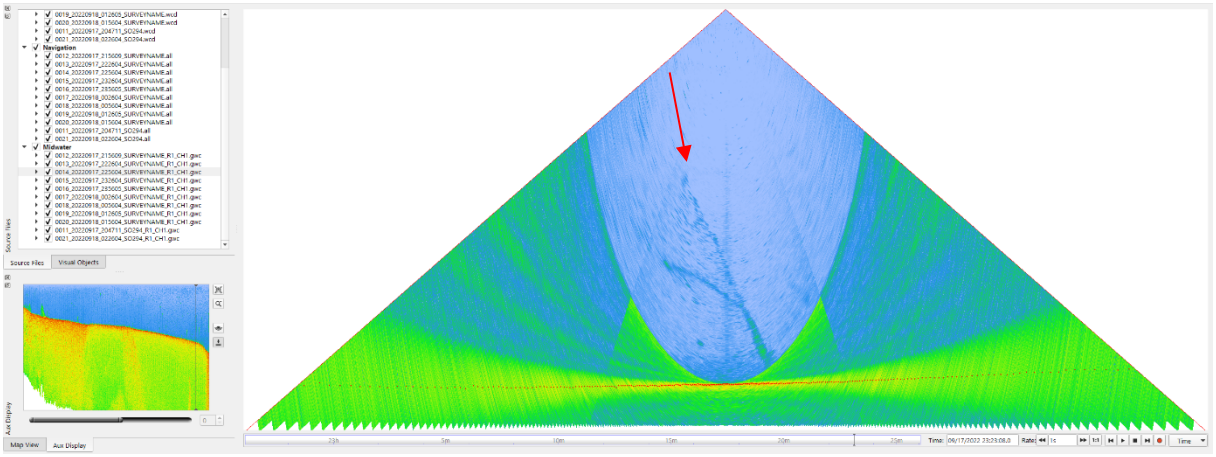

Figure 12. Gas flare 0014_4, 66.1 m high, high confidence.

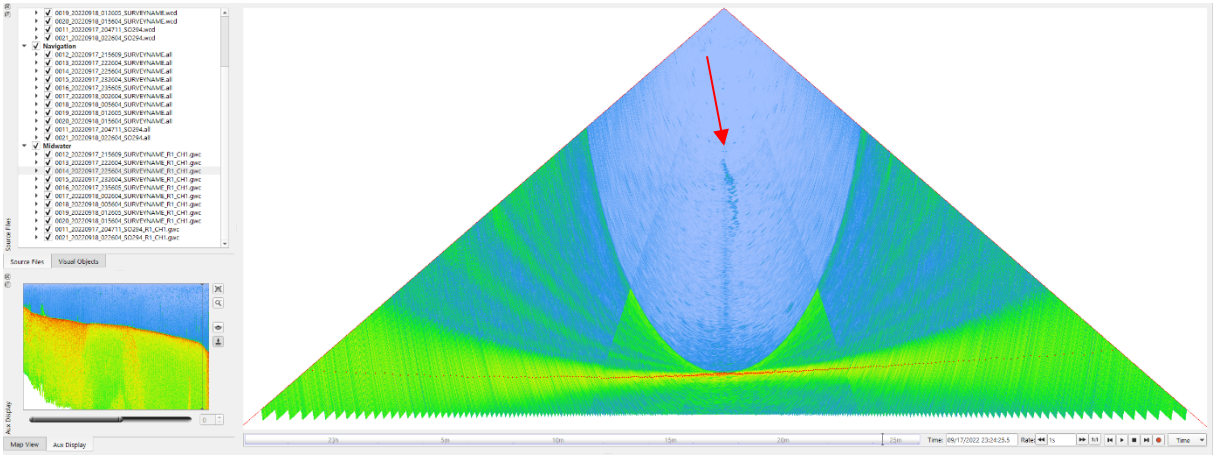

Figure 13. Gas flare 0014_5, 69.9 m high, medium confidence.

Track 0015

Table 5. Gas flares from track 0015 (track ID 0015_20220917_232604).

Flare ID	Latitude	Longitude	Depth (m)	Height (m)	Time (UTC)	Position	Confidence
0015_1	48.57309706	-125.0954869	122.68	35.9	2022-09-17 23:27:13	centre	high
0015_3	48.57866739	-125.1073941	110.17	17.1	2022-09-17 23:33:42	centre	high
0015_4	48.57920940	-125.1084722	109.13	19.8	2022-09-17 23:34:18	centre	low
0015_5	48.58228545	-125.1131264	105.88	45.7	2022-09-17 23:37:13	centre	low
0015_6	48.58374490	-125.1177135	104.32	44.9	2022-09-17 23:39:30	centre	high
0015_7	48.58676820	-125.1246597	105.22	10.8	2022-09-17 23:43:19	centre	medium
0015_8	48.58826023	-125.1265557	105.76	15.4	2022-09-17 23:44:38	centre	medium
0015_9	48.58847057	-125.1269144	106.33	15.1	2022-09-17 23:44:51	centre	medium
0015_11	48.59419222	-125.1444739	112.89	29.6	2022-09-17 23:53:58	port	medium

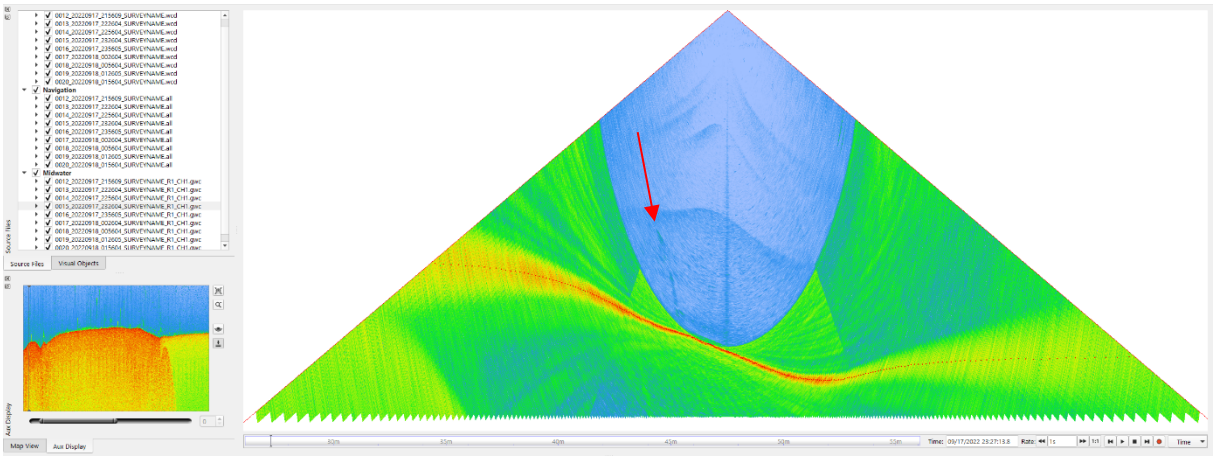

Figure 14. Gas flare 0015_1, 35.9 m high, high confidence.

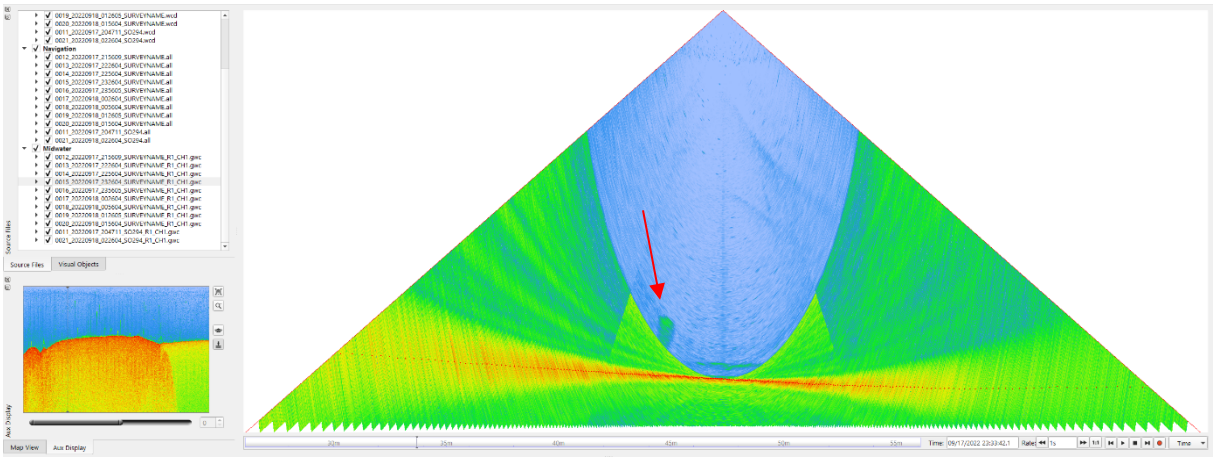

Figure 15. Gas flare 0015_3, 17.1 m high, high confidence

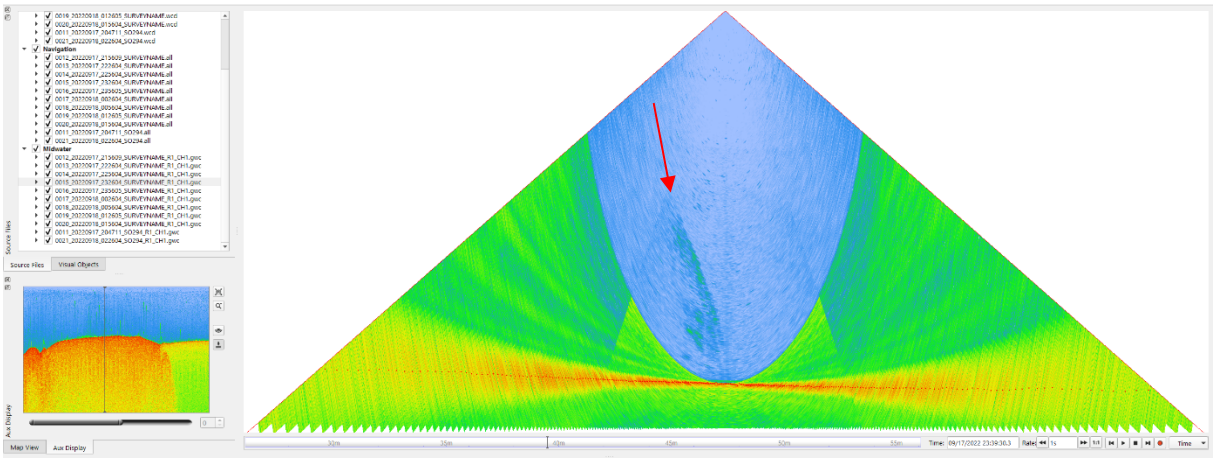

Figure 16. Gas flare 0015_6, 44.9 m high, high confidence.

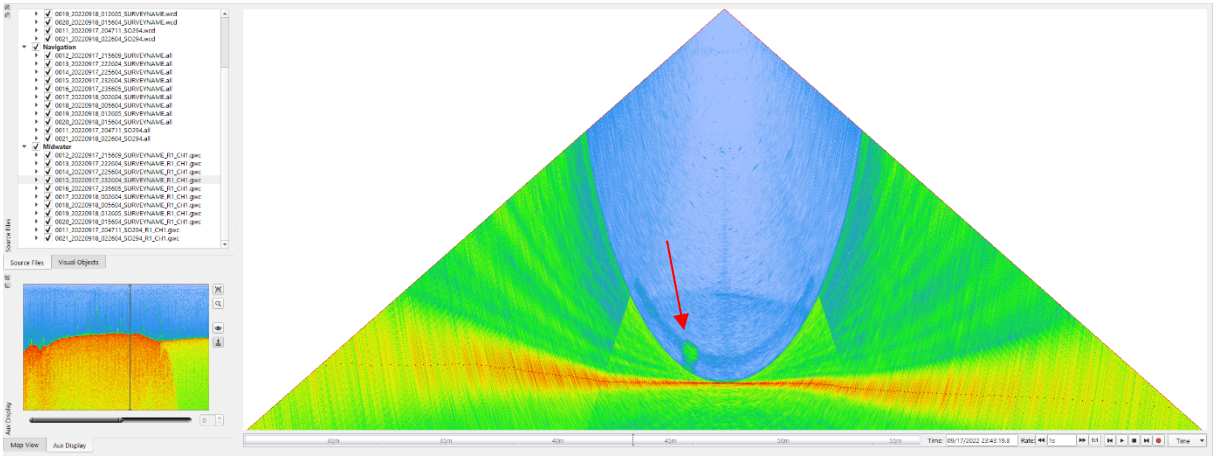

Figure 17. Gas flare 0015_7, 10.8 m high, medium confidence.

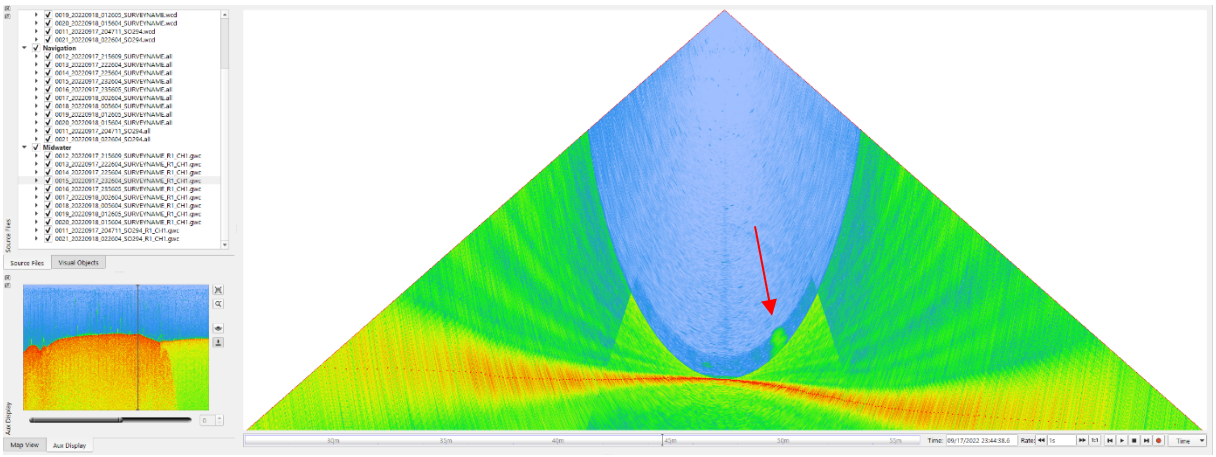

Figure 18. Gas flare 0015_8, 15.4 m high, medium confidence.

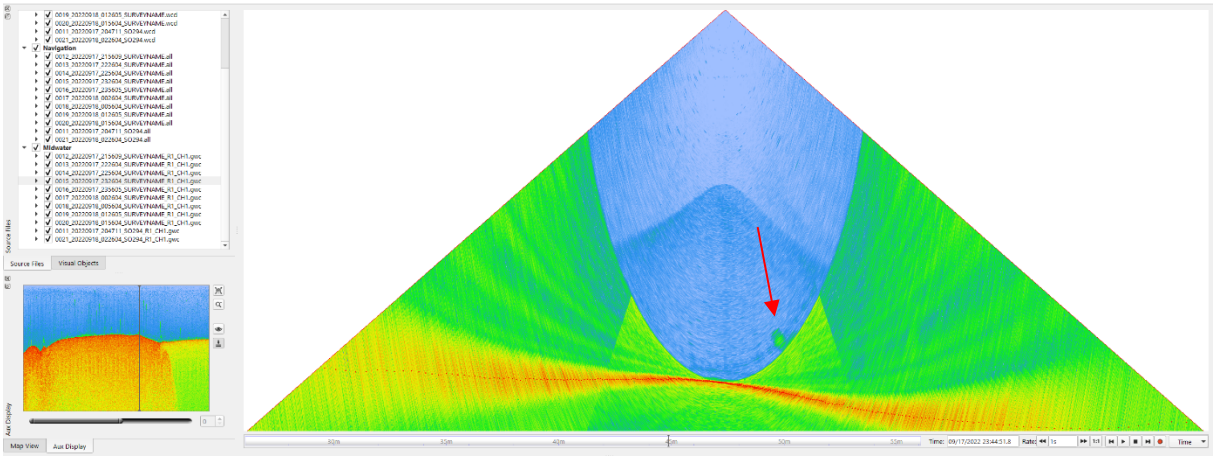

Figure 19. Gas flare 0015_9, 15.1 m high, medium confidence.

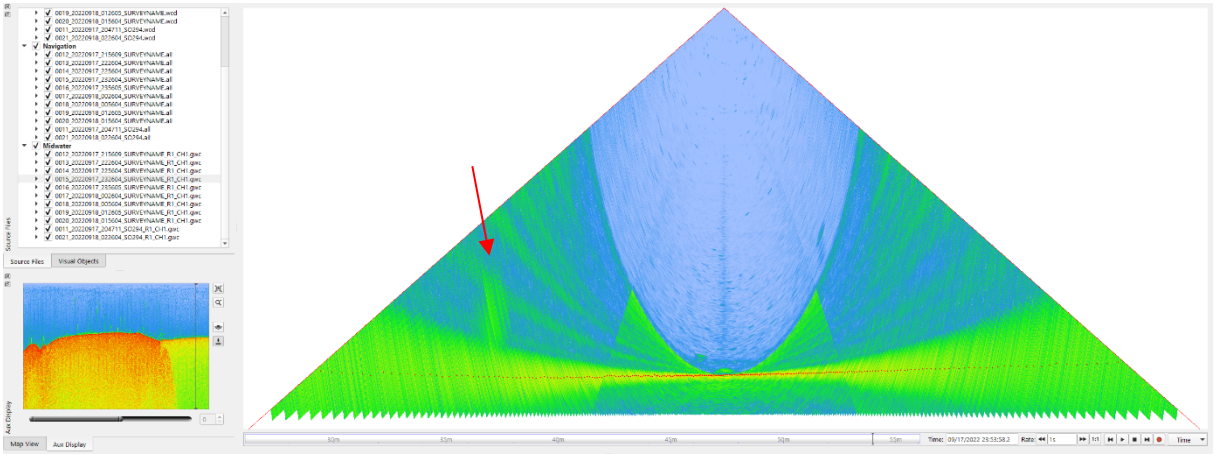

Figure 20. Gas flare 0015_11, 29.6 m high, medium confidence.

Track 0016

Table 6. Gas flares from track 0016 (track ID 0016_20220917_235605)

Flare ID	Latitude	Longitude	Depth (m)	Height (m)	Time (UTC)	Position	Confidence
0016_1	48.59952937	-125.14957134	109.50	19.9	2022-09-17 23:58:01	starboard	low
0016_2	48.59891120	-125.15145495	111.69	20.1	2022-09-17 23:58:31	centre	high
0016_3	48.60147421	-125.15848470	110.80	10.7	2022-09-18 0:02:19	centre	medium
0016_4	48.60114876	-125.16026354	110.34	22.4	2022-09-18 0:02:54	port	low
0016_6	48.60175276	-125.16036206	110.35	54.9	2022-09-18 0:03:10	centre	medium
0016_7	48.60202093	-125.16273020	110.56	24.3	2022-09-18 0:04:12	port	medium
0016_8	48.60258966	-125.16357871	109.87	20.0	2022-09-18 0:04:46	port	low
0016_10	48.60369765	-125.16300038	110.78	12.2	2022-09-18 0:04:57	centre	low
0016_12	48.60492994	-125.16776001	110.33	10.4	2022-09-18 0:07:20	centre	low
0016_13	48.60550593	-125.16763918	110.32	8.4	2022-09-18 0:07:30	centre	medium
0016_14	48.60561092	-125.16754412	109.77	10.1	2022-09-18 0:07:30	centre	medium
0016_16	48.60610812	-125.16913819	110.20	8.4	2022-09-18 0:08:19	centre	high
0016_17	48.60814281	-125.17382222	109.80	18.2	2022-09-18 0:10:59	centre	low
0016_18	48.60834583	-125.17463057	109.78	13.5	2022-09-18 0:11:23	centre	medium
0016_19	48.60843706	-125.17739661	109.87	26.3	2022-09-18 0:12:34	centre	medium
0016_26	48.61127408	-125.18318155	109.52	9.0	2022-09-18 0:15:56	centre	medium
0016_28	48.61081349	-125.18516374	109.28	24.2	2022-09-18 0:16:34	port	medium
0016_29	48.61201632	-125.18436851	109.53	13.6	2022-09-18 0:16:41	centre	medium
0016_30	48.61305670	-125.18651681	108.72	19.4	2022-09-18 0:17:56	centre	medium
0016_32	48.61558266	-125.19353888	108.86	11.1	2022-09-18 0:21:45	centre	low
0016_34	48.61640044	-125.19611379	109.11	6.2	2022-09-18 0:23:06	centre	low
0016_35	48.61725872	-125.19706110	108.89	18.0	2022-09-18 0:23:48	centre	medium

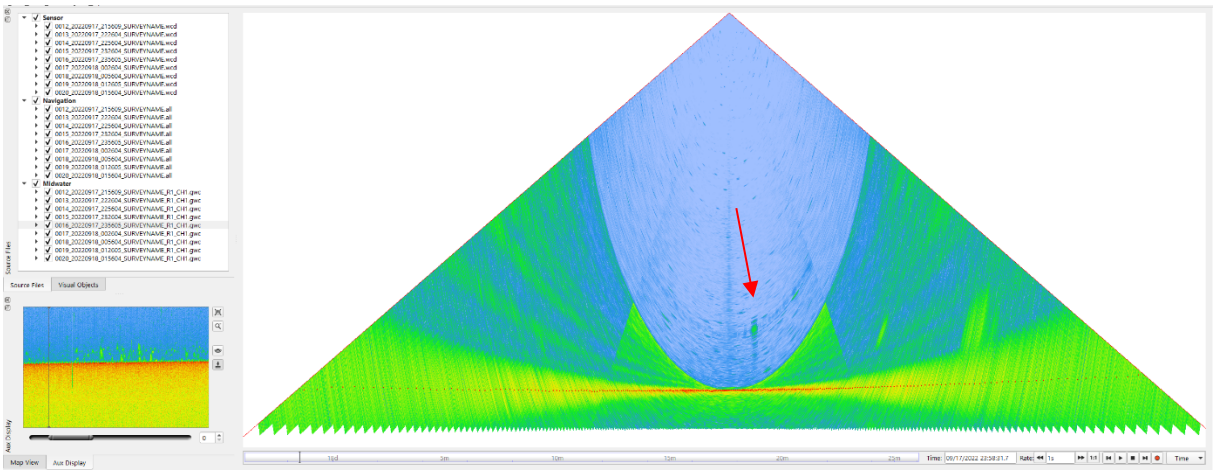

Figure 21. Gas flare 0016_2, 20.1 m high, high confidence.

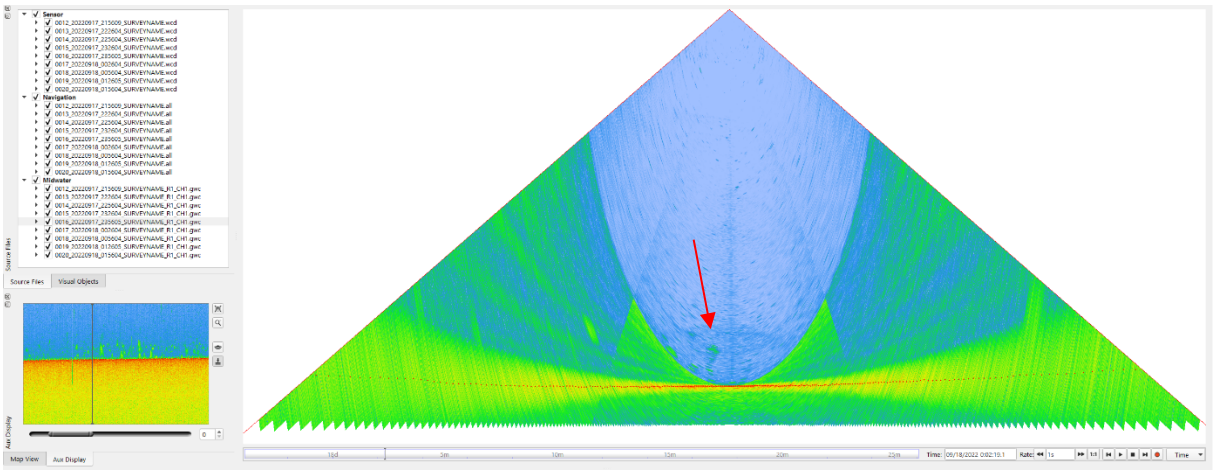

Figure 22. Gas flare 0016_3, 10.7 m high, medium confidence.

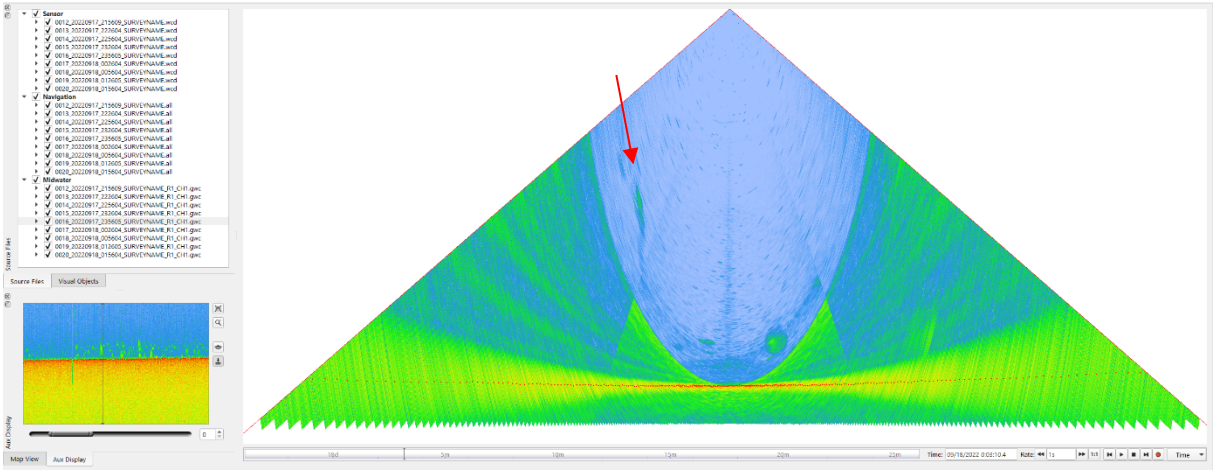

Figure 23. Gas flare 0016_6, 54.9 m high, medium confidence.

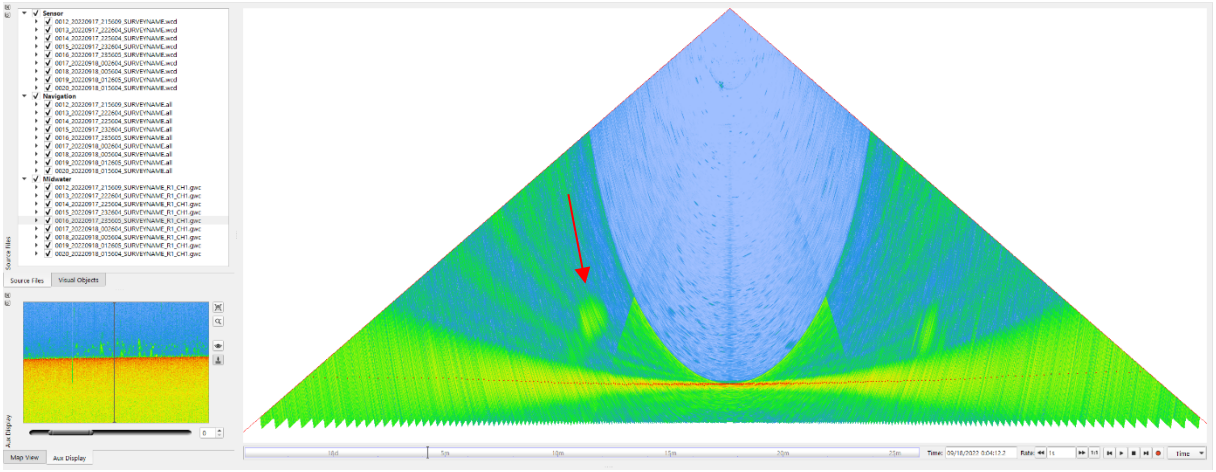

Figure 24. Gas flare 0016_7, 24.3 m high, medium confidence.

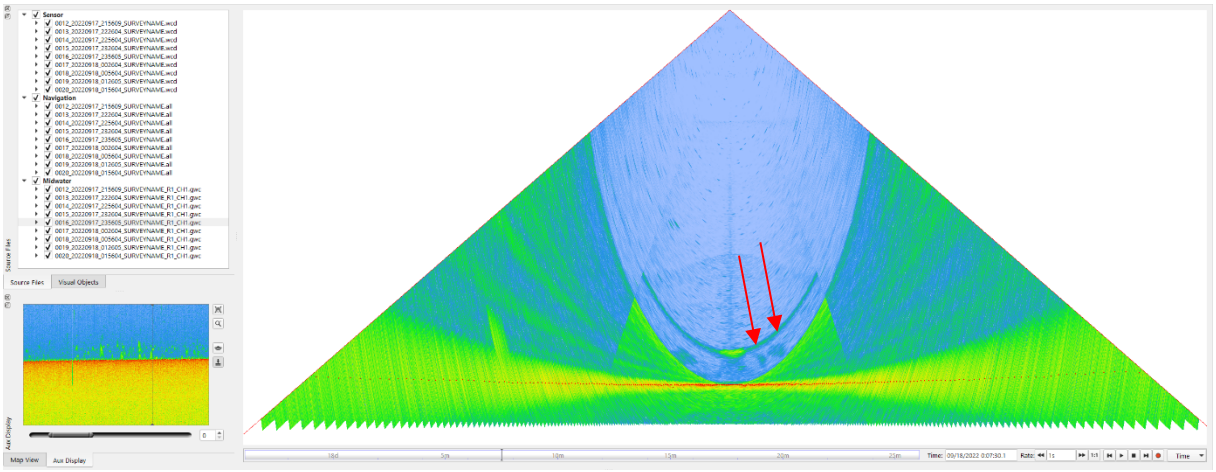

Figure 25. Gas flare 0016_13, 8.4 m high, medium confidence (left) and gas flare 0016_14, 10.1 m high, medium confidence (right).

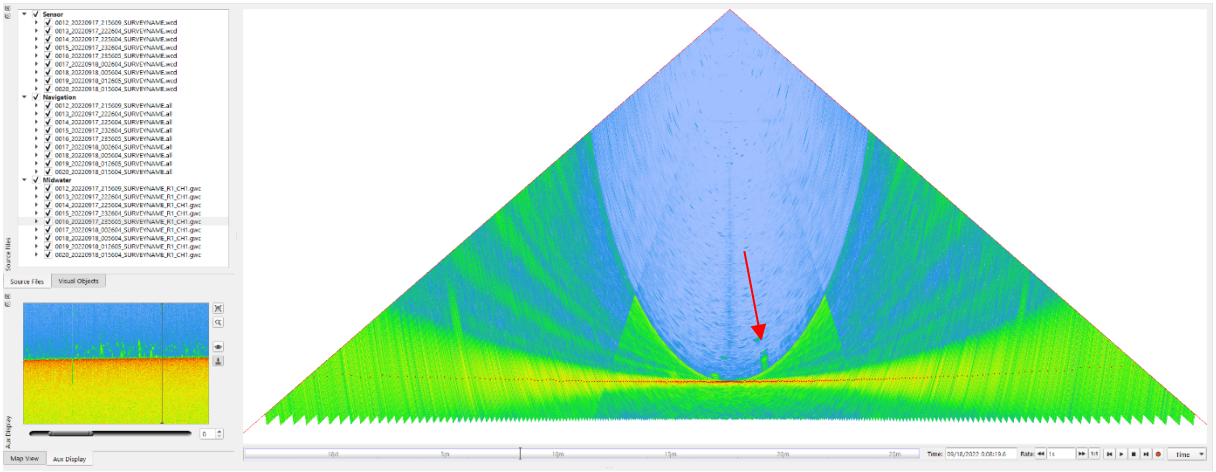

Figure 26. Gas flare 0016_16, 8.4 m high, high confidence.

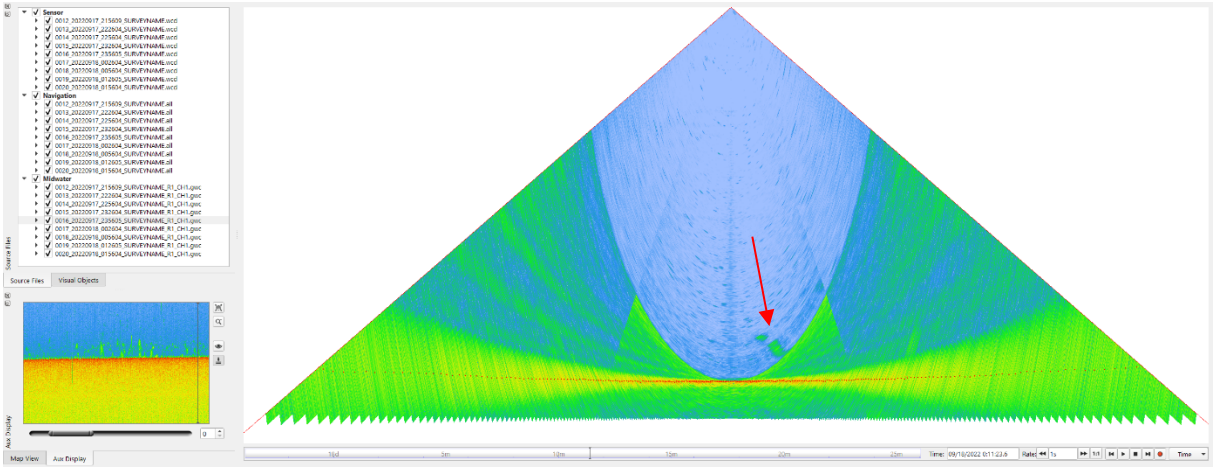

Figure 27. Gas flare 0016_18, 13.5 m high, medium confidence.

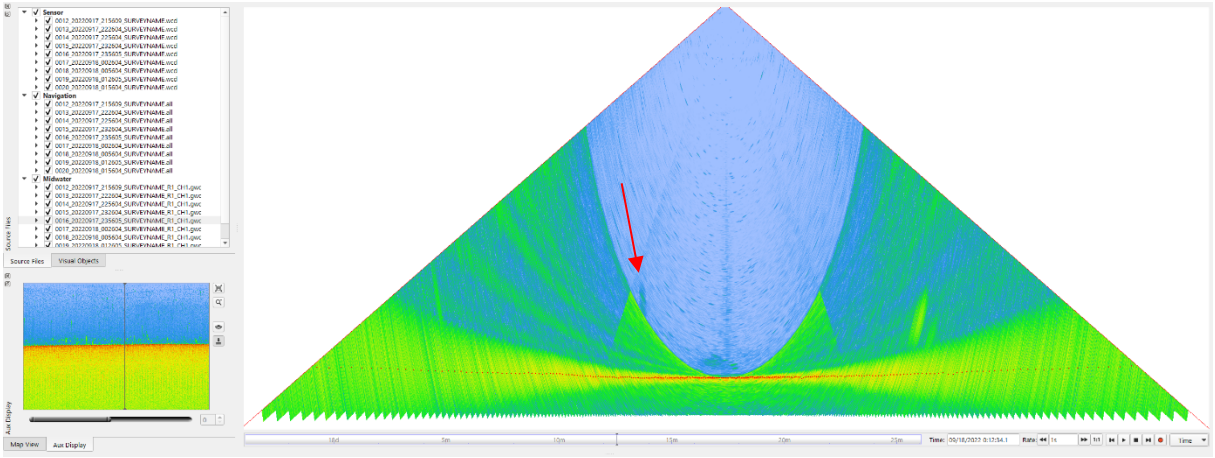

Figure 28. Gas flare 0016_19, 26.3 m high, medium confidence.

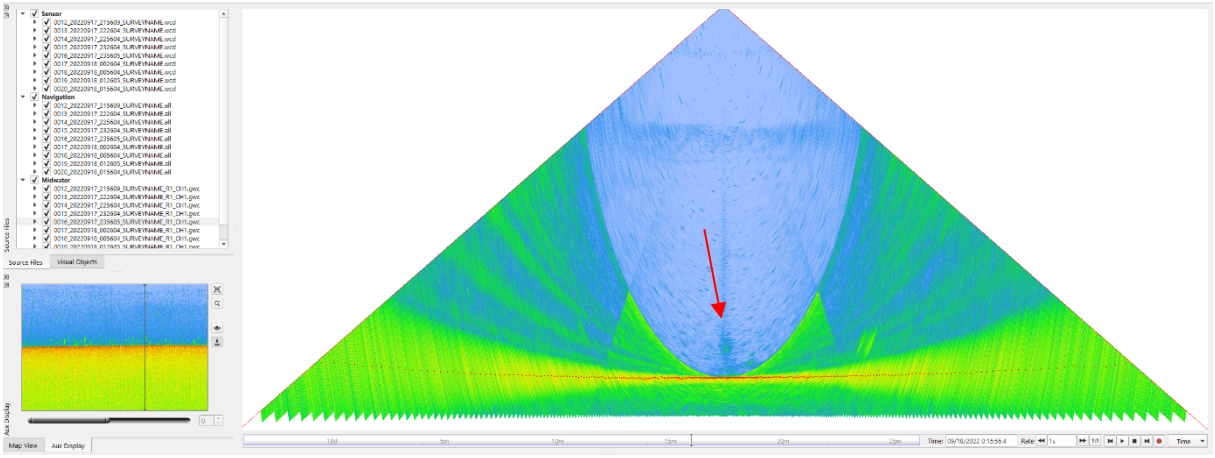

Figure 29. Gas flare 0016_26, 9.0 m high, medium confidence.

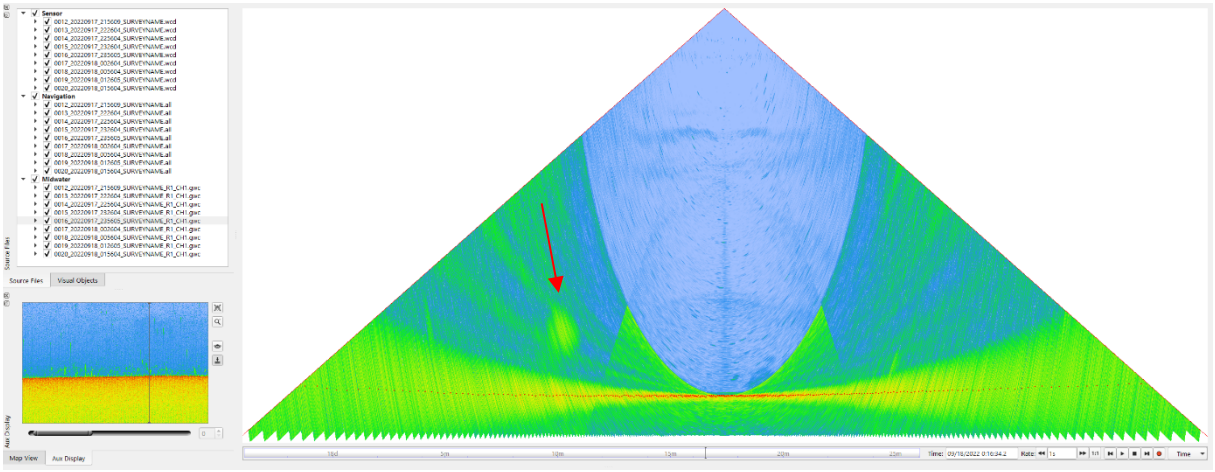

Figure 30. Gas flare 0016_28, 24.2 m high, medium confidence.

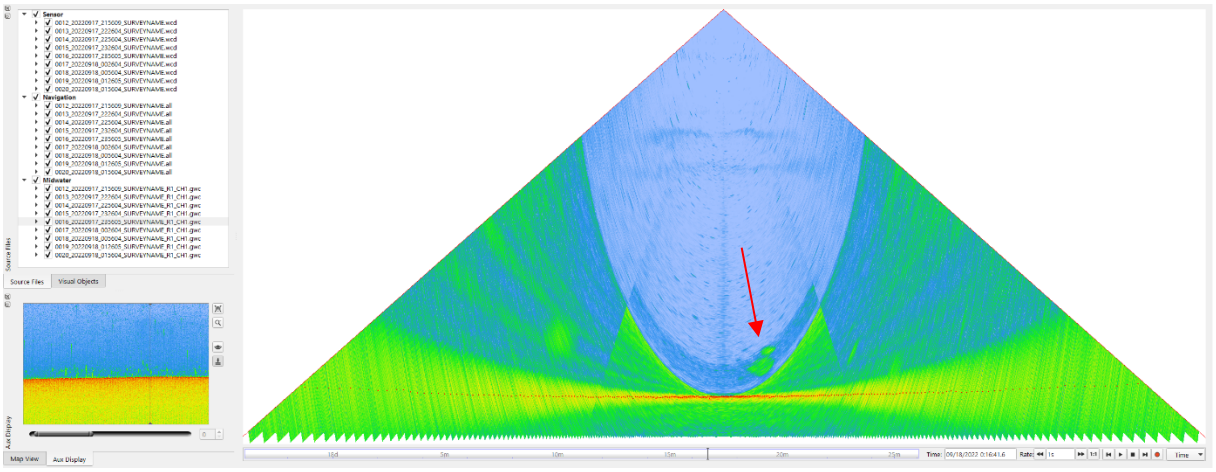

Figure 31. Gas flare 0016_29, 13.6 m high, medium confidence.

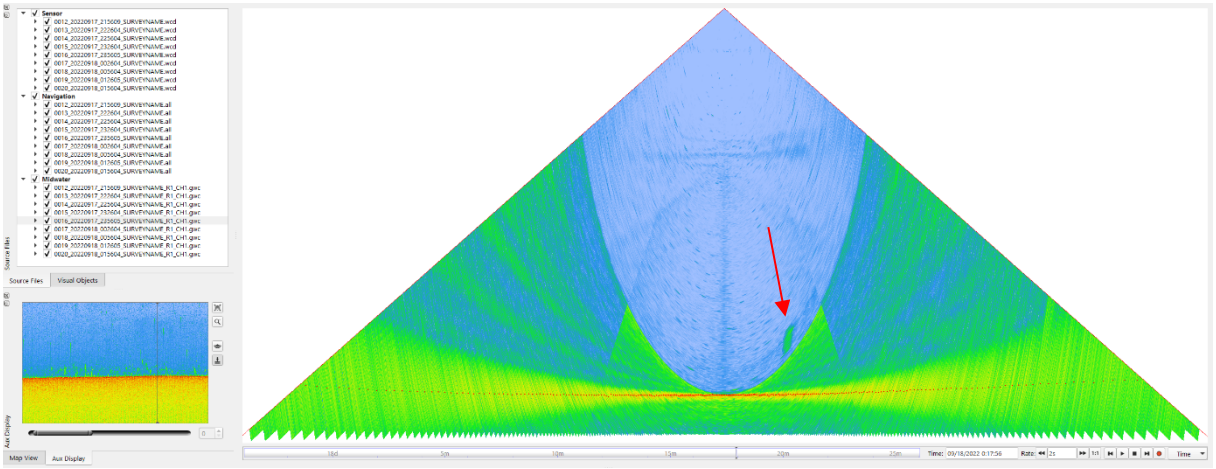

Figure 32. Gas flare 0016_30, 19.4 m high, medium confidence.

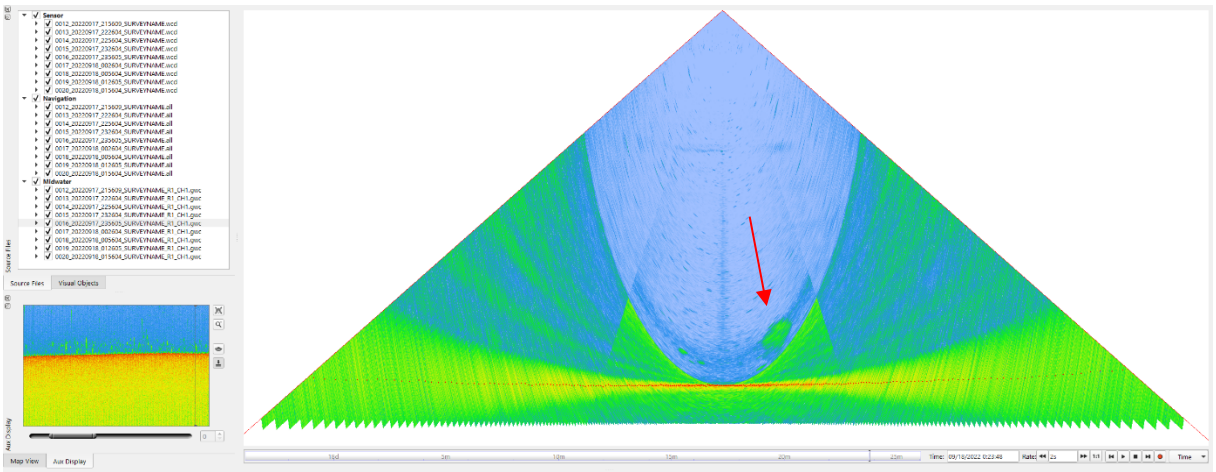

Figure 33. Gas flare 0016_35, 18.0 m high, medium confidence.

Track 0017

Table 7. Gas flares from track 0016 (track ID 0017_20220918_002604).

Flare ID	Latitude	Longitude	Depth (m)	Height (m)	Time (UTC)	Position	Confidence
0017_1	48.61992423	-125.20182206	108.96	16.7	2022-09-18 0:26:41	starboard	low
0017_2	48.62049228	-125.20523874	109.78	10.7	2022-09-18 0:28:16	centre	medium
0017_3	48.62115687	-125.20820643	109.82	33.6	2022-09-18 0:29:41	centre	high
0017_4	48.62212697	-125.21218200	109.63	22.2	2022-09-18 0:31:37	port	medium
0017_7	48.62395533	-125.21290772	109.98	11.2	2022-09-18 0:32:37	centre	low
0017_8	48.62659013	-125.22124923	110.01	22.8	2022-09-18 0:36:54	centre	high
0017_9	48.62677449	-125.22132635	110.03	9.7	2022-09-18 0:37:00	centre	medium
0017_10	48.62905357	-125.22235324	109.20	21.1	2022-09-18 0:38:14	starboard	low
0017_11	48.62823089	-125.22341347	110.11	13.5	2022-09-18 0:38:23	centre	medium
0017_12	48.62813046	-125.22403298	110.74	71.4	2022-09-18 0:38:37	centre	high
0017_14	48.63140846	-125.23260926	110.23	24.0	2022-09-18 0:43:22	centre	medium
0017_15	48.63248476	-125.23370278	110.81	13.5	2022-09-18 0:44:13	centre	high
0017_16	48.63419936	-125.24220600	109.82	26.2	2022-09-18 0:48:26	port	medium
0017_17	48.63837894	-125.24566764	110.24	19.8	2022-09-18 0:51:37	starboard	low
0017_18	48.63837345	-125.24969841	110.27	15.9	2022-09-18 0:53:19	centre	medium
0017_19	48.63900162	-125.24934479	110.77	19.9	2022-09-18 0:53:26	centre	medium
0017_20	48.63911608	-125.25105098	110.55	6.5	2022-09-18 0:54:11	centre	medium
0017_21	48.63990580	-125.25125421	110.47	15.7	2022-09-18 0:54:35	centre	medium
0017_22	48.64056634	-125.25382560	110.55	9.4	2022-09-18 0:55:54	centre	high

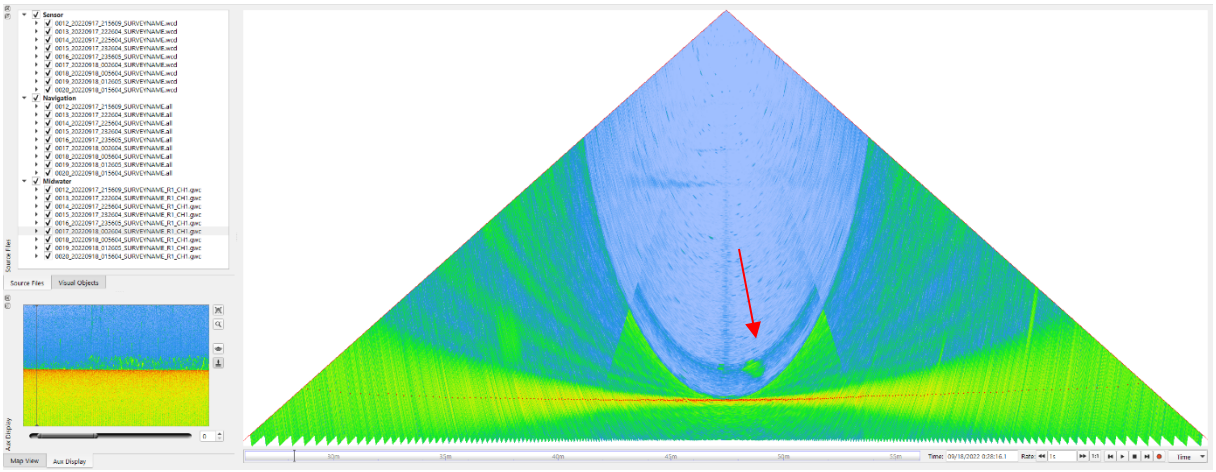

Figure 34. Gas flare 0017_2, 10.7 m high, medium confidence.

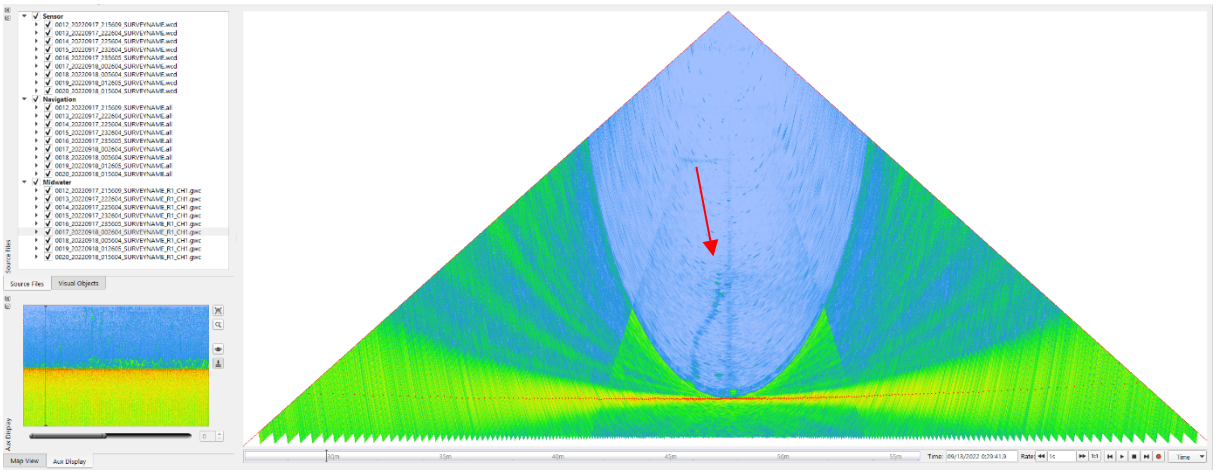

Figure 35. Gas flare 0017_3, 33.6 m high, high confidence.

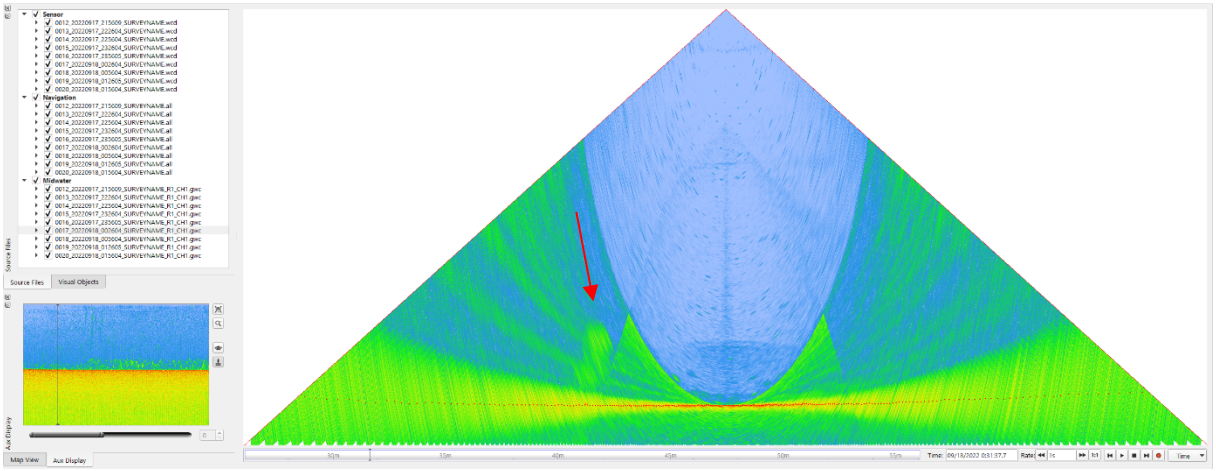

Figure 36. Gas flare 0017_4, 22.2 m high, medium confidence.

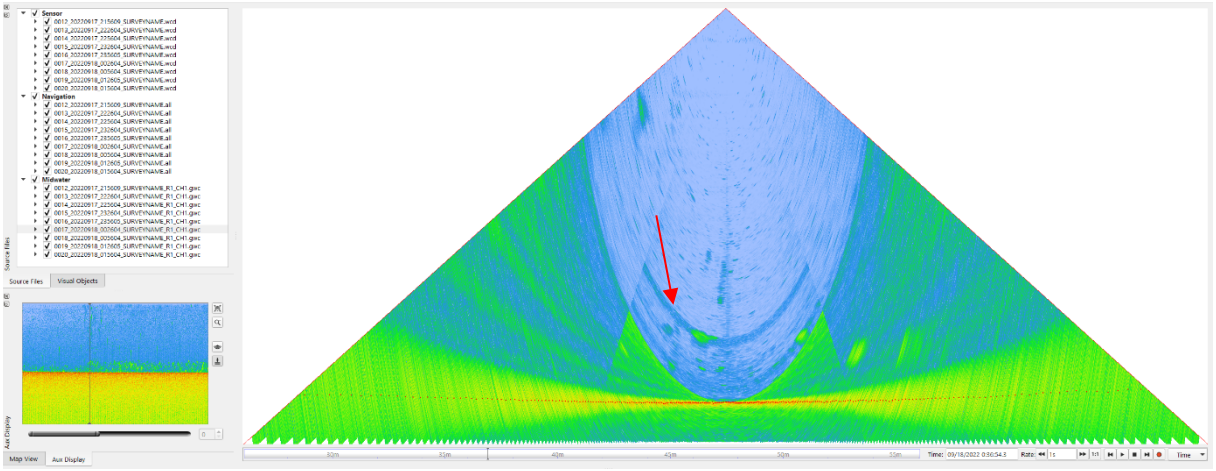

Figure 37. Gas flare 0017_8, 22.8 m high, high confidence.

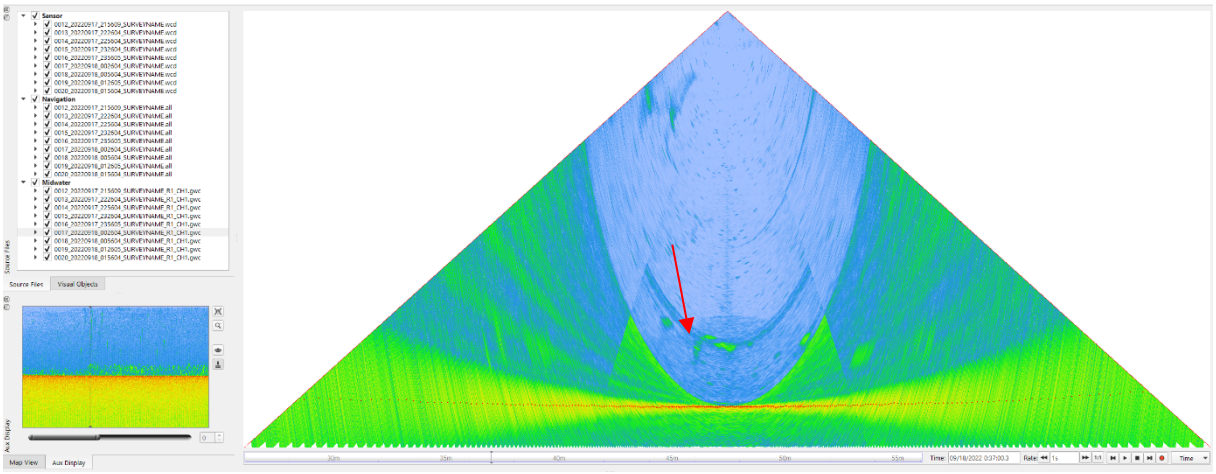

Figure 38. Gas flare 0017_9, 9.7 m high, medium confidence.

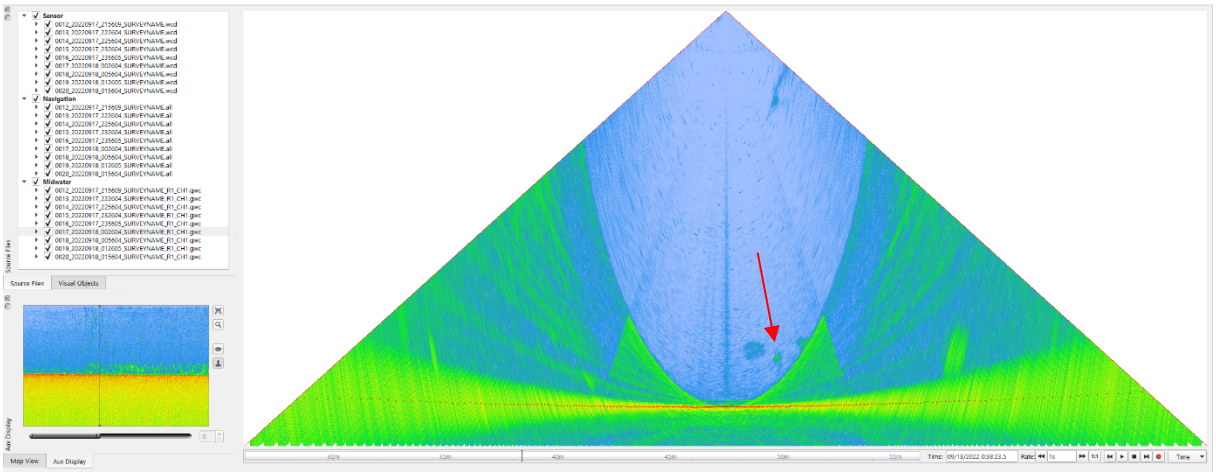

Figure 39. Gas flare 0017_11, 13.5 m high, medium confidence.

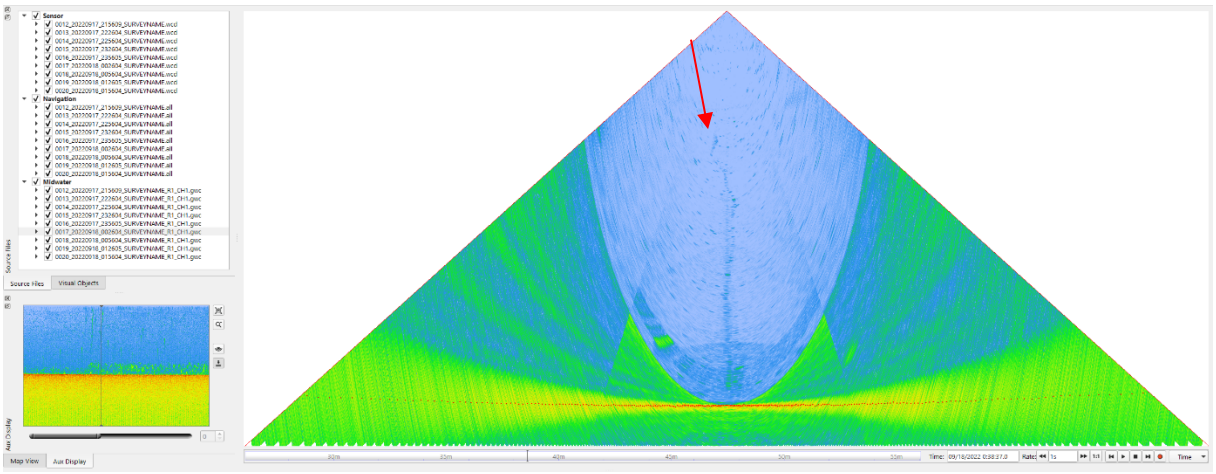

Figure 40. Gas flare 0017_12, 71.4 m high, high confidence.

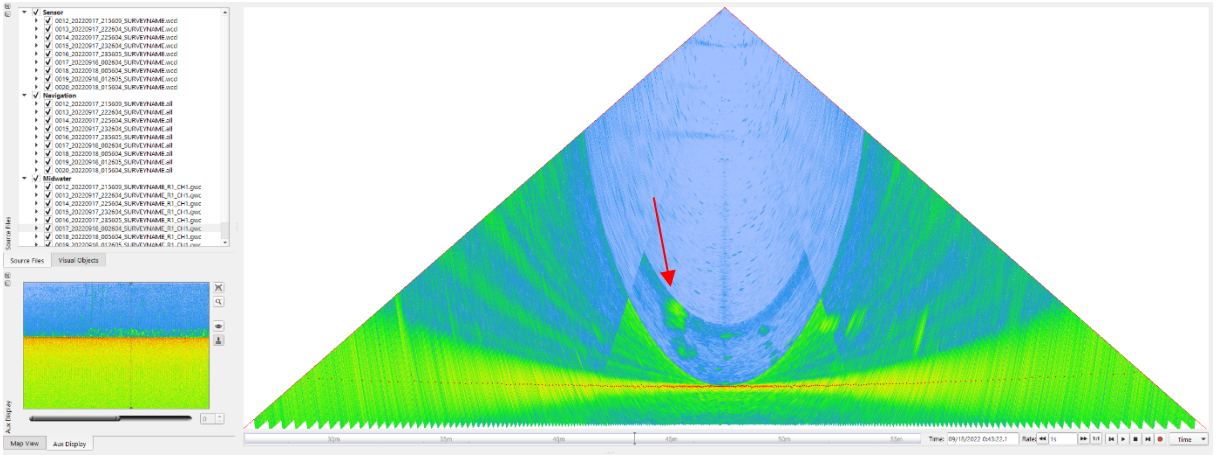

Figure 41. Gas flare 0017_14, 24.0 m high, medium confidence.

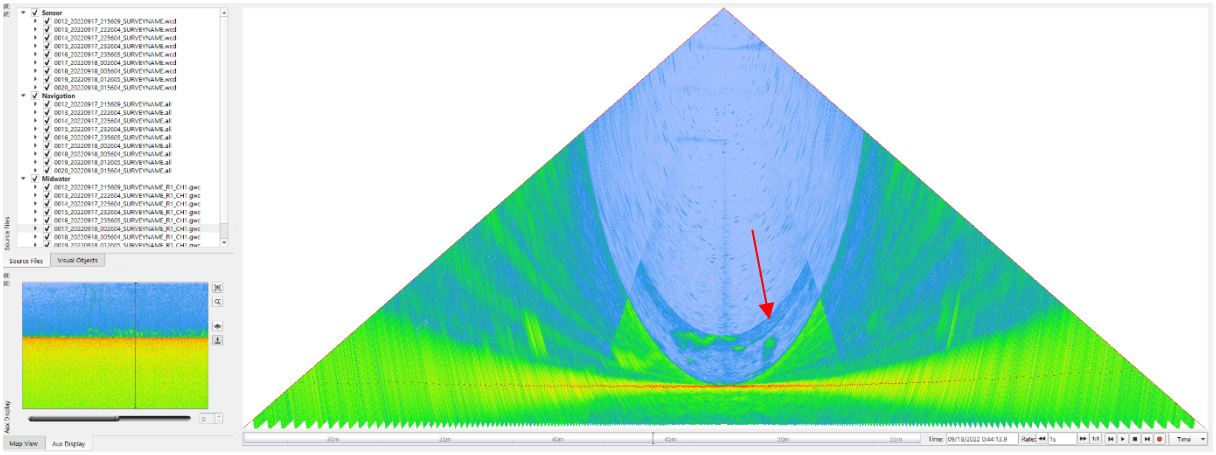

Figure 42. Gas flare 0017_15, 13.5 m high, high confidence.

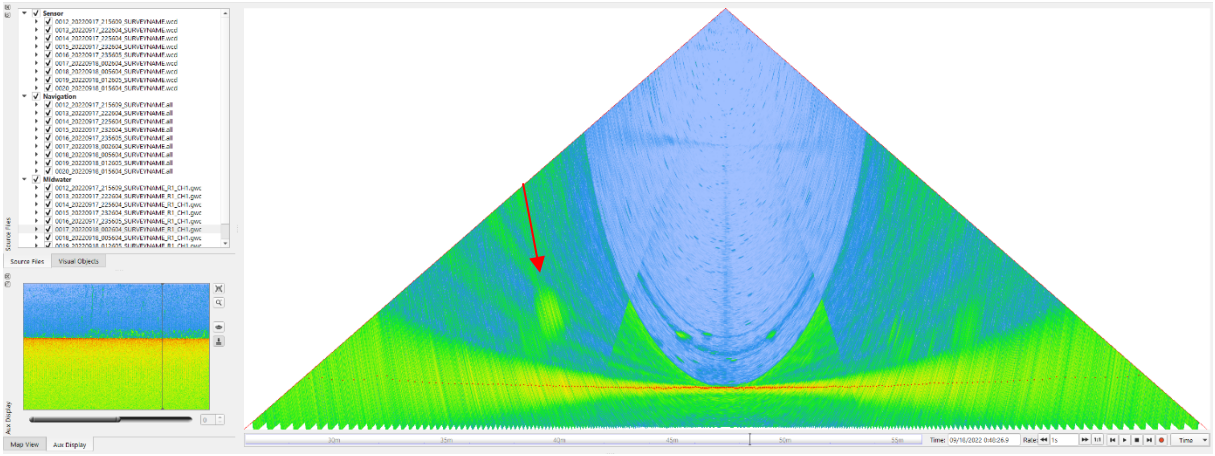

Figure 43. Gas flare 0017_16, 26.2 m high, medium confidence.

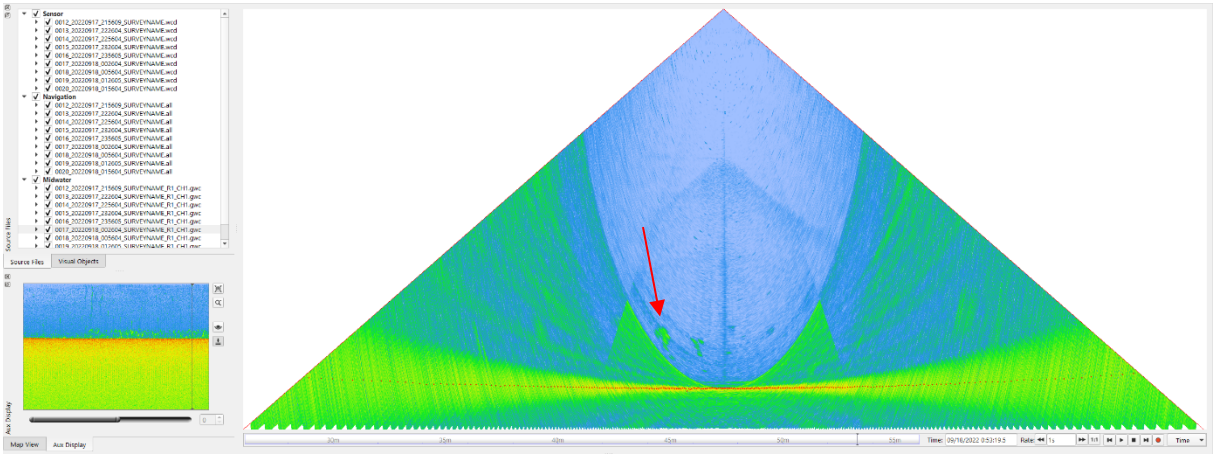

Figure 44. Gas flare 0017_18, 15.9 m high, medium confidence.

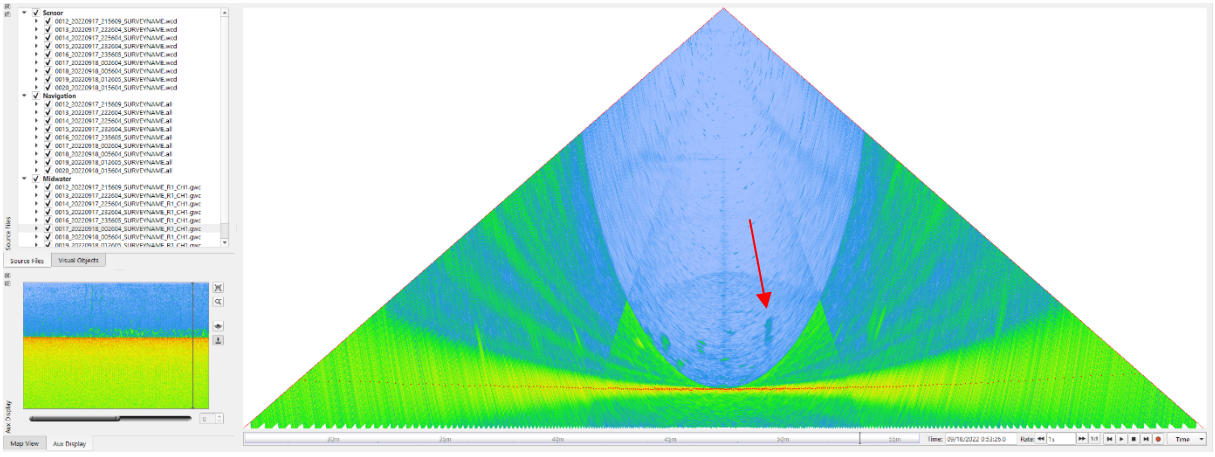

Figure 45. Gas flare 0017_19, 19.9 m high, medium confidence.

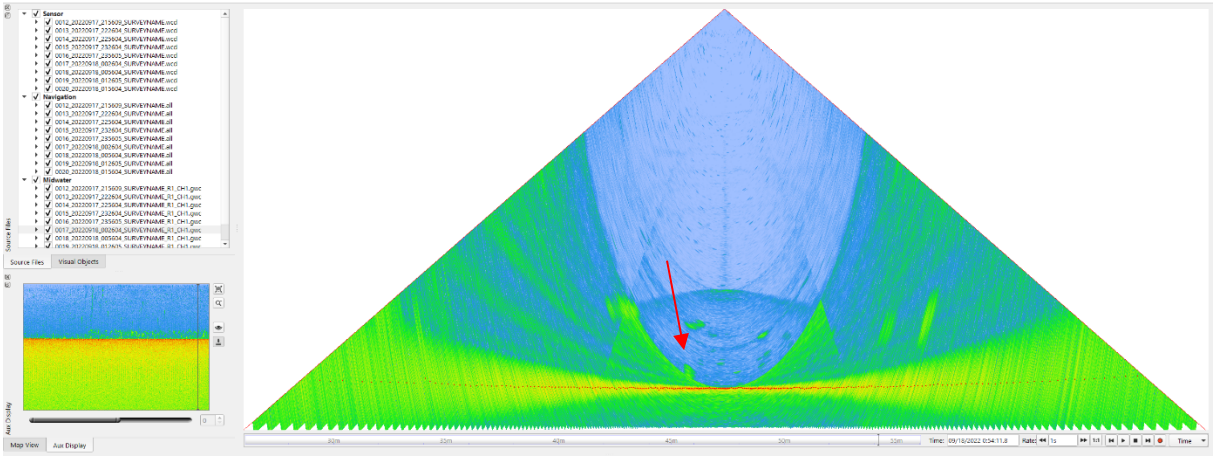

Figure 46. Gas flare 0017_20, 6.5 m high, medium confidence.

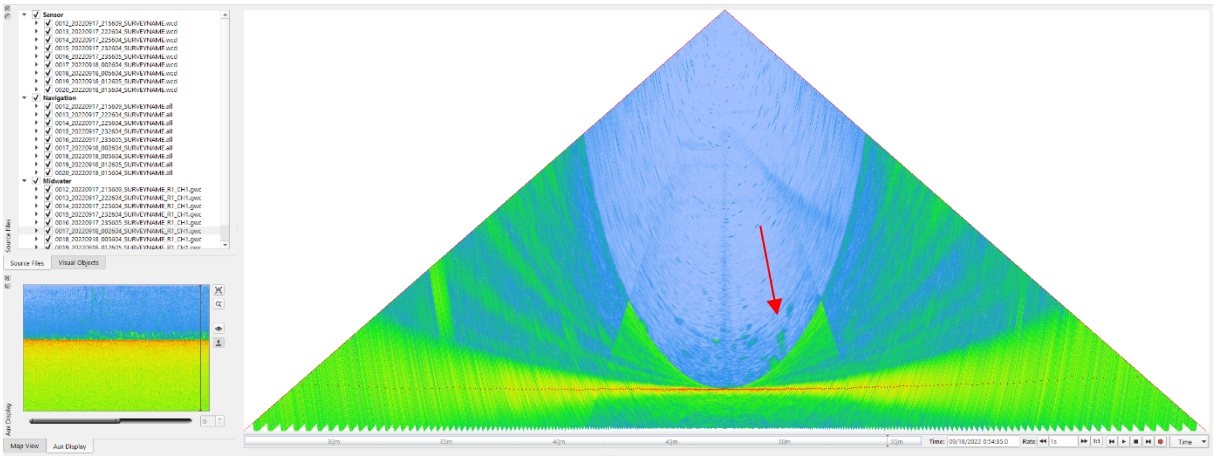

Figure 47. Gas flare 0017_21, 15.7 m high, medium confidence.

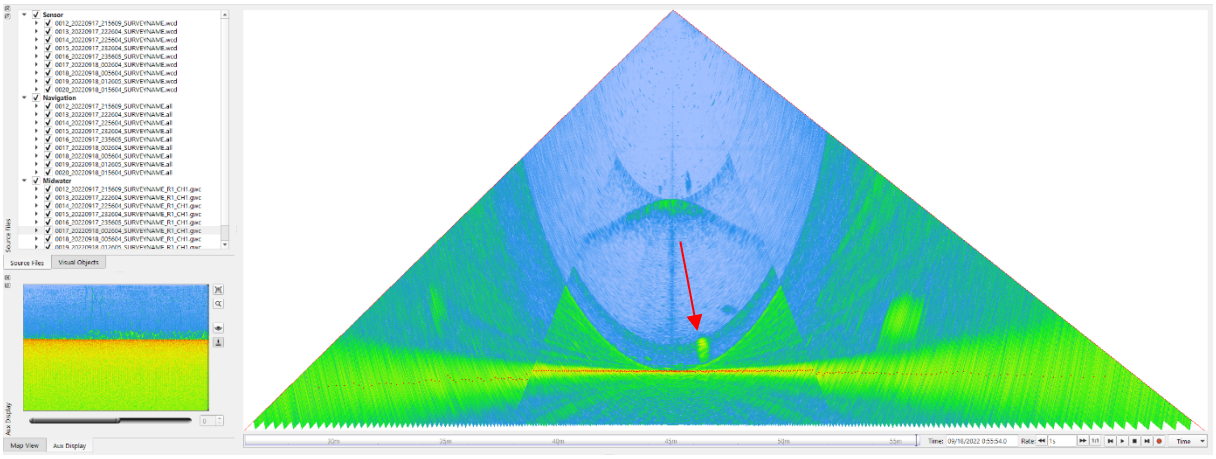

Figure 48. Gas flare 0017_22, 9.4 m high, high confidence.

Track 0018

Table 8. Gas flares from track 0018 (track ID 0018_20220918_005604).

Flare ID	Latitude	Longitude	Depth (m)	Height (m)	Time (UTC)	Position	Confidence
0018_1	48.64027671	-125.25914283	110.91	96.6	2022-09-18 0:58:32	centre	medium
0018_2	48.64079304	-125.26031776	110.98	90.5	2022-09-18 0:59:04	centre	medium
0018_3	48.64019692	-125.26071884	111.26	92.0	2022-09-18 0:59:20	centre	high
0018_4	48.64003919	-125.26094019	110.98	23.4	2022-09-18 0:59:27	centre	medium
0018_5	48.64107798	-125.26133559	110.72	67.3	2022-09-18 0:59:30	centre	medium
0018_6	48.64022349	-125.26149317	111.28	59.7	2022-09-18 0:59:42	centre	medium
0018_7	48.64023644	-125.26219302	111.10	31.3	2022-09-18 1:00:01	centre	medium
0018_8	48.63972196	-125.26249288	110.88	71.3	2022-09-18 1:00:14	centre	medium
0018_9	48.63796444	-125.26616880	111.14	34.3	2022-09-18 1:02:15	port	low
0018_10	48.63862713	-125.26987265	111.60	19.7	2022-09-18 1:03:50	centre	low
0018_11	48.63817879	-125.27203319	112.27	13.0	2022-09-18 1:04:50	centre	high
0018_13	48.63185448	-125.27717652	112.71	104.2	2022-09-18 1:09:44	centre	medium
0018_14	48.63196176	-125.27805926	113.78	89.8	2022-09-18 1:09:50	centre	high
0018_15	48.63174978	-125.27791626	113.75	88.6	2022-09-18 1:09:56	centre	high
0018_17	48.62902501	-125.27954579	113.76	23.1	2022-09-18 1:11:55	centre	high
0018_18	48.62879630	-125.27949560	114.30	94.2	2022-09-18 1:12:02	centre	medium
0018_19	48.62364203	-125.28361305	115.33	97.6	2022-09-18 1:15:58	centre	medium
0018_20	48.62307448	-125.28510724	115.82	17.5	2022-09-18 1:16:36	centre	high
0018_21	48.62278993	-125.28484641	116.29	96.0	2022-09-18 1:16:44	centre	medium
0018_22	48.62262215	-125.28540780	115.97	7.8	2022-09-18 1:16:56	centre	medium
0018_23	48.62174594	-125.28686720	116.11	44.6	2022-09-18 1:17:45	centre	low
0018_24	48.61768065	-125.28814460	117.37	78.0	2022-09-18 1:20:30	centre	high
0018_25	48.61781709	-125.28883581	117.80	42.7	2022-09-18 1:20:32	centre	high
0018_26	48.61691954	-125.28856181	117.21	17.6	2022-09-18 1:21:03	centre	low

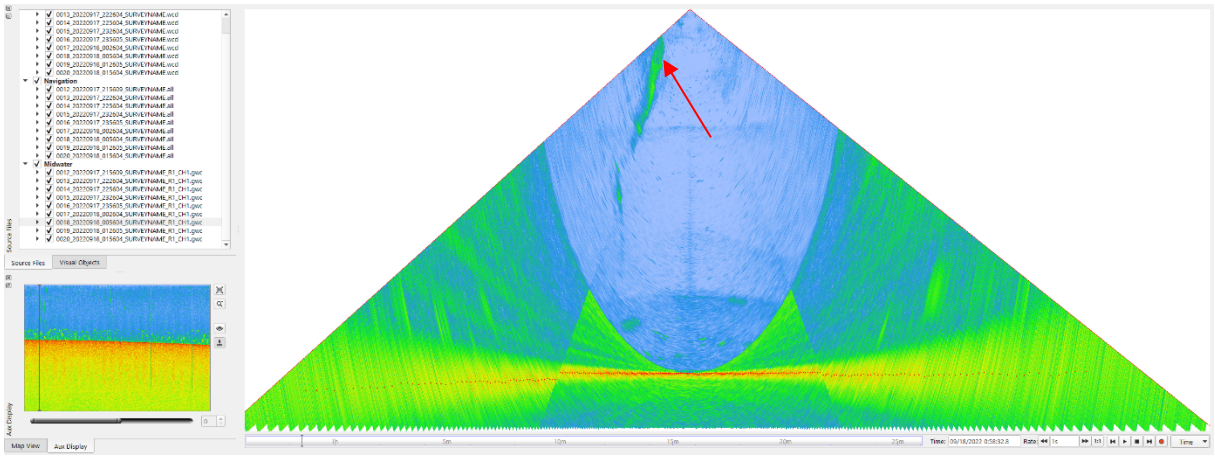

Figure 49. Gas flare 0018_1, 96.6 m high, medium confidence.

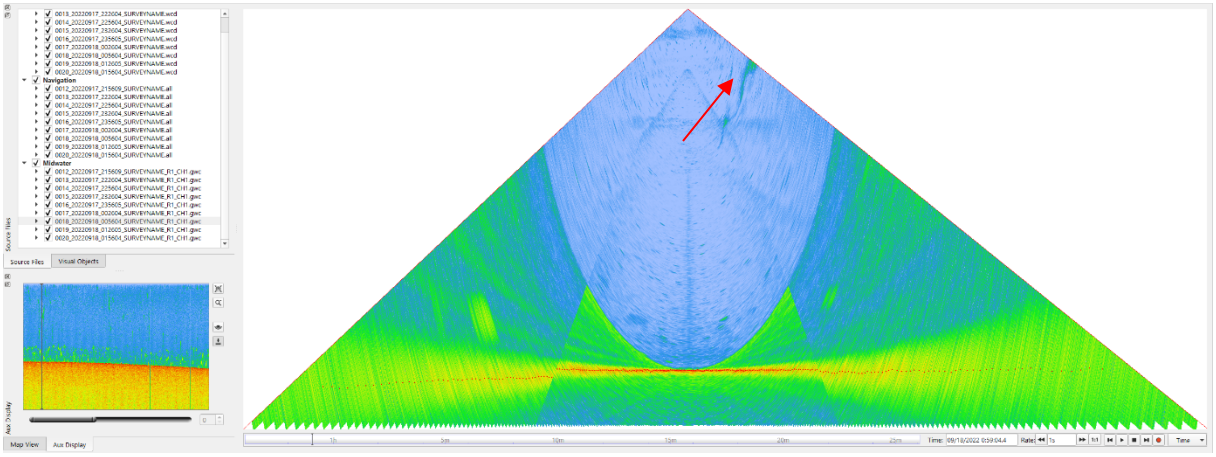

Figure 50. Gas flare 0018_2, 90.5 m high, medium confidence.

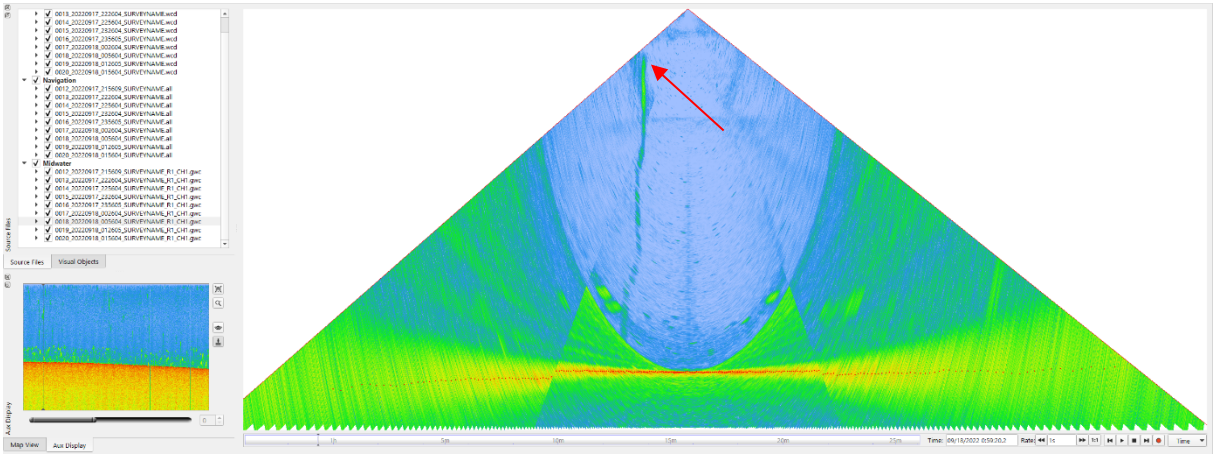

Figure 51. Gas flare 0018_3, 92.0 m high, high confidence.

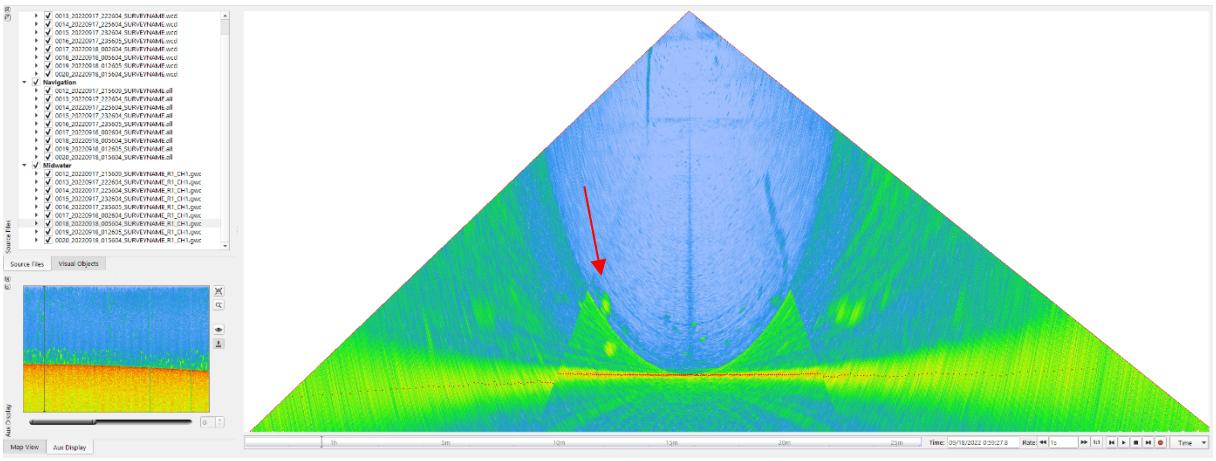

Figure 52. Gas flare 0018_4, 23.4 m high, medium confidence.

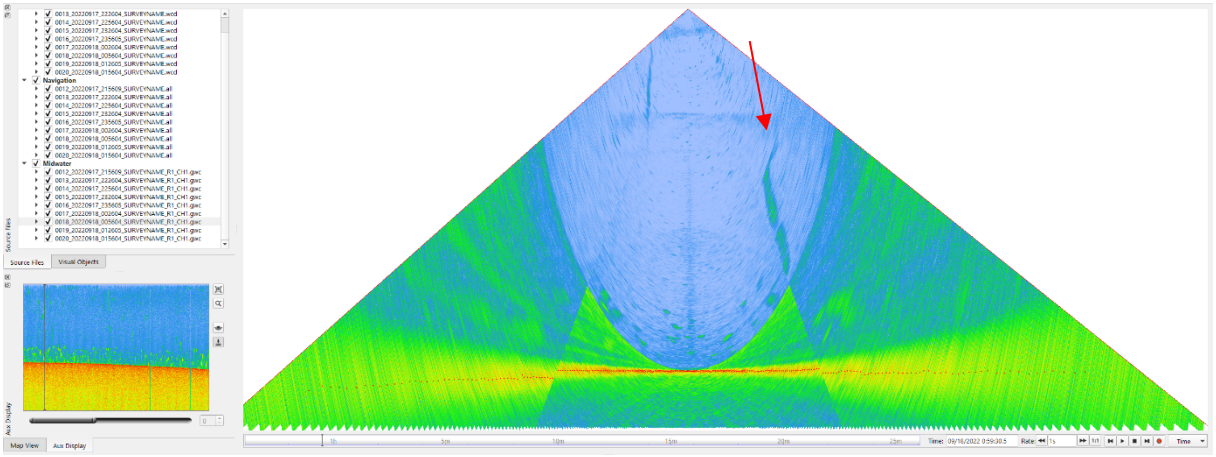

Figure 53. Gas flare 0018_5. 67.3 m high, medium confidence.

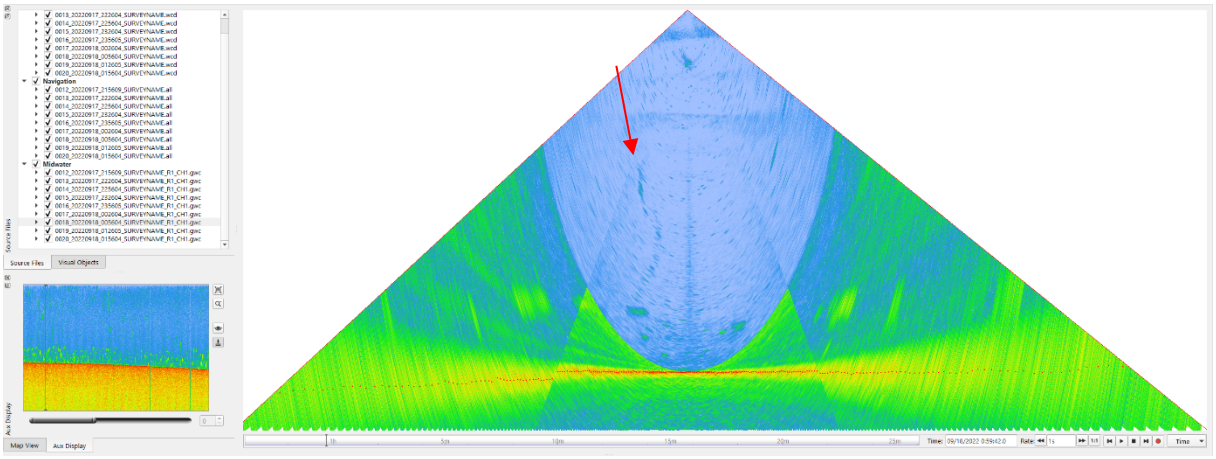

Figure 54. Gas flare 0018_6, 59.7 m high, medium confidence.

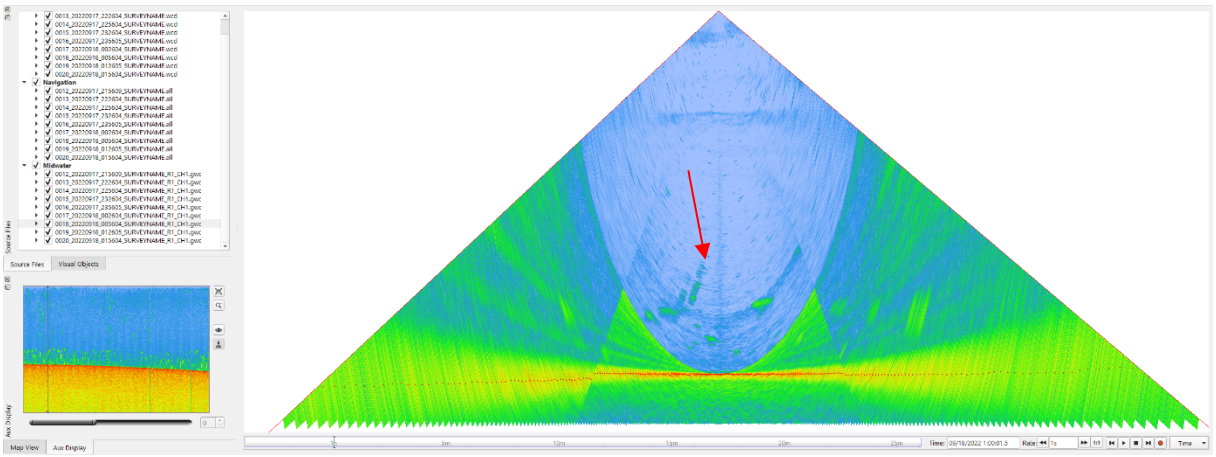

Figure 55. Gas flare 0018_7, 31.3 m high, medium confidence.

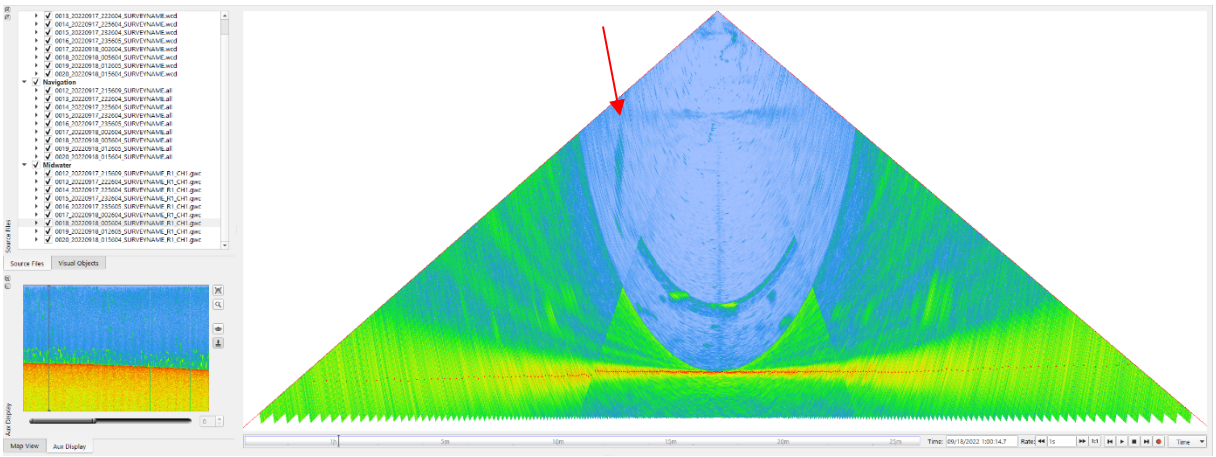

Figure 56. Gas flare 0018_8, 71.3 m high, medium confidence.

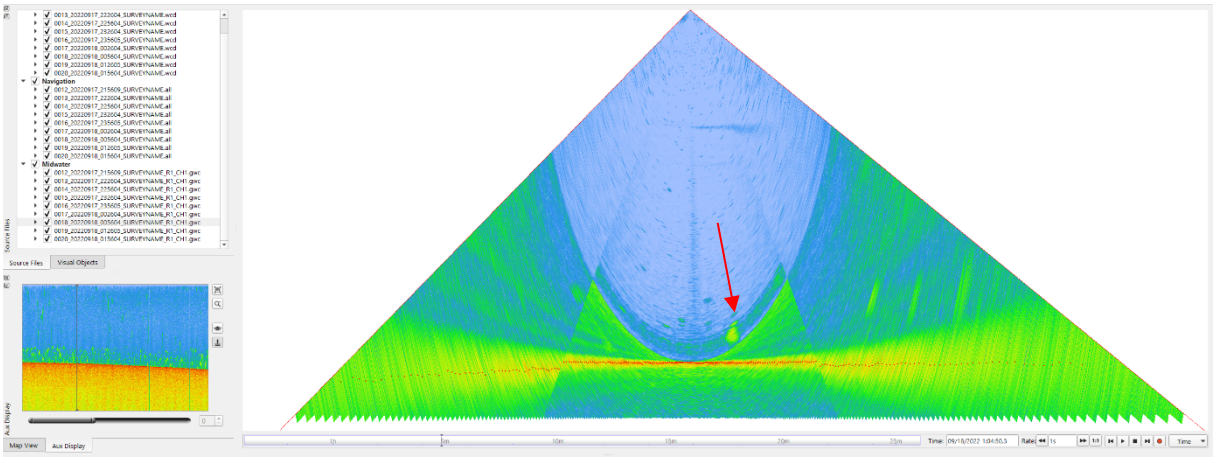

Figure 57. Gas flare 0018_11, 13.0 m high, high confidence.

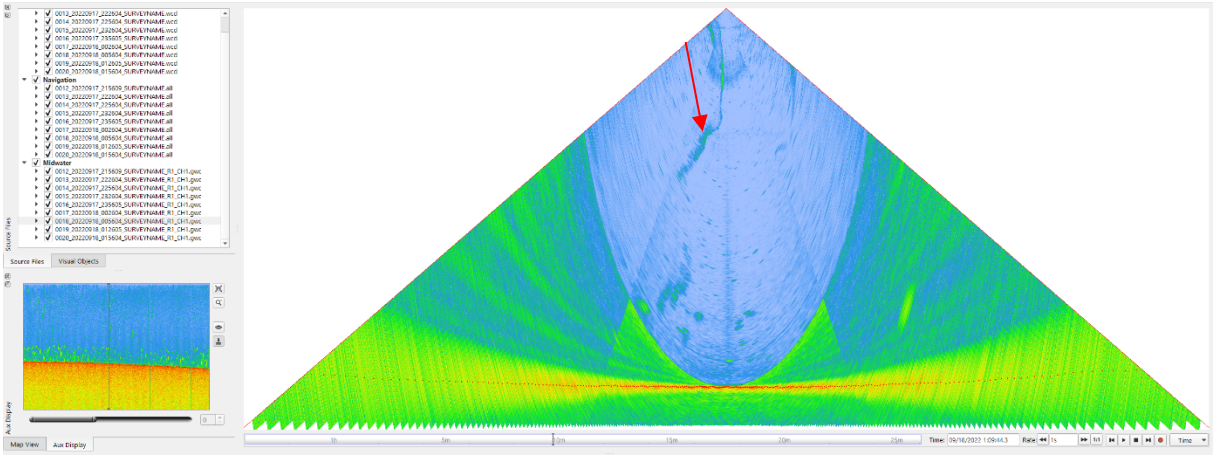

Figure 58. Gas flare 0018_13, 104.2 m high, medium confidence.

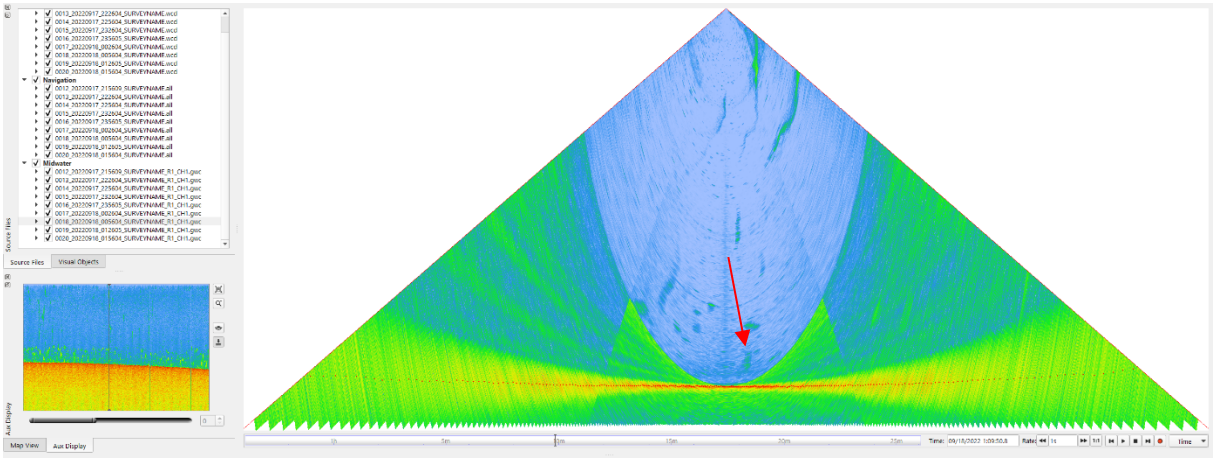

Figure 59. Gas flare 0018_14, 89.8 m high, high confidence.

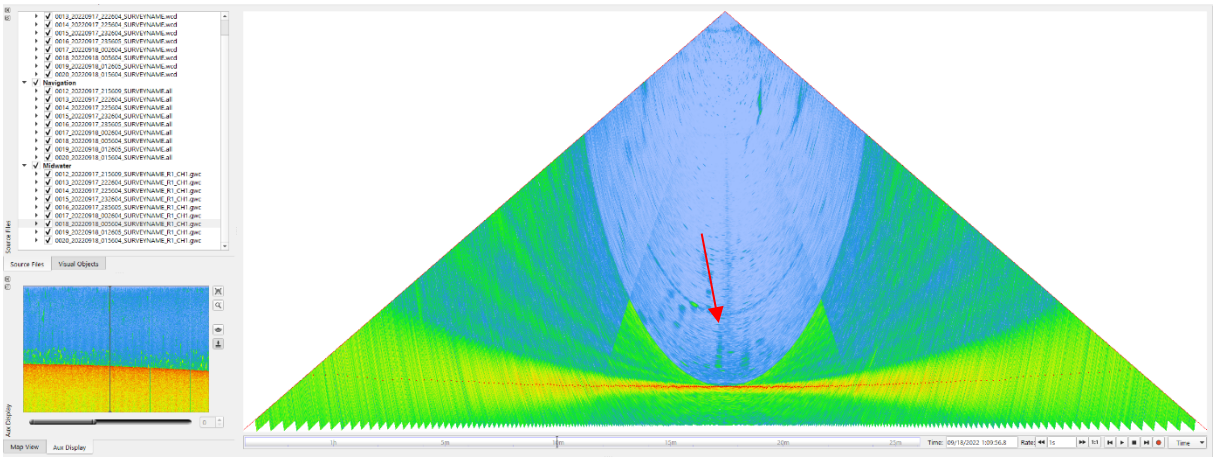

Figure 60. Gas flare 0018_15, 88.6 m high, high confidence.

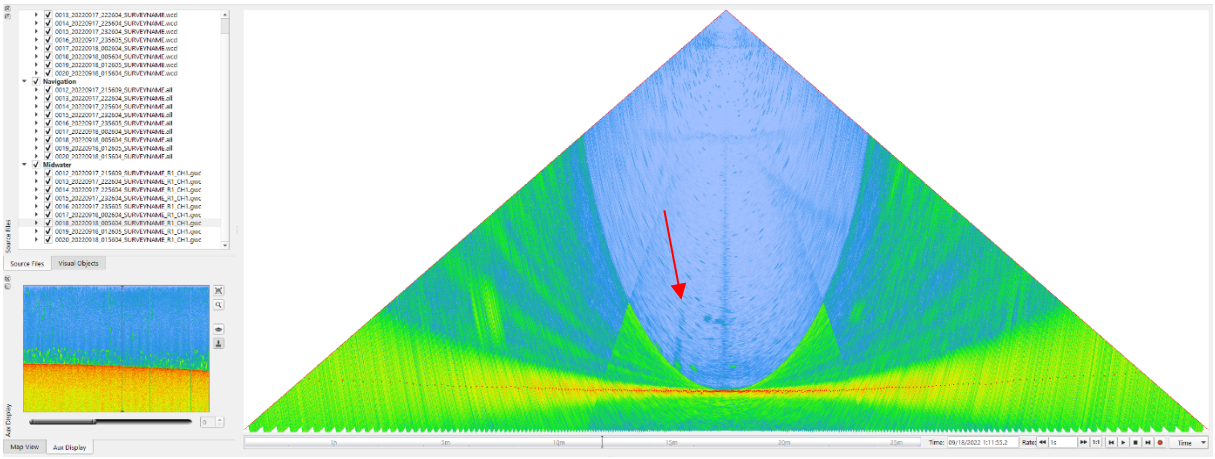

Figure 61. Gas flare 0018_17, 23.1 m high, high confidence.

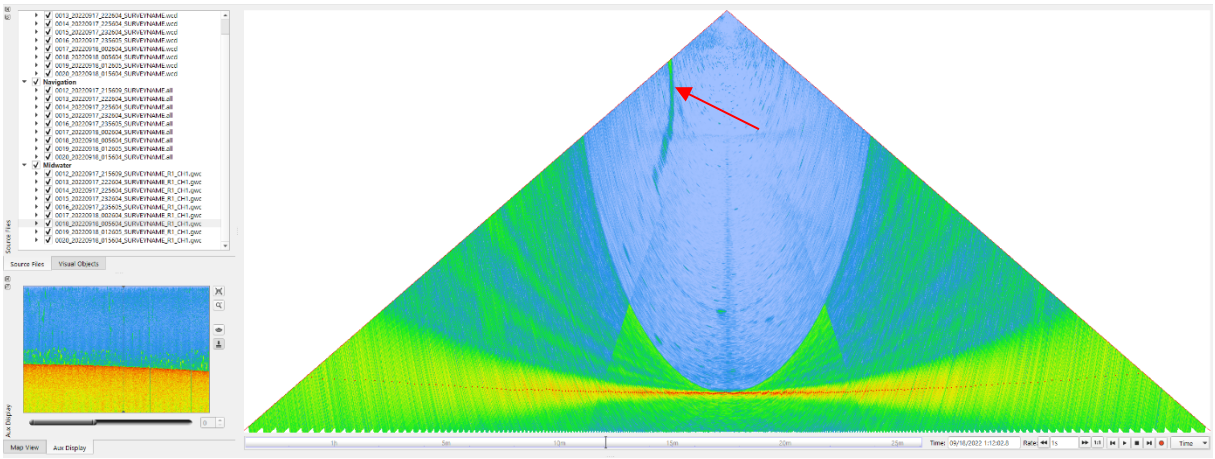

Figure 62. Gas flare 0018_18, 94.2 m high, medium confidence.

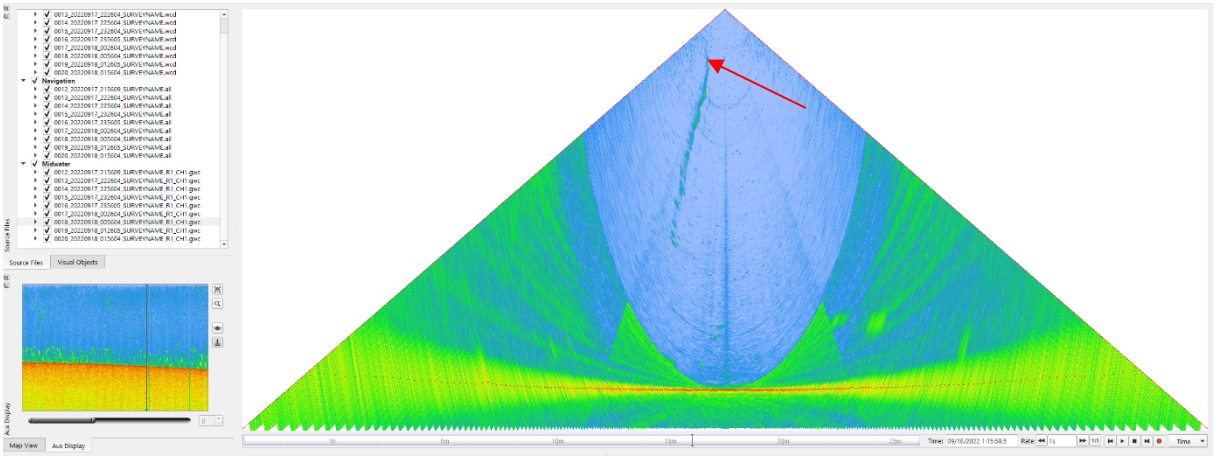

Figure 63. Gas flare 0018_19, 97.6 m high, medium confidence.

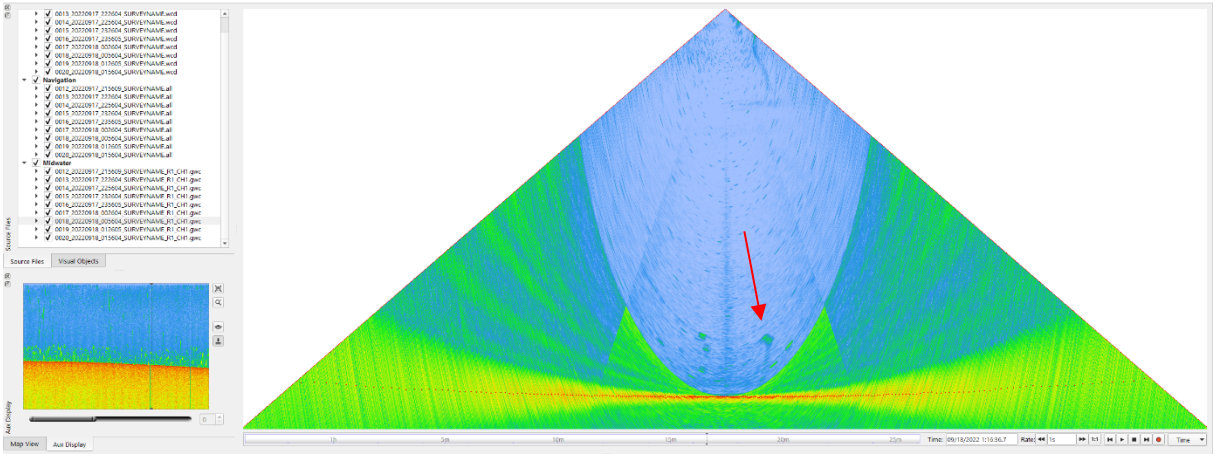

Figure 64. Gas flare 0018_20, 17.5 m high, high confidence.

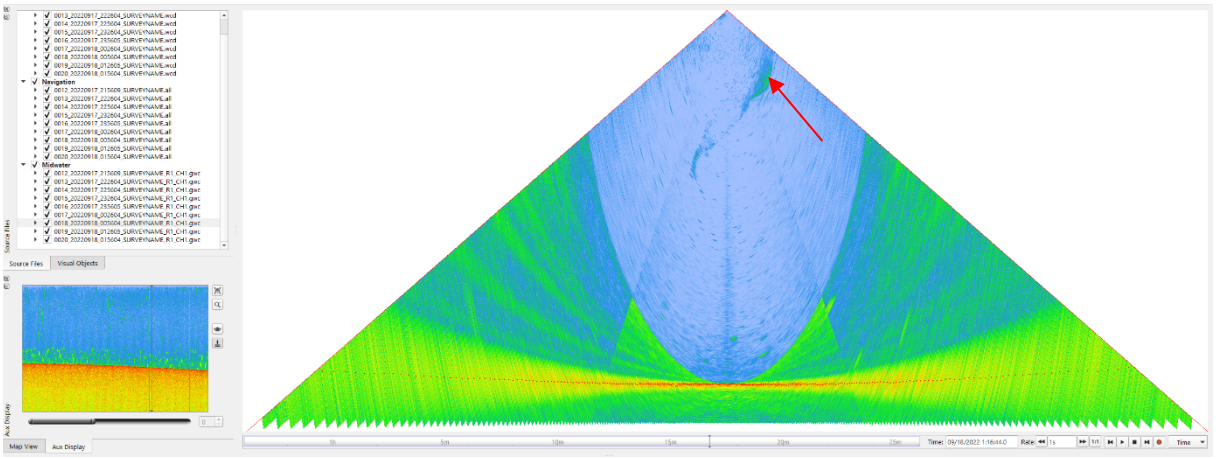

Figure 65. Gas flare 0018_21, 96.0 m high, medium confidence.

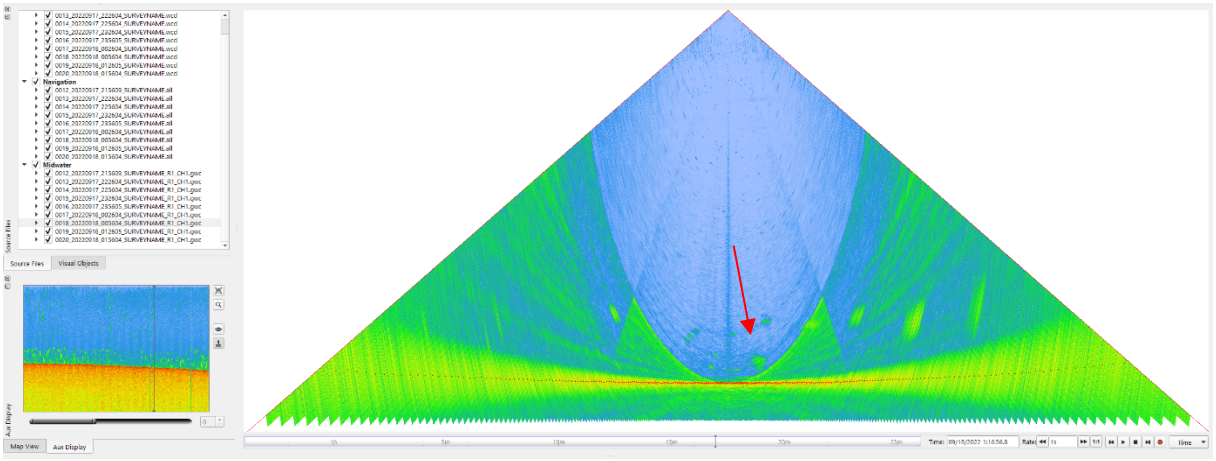

Figure 66. Gas flare 0018_22, 7.8 m high, medium confidence.

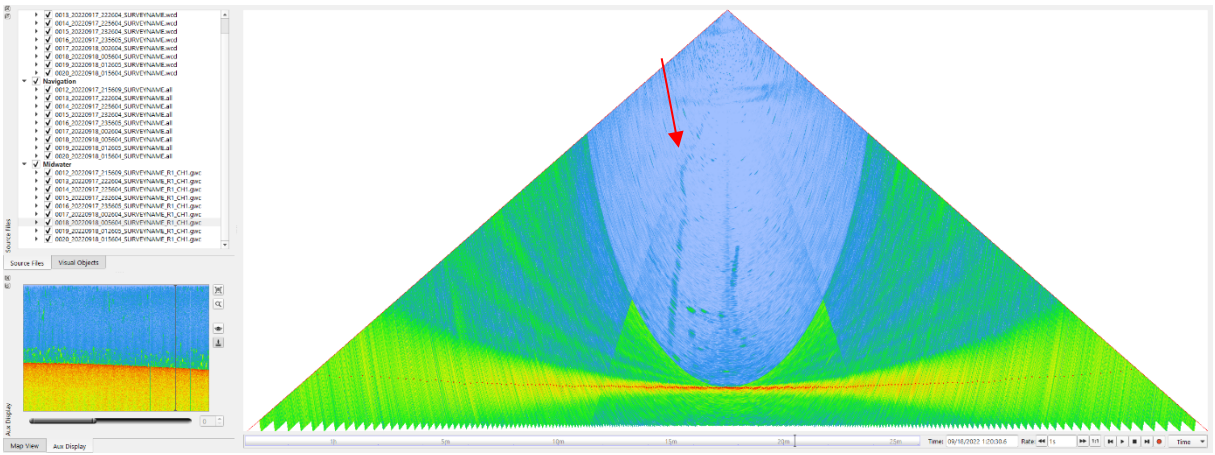

Figure 67. Gas flare 0018_24, 78.0 m high, high confidence.

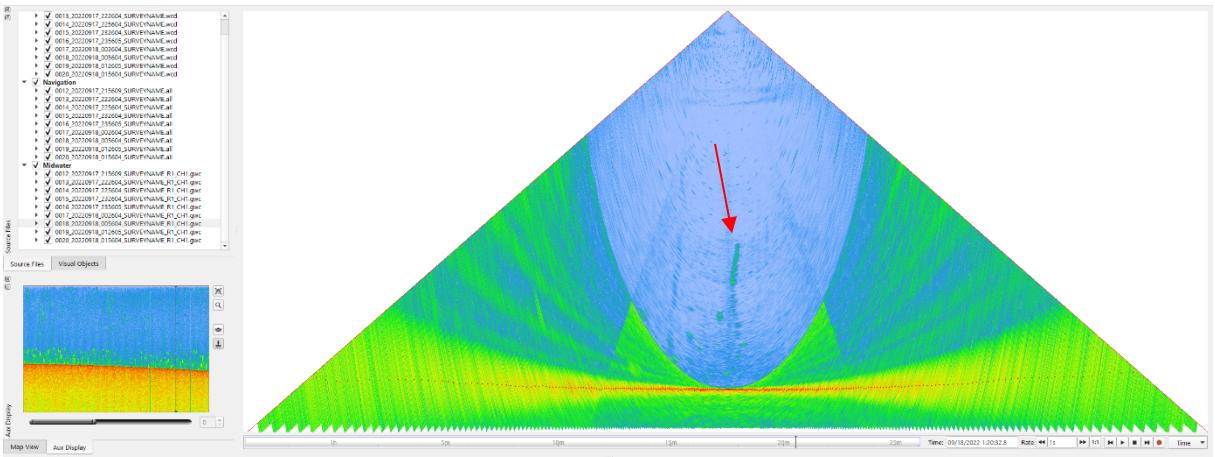

Figure 68. Gas flare 0018_25, 42.7 m high, high confidence.

Track 0019

Table 9. Gas flares from track 0016 (track ID 0019_20220918_012605).

Flare ID	Latitude	Longitude	Depth (m)	Height (m)	Time (UTC)	Position	Confidence
0019_1	48.60286208	-125.29884610	123.24	58.6	2022-09-18 1:31:49	centre	medium
0019_2	48.59066786	-125.30834207	130.53	91.7	2022-09-18 1:41:16	centre	medium
0019_3	48.58086434	-125.31548077	108.80	76.6	2022-09-18 1:48:48	centre	medium
0019_4	48.58095884	-125.31584060	109.07	40.9	2022-09-18 1:48:48	centre	medium
0019_5	48.58024095	-125.31452223	107.82	29.0	2022-09-18 1:49:02	port	medium
0019_6	48.57947457	-125.31772907	110.42	22.7	2022-09-18 1:50:03	centre	medium
0019_7	48.57116778	-125.32290112	110.44	30.9	2022-09-18 1:56:02	centre	medium

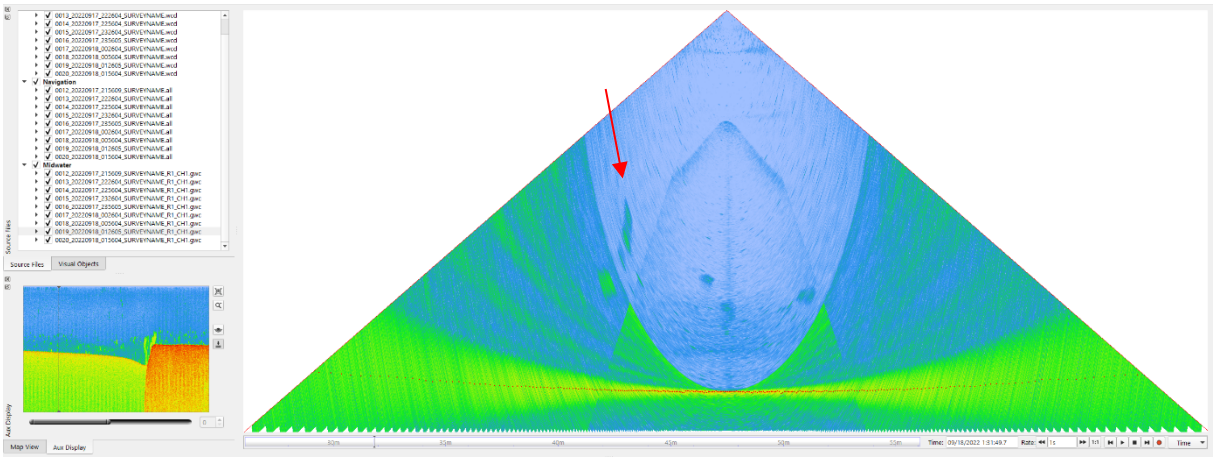

Figure 69. Gas flare 0019_1, 58.6 m high, medium confidence.

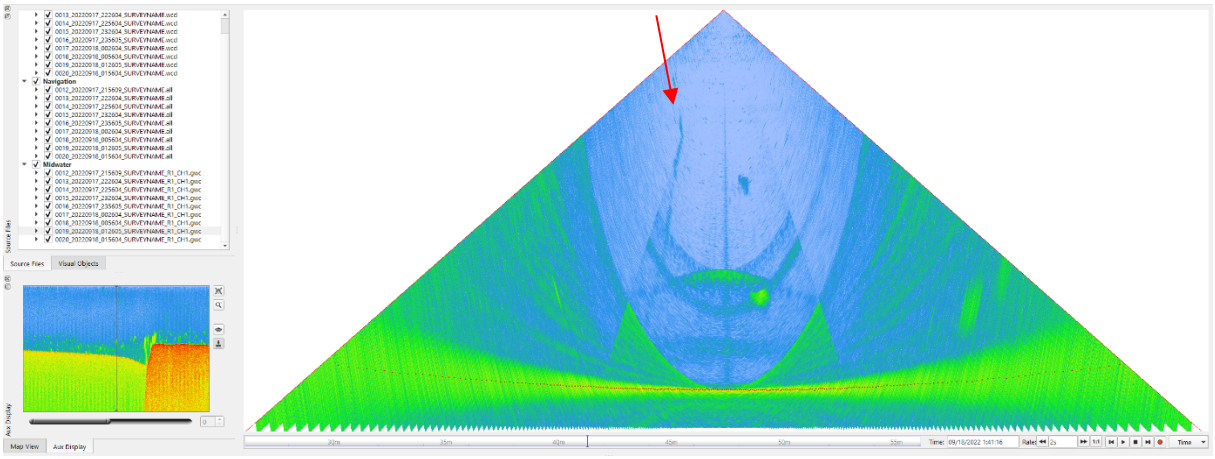

Figure 70. Gas flare 0019_2, 91.7 m high, medium confidence.

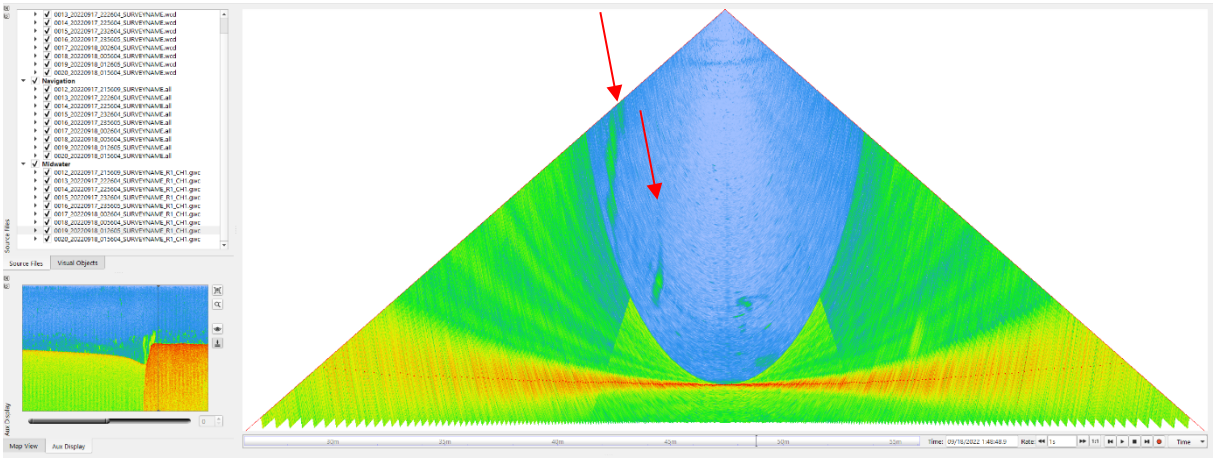

Figure 71. Gas flare 0019_3 (left), 76.6 m high, medium confidence, and gas flare 0019_4 (right), 40.9 m high, medium confidence.

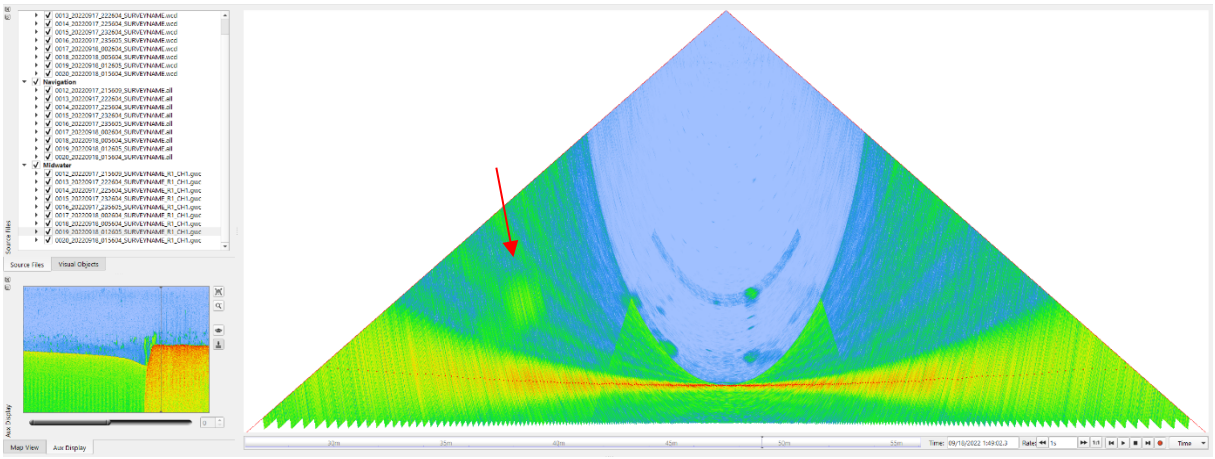

Figure 72. Gas flare 0019_5, 29.0 m high, medium confidence. Signal range decreased to improve image.

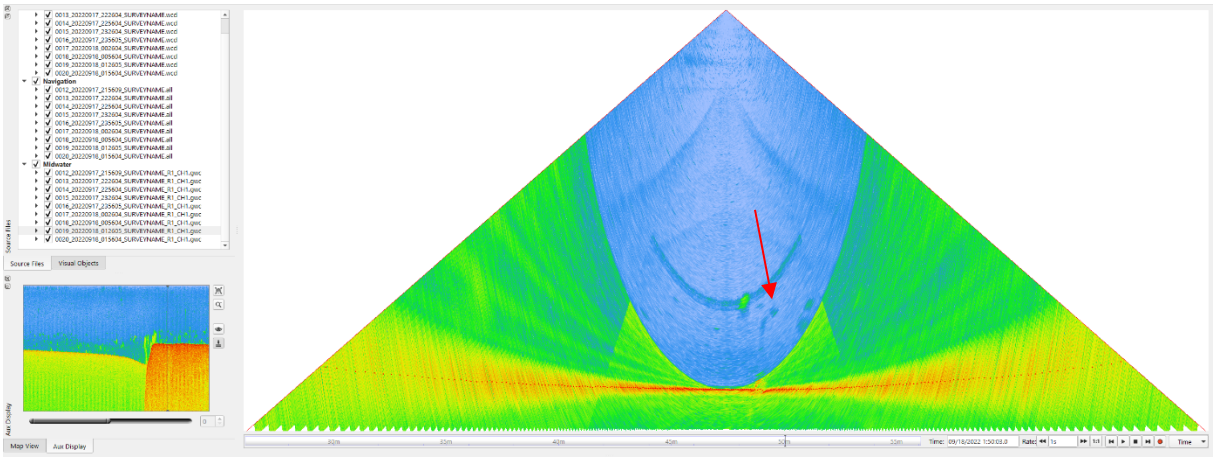

Figure 73. Gas flare 0019_6, 22.7 m high, medium confidence.

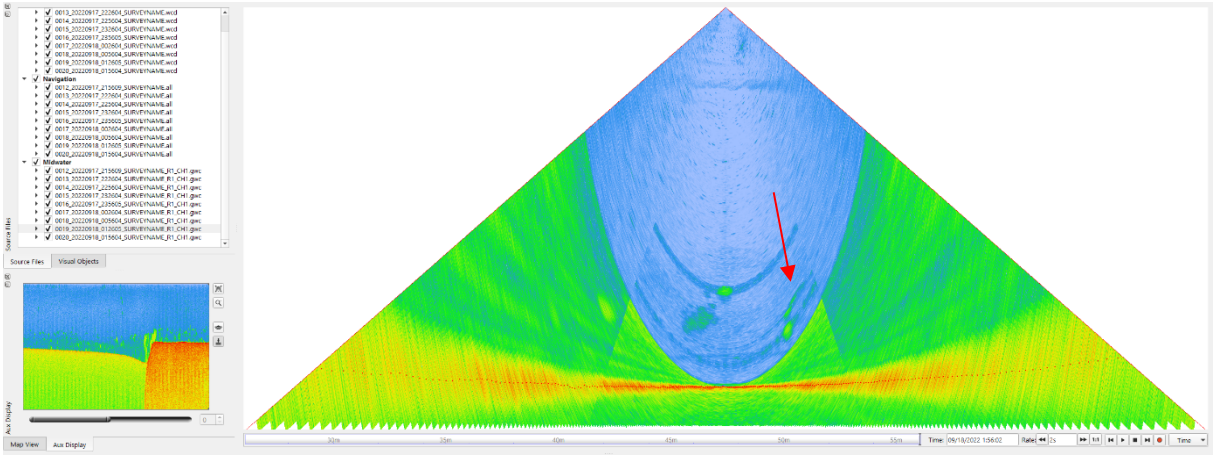

Figure 74. Gas flare 0019_7, 30.9 m high, medium confidence.

Track 0020

Table 10. Gas flares from track 0020 (track ID 0020_20220918_015604).

Flare ID	Latitude	Longitude	Depth (m)	Height (m)	Time (UTC)	Position	Confidence
0020_1	48.56883101	-125.32422737	110.88	59.3	2022-09-18 1:57:39	centre	medium
0020_2	48.56860630	-125.32389776	111.60	53.8	2022-09-18 1:57:46	centre	high
0020_3	48.56826255	-125.32363225	111.23	8.0	2022-09-18 1:57:59	centre	high
0020_4	48.56733557	-125.32328964	111.21	34.1	2022-09-18 1:58:38	centre	high
0020_5	48.56717386	-125.32382548	112.03	77.0	2022-09-18 1:58:45	centre	high
0020_6	48.56352074	-125.32075971	110.36	32.6	2022-09-18 2:01:27	port	low
0020_7	48.56160691	-125.32243128	113.72	43.2	2022-09-18 2:02:34	centre	medium
0020_8	48.56137886	-125.32248498	113.82	93.4	2022-09-18 2:02:43	centre	medium
0020_9	48.56069245	-125.32221314	113.55	86.3	2022-09-18 2:03:07	centre	medium
0020_10	48.56045382	-125.32326028	114.66	62.2	2022-09-18 2:03:22	centre	high
0020_11	48.56022504	-125.32341438	115.00	62.4	2022-09-18 2:03:33	centre	high
0020_12	48.56028078	-125.32373007	115.00	44.9	2022-09-18 2:03:33	centre	high
0020_13	48.55767693	-125.32389589	116.79	32.1	2022-09-18 2:05:17	port	medium
0020_15	48.53837334	-125.34612762	145.38	95.7	2022-09-18 2:22:19	centre	medium

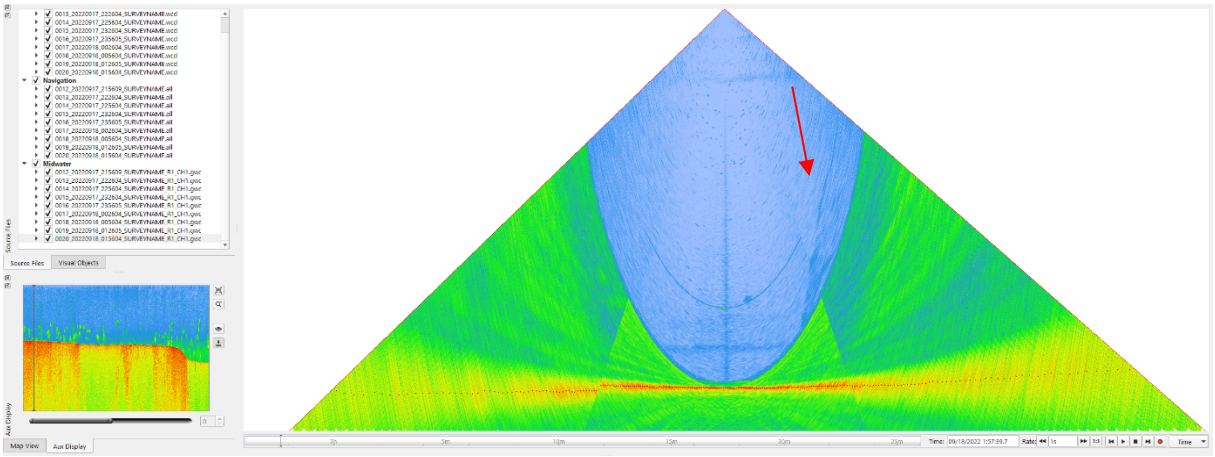

Figure 75. Gas flare 0020_1, 59.3 m high, medium confidence.

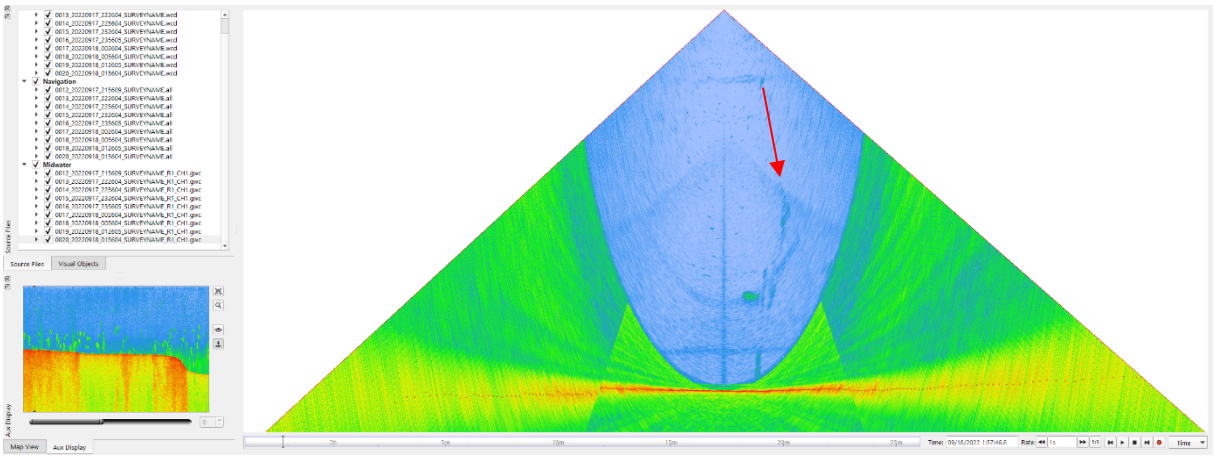

Figure 76. Gas flare 0020_2, 53.8 m high, high confidence.

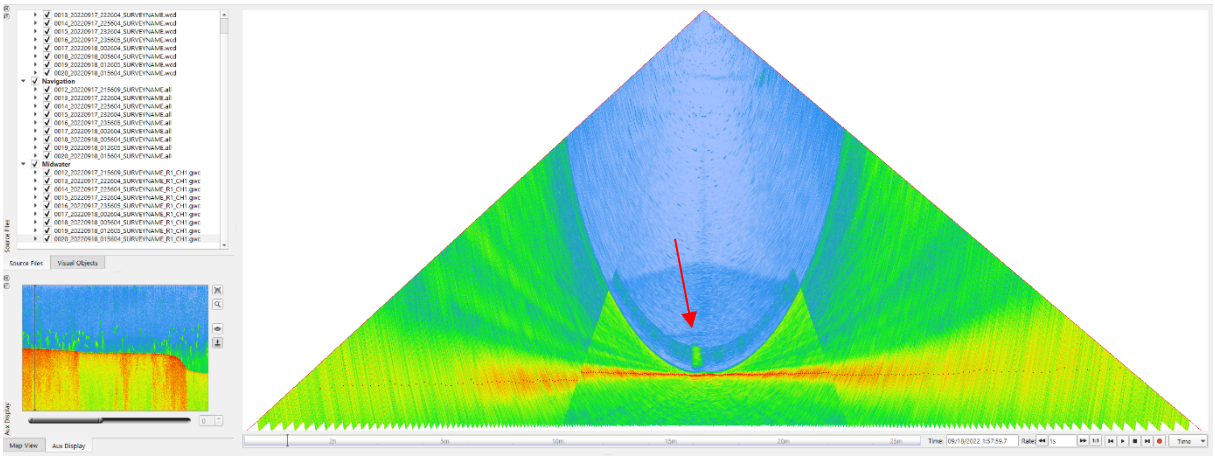

Figure 77. Gas flare 0020_3, 8.0 m high, high confidence.

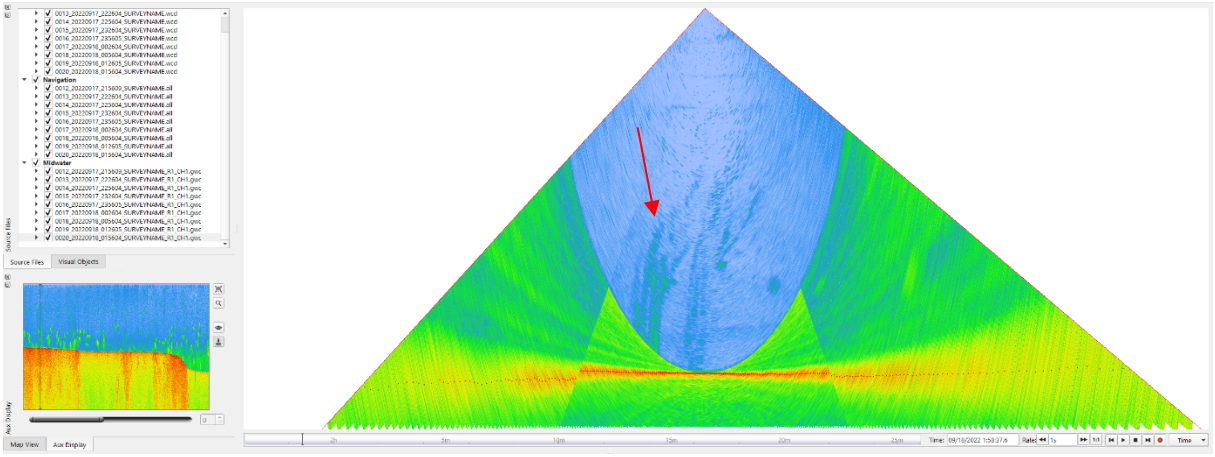

Figure 78. Gas flare 0020_4, 34.1 m high, high confidence.

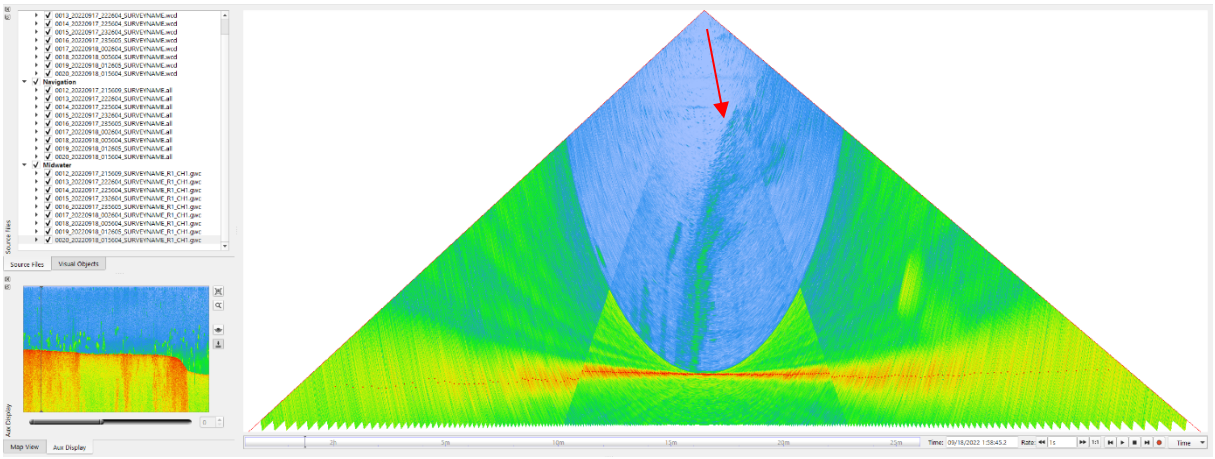

Figure 79. Gas flare 0020_5, 77.0 m high, high confidence.

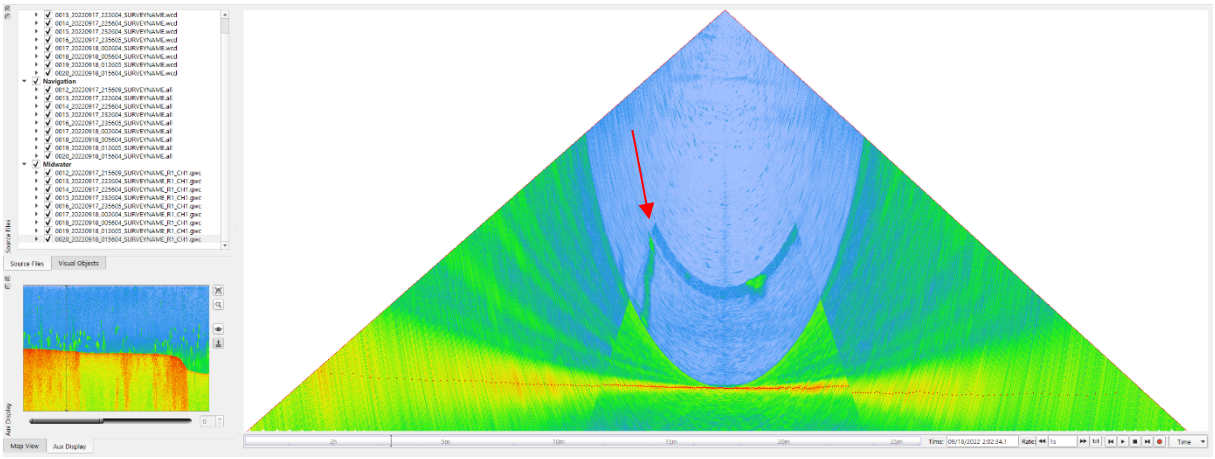

Figure 80. Gas flare 0020_7, 43.2 m high, medium confidence.

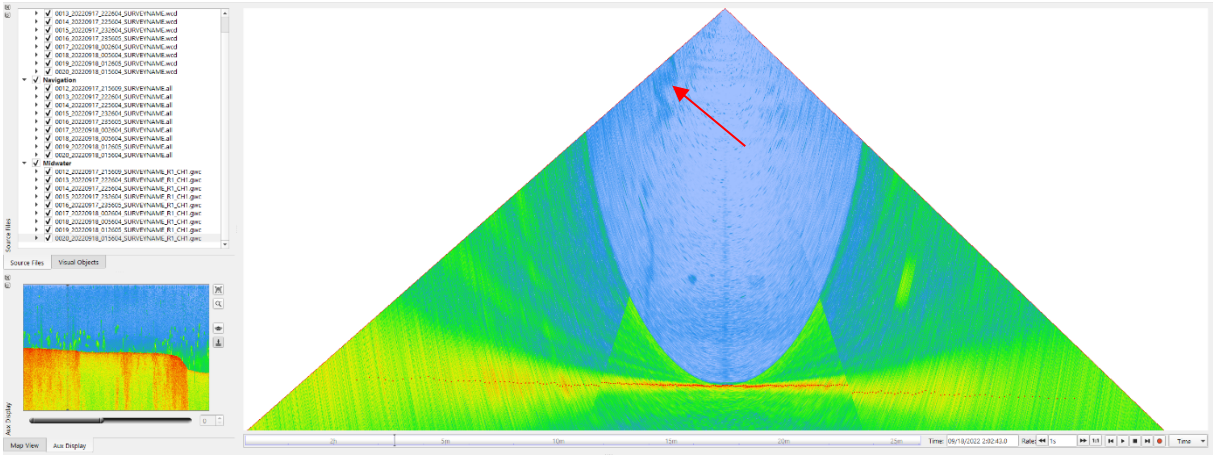

Figure 81. Gas flare 0020_8, 93.4 m high, medium confidence.

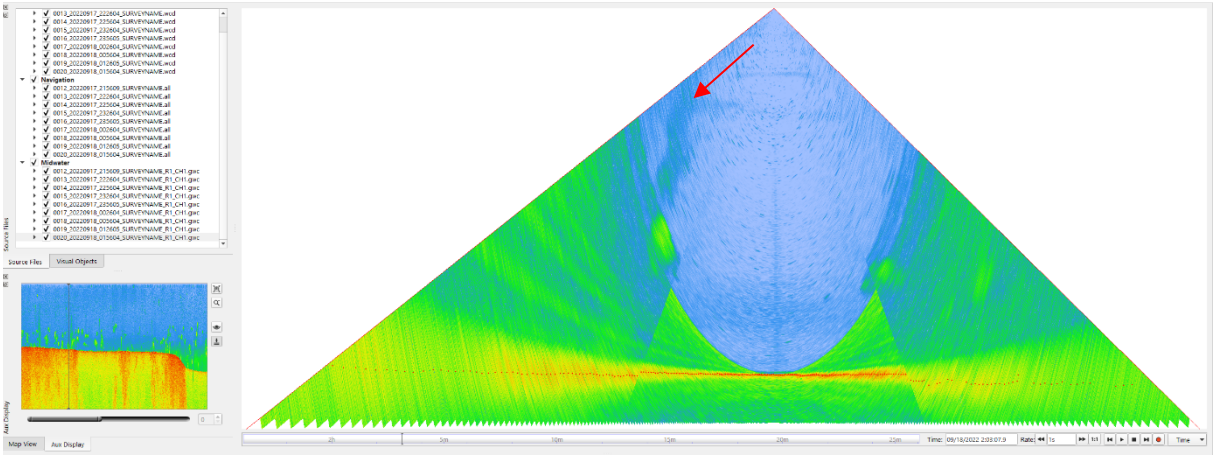

Figure 82. Gas flare 0020_9, 86.3 m high, medium confidence.

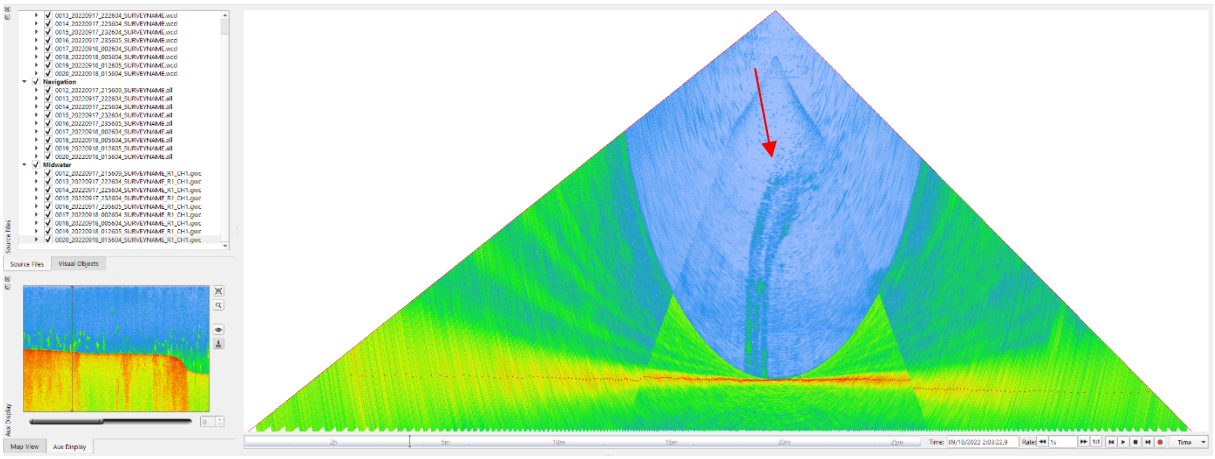

Figure 83. Gas flare 0020_10, 62.2 m high, high confidence.

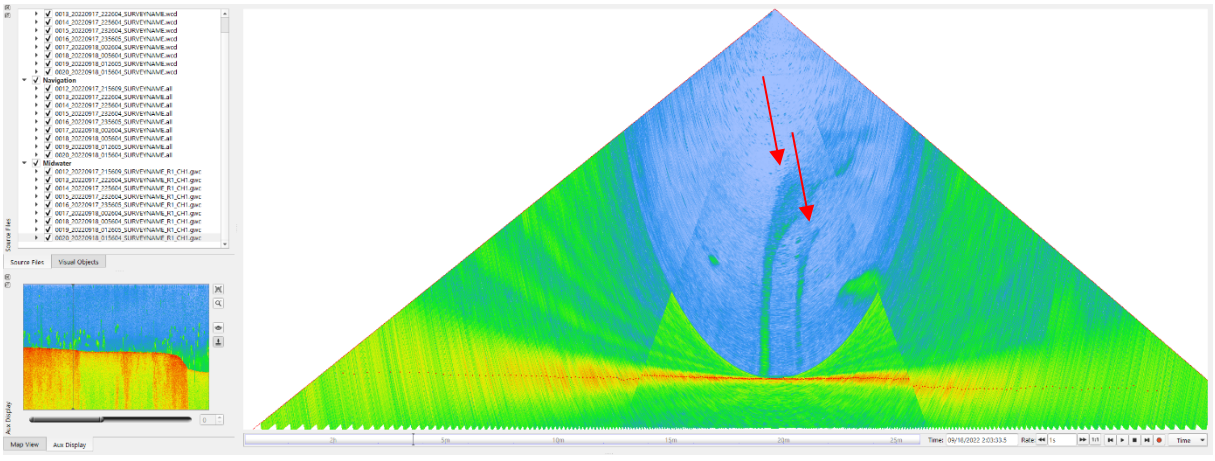

Figure 84. Gas flare 0020_11 (left), 62.4 m high, high confidence, and gas flare 0020_12 (right), 44.9 m high, high confidence.

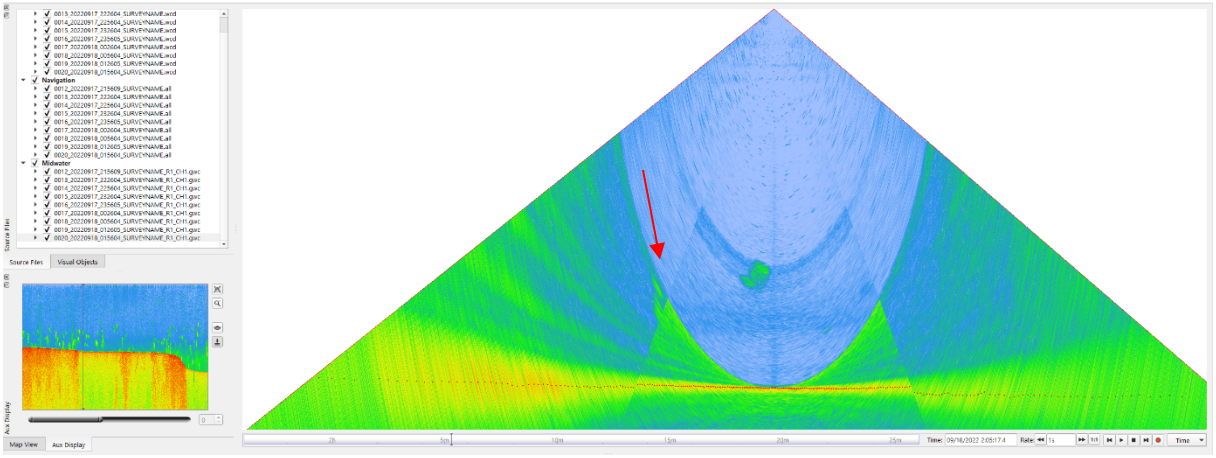

Figure 85. Gas flare 0020_13, 32.1 m high, medium confidence.

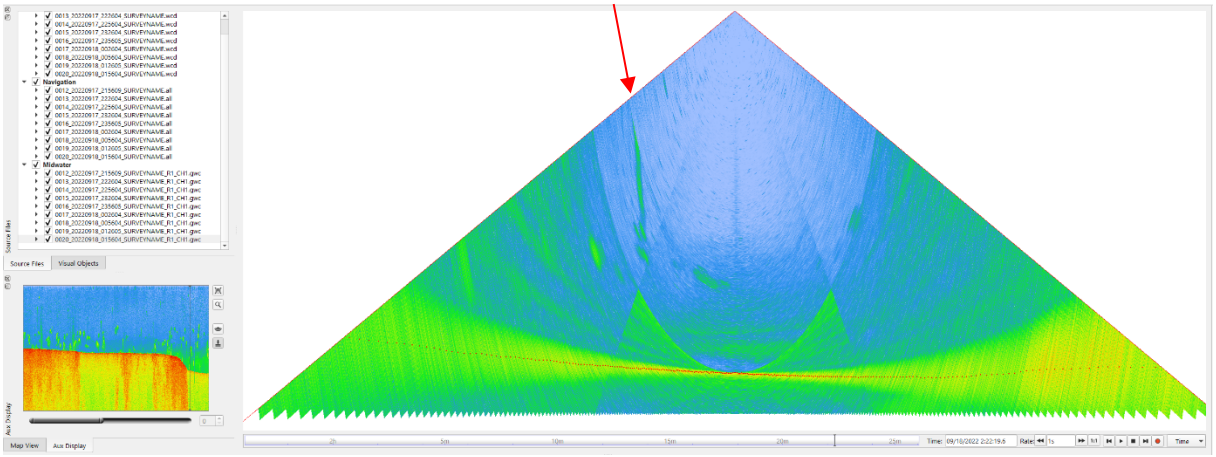

Figure 86. Gas flare 0020_15, 95.7 m high, medium confidence.

Track 0021

Table 11. Gas flare from track 0021 (track ID 0021_20220918_022604).

Flare ID	Latitude	Longitude	Depth (m)	Height (m)	Time (UTC)	Position	Confidence
0021_1	48.52901789	-125.35694275	152.29	116.2	2022-09-18 2:29:59	centre	medium

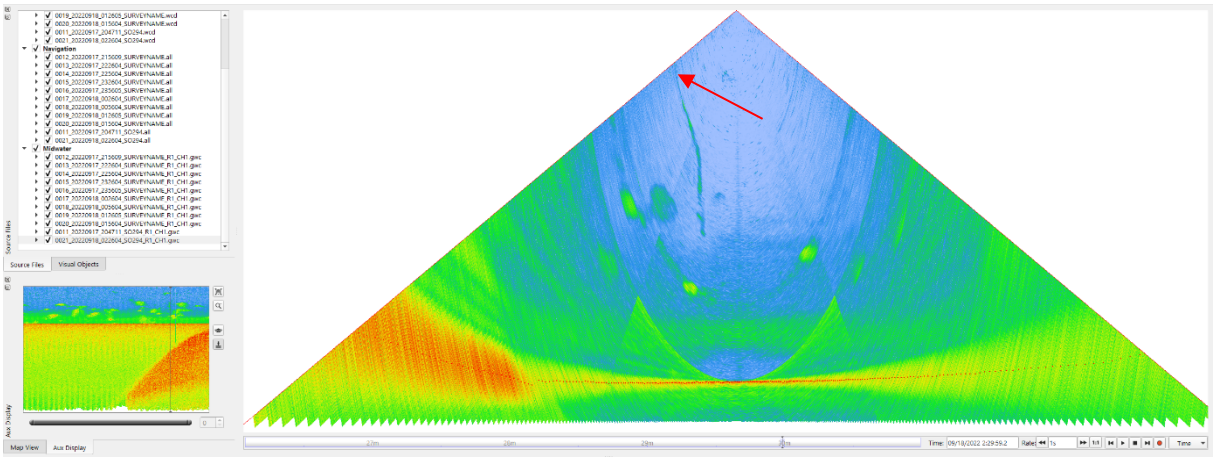

Figure 87. Gas flare 0021_1, 116.2 m high, medium confidence.

Noise and fish

Table 12. High strength anomalies interpreted to be fish, marine mammals and plankton.

Flare ID	Latitude	Longitude	Depth (m)	Height (m)	Time (UTC)	Position
0015_2	48.57526888	-125.10005315	123.92	29.1	2022-09-17 23:29:41	centre
0015_10	48.58866937	-125.12840788	108.03	18.2	2022-09-17 23:45:29	centre
0016_5	48.60229677	-125.15948547	110.64	19.4	2022-09-18 0:03:01	centre
0016_9	48.60306999	-125.16312622	110.82	13.4	2022-09-18 0:04:46	centre
0016_11	48.60449189	-125.16544757	110.61	18.7	2022-09-18 0:06:14	centre
0016_15	48.60582556	-125.16938811	110.61	2.7	2022-09-18 0:08:19	centre
0016_20	48.61022648	-125.18129563	109.16	13.9	2022-09-18 0:14:47	centre
0016_21	48.60973437	-125.18174577	108.62	17.9	2022-09-18 0:14:47	port
0016_22	48.61092351	-125.18233201	109.06	20.0	2022-09-18 0:15:28	centre
0016_23	48.60974706	-125.18397631	107.92	27.8	2022-09-18 0:15:40	port
0016_24	48.61014670	-125.18359700	108.70	22.9	2022-09-18 0:15:40	port
0016_25	48.61192739	-125.18190684	108.57	19.7	2022-09-18 0:15:40	starboard
0016_27	48.61147977	-125.18353366	109.80	16.3	2022-09-18 0:16:09	centre
0016_31	48.61287400	-125.18774617	109.32	10.5	2022-09-18 0:18:22	centre
0016_33	48.61572796	-125.19424537	109.31	15.9	2022-09-18 0:22:05	centre
0017_5	48.62257852	-125.21295054	110.20	6.7	2022-09-18 0:32:07	port
0017_6	48.62299202	-125.21255799	109.68	9.0	2022-09-18 0:32:07	centre
0017_13	48.63118910	-125.23193818	110.57	4.3	2022-09-18 0:43:00	centre
0018_12	48.63404401	-125.27453635	113.81	29.3	2022-09-18 1:07:55	port
0018_16	48.62979125	-125.27929100	114.32	6.5	2022-09-18 1:11:24	centre
0020_14	48.54507238	-125.34051245	120.10	25.8	2022-09-18 2:17:15	centre

Flares with Overlap

Table 13. Identified flares in SO294 that overlap with previously located flares within the footprint of the multibeam sonar. F = Flares located by the CCGS Franklin 2022 expedition, and R = Flares located by Riedel et al. (2018).

Flare ID	Longitude	Latitude	Depth (m)	Height (m)	Time (UTC)	Position	Confidence	Overlap with sonar footprint (F=CCGS Franklin cruise, R=Riedel et al. (2018) compilation)
0014_1	-125.037842	48.557231	-70.98	23.0	2022-09-17 22:58:19	centre	high	F
0014_3	-125.086790	48.569851	-118.46	34.5	2022-09-17 23:22:48	centre	medium	F
0014_4	-125.087295	48.570239	-120.64	66.1	2022-09-17 23:23:08	centre	high	F
0014_5	-125.089949	48.571051	-126.55	69.9	2022-09-17 23:24:25	centre	medium	F
0015_11	-125.144474	48.594192	-112.89	29.6	2022-09-17 23:53:58.2	port	medium	F
0015_5	-125.113126	48.582285	-105.88	45.7	2022-09-17 23:37:13	centre	low	R
0016_10	-125.163000	48.603698	-110.78	12.2	2022-09-18 0:04:57.4	centre	low	F
0016_12	-125.167760	48.604930	-110.33	10.4	2022-09-18 0:07:20.4	centre	low	F
0016_2	-125.151455	48.598911	-111.69	20.1	2022-09-17 23:58:31.7	centre	high	F
0016_32	-125.193539	48.615583	-108.86	11.1	2022-09-18 0:21:45	centre	low	F
0016_34	-125.196114	48.616400	-109.11	6.2	2022-09-18 0:23:06	centre	low	F
0016_7	-125.162730	48.602021	-110.56	24.3	2022-09-18 0:04:12.2	port	medium	F
0016_8	-125.163579	48.602590	-109.87	20.0	2022-09-18 0:04:46.1	port	low	F
0017_22	-125.253826	48.640566	-110.55	9.4	2022-09-18 0:55:54.0	centre	high	F
0018_1	-125.259143	48.640277	-110.91	96.6	2022-09-18 0:58:32.8	centre	medium	F
0018_10	-125.269873	48.638627	-111.60	19.7	2022-09-18 1:03:50.6	centre	low	F
0018_11	-125.272033	48.638179	-112.27	13	2022-09-18 1:04:50.3	centre	high	F
0018_13	-125.277177	48.631854	-112.71	104.2	2022-09-18 1:09:44.3	centre	medium	R
0018_14	-125.278059	48.631962	-113.78	89.8	2022-09-18 1:09:50.8	centre	high	R
0018_15	-125.277916	48.631750	-113.75	88.6	2022-09-18 1:09:56.8	centre	high	R
0018_19	-125.283613	48.623642	-115.33	97.6	2022-09-18 1:15:58.5	centre	medium	R
0018_2	-125.260318	48.640793	-110.98	90.5	2022-09-18 0:59:04.4	centre	medium	F
0018_20	-125.285107	48.623074	-115.82	17.5	2022-09-18 1:16:36.7	centre	high	R

0018_21	-125.284846	48.622790	-116.29	96	2022-09-18 1:16:44.0	centre	medium	R
0018_22	-125.285408	48.622622	-115.97	7.8	2022-09-18 1:16:56.8	centre	medium	R
0018_23	-125.286867	48.621746	-116.11	44.6	2022-09-18 1:17:45.2	centre	low	R
0019_3	-125.315481	48.580864	-108.80	76.6	2022-09-18 1:48:48.9	centre	medium	F
0019_4	-125.315841	48.580959	-109.07	40.9	2022-09-18 1:48:48.9	centre	medium	F
0019_5	-125.314522	48.580241	-107.82	29	2022-09-18 1:49:02.3	port	medium	F
0019_6	-125.317729	48.579475	-110.42	22.7	2022-09-18 1:50:03.0	centre	medium	F
0019_7	-125.322901	48.571168	-110.44	30.9	2022-09-18 1:56:02.9	centre	medium	R
0020_1	-125.324227	48.568831	-110.88	59.3	2022-09-18 1:57:39.7	centre	medium	F,R
0020_10	-125.323260	48.560454	-114.66	62.2	2022-09-18 2:03:22.9	centre	high	F,R
0020_11	-125.323414	48.560225	-115.00	62.4	2022-09-18 2:03:33.5	centre	high	F,R
0020_12	-125.323730	48.560281	-115.00	44.9	2022-09-18 2:03:33.5	centre	high	F,R
0020_13	-125.323896	48.557677	-116.79	32.1	2022-09-18 2:05:17.4	port	medium	F,R
0020_2	-125.323898	48.568606	-111.60	53.8	2022-09-18 1:57:46.8	centre	high	F,R
0020_3	-125.323632	48.568263	-111.23	8	2022-09-18 1:57:59.7	centre	high	F,R
0020_4	-125.323290	48.567336	-111.21	34.1	2022-09-18 1:58:38.6	centre	high	F,R
0020_5	-125.323825	48.567174	-112.03	77	2022-09-18 1:58:45.2	centre	high	F,R
0020_6	-125.320760	48.563521	-110.36	32.6	2022-09-18 2:01:27.1	port	low	F
0020_7	-125.322431	48.561607	-113.72	43.2	2022-09-18 2:02:34.1	centre	medium	F,R
0020_8	-125.322485	48.561379	-113.82	93.4	2022-09-18 2:02:43.0	centre	medium	F,R
0020_9	-125.322213	48.560692	-113.55	86.3	2022-09-18 2:03:07.9	centre	medium	F,R

Conclusion

Active venting is widespread in the Swiftsure Bank survey area, with a total of 109 mapped gas flares. This collection of data can be used for future cold seep studies on Swiftsure Bank and will be added into the review of the area for potential marine conservation.

Acknowledgements

We acknowledge the Pacheedaht First Nation, Ditidaht First Nation, Huu-ay-aht First Nations, Maa-nulth Treaty Nations, and Nuu-chah-nulth Tribal Council Nations on whose marine traditional territories we conducted our scientific survey.

We thank Captain Tilo Birnbaum and the crew of the RV Sonne for their part in the safe operation of the ship without which this survey could not have been a success.

We thank GEOMAR Helmholtz Research Institute for allowing this survey to happen on transit during their larger program. The cruise and scientific work were financed by the Federal Ministry of Education and Research (BMBF) under grants 03G0294A (CLOCKS), with extra funding and use of large-scale equipment from GEOMAR. Additional funding was provided through the Japan Society for the promotion of Science (JSPS), Japan Agency for Marine-Earth Science and Technology (JAMSTEC), University of Tokyo, Kobe University, Geological Survey of Canada (Public Safety Geoscience Program), Ocean Networks Canada, and the University of Alberta for the land MT-Program.

This work was completed under the Marine Geoscience for Marine Spatial Planning and the Public Safety Geoscience programs.

References

DFO. 2018. Assessment of Canadian Pacific Cold Seeps against Criteria for Determining Ecologically and Biologically Significant Areas. DFO Can. Sci. Advis. Sec. Sci. Resp. 2018/002.

Dıaz-del-Rıo, V., Somoza, L., Martınez-Frias, J., Mata, M.P., Delgado, A., Hernandez-Molina, F.J., Lunar, R., Martın-Rubı, J.A., Maestro, A., Fernández-Puga, M.C. and León, R., 2003. Vast fields of hydrocarbon-derived carbonate chimneys related to the accretionary wedge/olistostrome of the Gulf of Cádiz. *Marine geology*, *195*(1-4), pp.177-200.

Johns, M.J., Trotter, J.A., Barnes, C.R. and Narayan, Y.R., 2012. Biostratigraphic, strontium isotopic, and geologic constraints on the landward movement and fragmentation of terranes within the Tofino Basin, British Columbia. *Canadian Journal of Earth Sciences*, *49*(7), pp.819-856.

Luternauer, J.L., Linden, R.H., Westrheim, S.J. and Thomson, R.E., 1986. Sedimentology of amphitrite bank, a commercially exploited groundfish habitat—Southwestern continental shelf, British Columbia, Canada. *Environmental Geology and Water Sciences*, *8*(3), pp.107-121.

Riedel, M., Scherwath, M., Römer, M., Veloso, M., Heesemann, M., Spence, G.D. 2018. Distributed natural gas venting offshore along the Cascadia margin. *Nature Communications.* (2018)9:3264. DOI: 10.1038/s41467-018-05736-x.

Römer, M., Riedel, M., Scherwath, M., Heesemann, M. & Spence, G. D. Tidally controlled gas bubble emissions: A comprehensive study using long-term monitoring data from the NEPTUNE cabled observatory offshore Vancouver Island. Geochem. Geophys. Geosyst. 17, 3797–3814 (2016).

Quality Positioning Services. 2018. Fledermaus v7.8 Manual. pp.560

Yorath, C.J., 1980. The Apollo structure in Tofino basin, Canadian Pacific continental shelf. *Canadian Journal of Earth Sciences*, *17*(6), pp.758-775.

Appendix A

CCGS Franklin 2022002PGC water column survey observations using EK60 Echosounder

Date	Time (UTC)	Latitude	Longitude	Depth (m)	Top (m)	Bottom (m)	flare height vertical (m above seabed)	Intensity (dense/ diffuse)	Orientation (vertical/ incline/ T-shape)	Seabed (flat/ridge/ depression)	Bottom hardness	Comments
2022-04-11	19:32	48.584000	-125.105267				attached (30 m)		vertical			SOL line 2. Just before this, we see a vertical line @ 1926 that looks "Plume-like". It's connected to the seabed, vertical.
2022-04-11	19:53	48.573200	-125.164300									Just before this timestamp, we see activity at seafloor. Attached bulbous feature. Preceding it, we see undulating lower water column activity. Following it, we see continued activity extending ~20-25 m into water column. Position from ship's GPS log.
2022-04-11	19:56	48.571000	-125.171083									Whale seen ~ 1/2 mile heading in direction away from ship and route. Going with whale wise guidelines, we continued while bridge keeping watch. Position from ship's GPS log.
2022-04-11	20:39	48.514300	-125.253333									Continued plume activity at bottom, extending ~25 m into water column. Position from ship's GPS log.
2022-04-11	21:00	48.478117	-125.321067									MS70 showing more plume-like structure
2022-04-11	21:40	48.447633	-125.392183									We see more linear flares on the MS70
2022-04-11	22:01	48.438167	-125.444983									extends up to ~ 60 m. disconnected from seabed
2022-04-11	22:13	48.436683	-125.472367	155								End of line 2
2022-04-11	22:44	48.406367	-125.472767									Start of Line 3. Second cross line across previously identified plume sites
2022-04-11	23:07	48.447667	-125.441783									Vertical plume extending ~30 m from seabed. Flat seafloor with low hardness (-29).
2022-04-11	23:17	48.462850	-125.426167	150			20	dense	vertical	flat	soft (-29)	High amplitude vertical feature 50 m above seabed. 20 m in height.
2022-04-11	23:30	48.483100	-125.406483	142			detached (15 m, 30 m above seafloor)	dense	vertical	flat	soft (-29)	EK80, also MS70 numerous detached structures (west of line 3). Good camera location
2022-04-12	00:11	48.545833	-125.339500	110			detached (5 m, 35 m above sea floor)	dense	vertical	incline	mid (-13)	Plume appears on incline and more plumes as seabed flattens, harder edge.
2022-04-12	00:23	48.563500	-125.324217	102			50	dense	vertical, branching	slight incline	mid (-10)	One large, prominent plume surrounded by small vertical plumes to the south and north. Good camera location.
2022-04-12	00:35	48.579233	-125.313717	100								Turning around to cross prominent plumes again to verify
2022-04-12	00:41	48.565700	-125.322050	100			attached (60 m above sea floor)	diffuse	vertical	flat but begins gradual decline after	mid-hard (-8)	Preceded by blob like plume, then long vertical flare connected to bed, 60m long. Surrounded by small blobs.
2022-04-12	00:48	48.558867	-125.323100	110			attached, extends 50 m	dense but diffuses over flare to top	vertical	slight decline	mid (-14)	Lots of activity, concentrated plume at seabed with one long flare, followed by other concentrations on down slope. Good camera location

2022-04-12	00:55	48.560900	-125.324900	115			attached (30 m)	dense then diffuses	vertical	slight incline	mid (-11)	Dense plumes 5 m high before slight incline, then two 30m flares side by side. Large, detached blob follows
2022-04-12	00:59	48.567883	-125.324000	100			detached (75 m above sea floor)	dense	vertical	slight incline	hard (-7)	Two dense plumes side by side.
2022-04-12	01:08	48.583583	-125.314900	100			detached	dense	vertical	edge of sharp decline	hard (-7)	Some pluming at edge of steep ridge.
2022-04-12	01:38	48.638383	-125.272667	100			detached	dense	vertical	flat	soft (-20)	Bubble stretching from 50m to 60m. Potential plumes 10m off the bottom.
2022-04-12	01:41	48.642983	-125.267600	100			detached	dense	vertical	flat	soft (-20)	Flare stretches to seabed, but detached, about 15m long. Followed by other plumes ahead closer to seabed.
2022-04-12	01:45	48.641667	-125.256467	100			detached	dense	vertical	flat	soft (-22)	Continued features.
2022-04-12	02:05	48.615383	-125.193550	99			attached	dense	vertical	flat	mid (-18)	short vertical just before this position
2022-04-12	02:18	48.603500	-125.164667	63.35			detached	dense	vertical	flat	mid (-19)	Depth between 63 and 82
2022-04-12	02:21	48.600000	-125.155000	89.15			detached	dense	vertical	flat	soft (-20)	Depth between 89 and 98
2022-04-12	02:25	48.595167	-125.142500	85.99			detached	dense	vertical	slight incline	soft (-21)	Depth between 85 and 98
2022-04-12	02:25	48.592667	-125.160000	99.31			detached	dense	vertical, several sections	slight incline	hard (-9)	Start of line 4, looks like fish groups
2022-04-12	02:25	48.576167	-125.099833	100.71			detached	diffuse	vertical, wider group	incline	hard (-11)	in a mass, looks like a fish group
2022-04-12	02:42	48.570667	-125.088167	100.71			detached	dense	vertical	incline	mid (-15)	About 92.5 m top and 102 m bottom, a weak reflection can be seen under the seabed.
2022-04-12	02:48	48.563667	-125.073000	86.33			detached	dense	vertical	incline	mid (-12)	top is at 67.72 m, bottom at 92.75 m, branched and curved at both the top and the bottom
2022-04-12	02:51	48.559000	-125.063167	78.88			attached	dense	vertical	slight	mid (-13)	top is at 74.13 m
2022-04-12	03:22	48.518500	-124.981833	62.4	46.69		attached	dense	vertical	incline	mid (-14)	one more less dense after
2022-04-12	03:45	48.491833	-124.923833	79.79	68.29		attached	diffuse	vertical	flat	hard (-9)	Start of the second line, Two more diffuse
2022-04-12	03:56	48.502500	-124.923167	73.14	65.6		detached, but near sea floor	diffuse	vertical	flat	hard (-9)	in a mass, possibly a group of fish
2022-04-12	04:11	48.518000	-124.954833	65.59	60.98		attached, but two sections	dense	vertical	slight incline	mid (-12)	one more attached after
2022-04-12	04:25	48.530500	-124.982333	40.31	37.07	40.05	detached	dense	vertical	incline	hard (-8)	one more small vertical group after
2022-04-12	04:36	48.541500	-125.003500	55.34	35.14		detached	dense	vertical	slight incline	hard (-5)	
2022-04-12	04:41	48.546167	-125.012667	37.57			detached, but near sea floor	dense	vertical	incline	mid (-14)	

2022-04-12	04:50	48.556167	-125.032600	53.98	35.14	37.64	detached	dense	vertical	incline	hard (-7)	
2022-04-12	04:52	48.558333	-125.037333	66.47	37.14		attached	dense	vertical	incline	hard (-11)	
2022-04-12	05:13	48.579833	-125.079667	104	37.71		detached	diffuse	vertical	incline	mid (-15)	a curved one. Break at the middle curve part
2022-04-12	05:16	48.583000	-125.086333	105.4	38.83	60.98	detached	diffuse	more horizontal group	slight incline	mid (-15)	end the line at 519 (1019) in a mass, is more dense upper part with gradually diffusing downward, possibly fish group
2022-04-12	05:24	48.589000	-125.082167	99.49	37.71		attached	diffuse	vertical, wide group	slight incline	mid (-14)	Start line at 5:27 (1027), in a mass, upper part is more dense, with the diffuse lower part attached the sea floor, possibly fish group
2022-04-12	05:54	48.555000	-125.001667	48.64	33.71	40.73	detached	dense	vertical	sharp incline	hard (-7)	bottom is very close to the sea floor
2022-04-12	06:47	48.530333	-124.953833	63.07	52.76	55.74	detached	dense	vertical	sharp incline	hard (-8)	a group of vertical plumes, measured the largest one
2022-04-12	07:06	48.503000	-124.898167	74.59	37.87	44.42	detached	diffuse	more horizontal group	slight incline	mid (-15)	Start a new line at 00:11. a more horizontal group, likely fish
2022-04-12	07:11	48.496667	-124.881167	179.2	43.04	100	detached	diffuse	vertical	sharp incline	mid (-15)	Diffuse above 50.06 m, at the bottom, followed by a diffuse attached inclined flare, and detached curved flare.
2022-04-12	07:31	48.510500	-124.885667	72.13	13.35		detached	diffuse	horizontally curved	flat	hard (-8)	Start a new line at 00:24. a more horizontal group, likely fish
2022-04-12	07:37	48.515667	-124.896833	69.84	29.98	52.63	detached	diffuse	horizontally curved	slight incline	hard (-7)	Fish group?
2022-04-12	07:59	48.537833	-124.939500	64.99	59		attached	dense	vertical	slight incline, rugged	hard (-9)	a diffused group above 20 m
2022-04-12	08:19	48.557500	-124.979167	39.45	16.17	35	detached	diffuse	horizontal	incline	hard (-7)	start to turn to a new line at 1:57
2022-04-12	08:32	48.568833	-125.004000	57.09	42.84	52	detached, near the sea floor	dense	vertical	sharp incline	hard (-6)	vertical flare
2022-04-12	08:40	48.576500	-125.020167	61.36	7.7	17	detached	dense	vertical	incline	hard (-5)	a group of vertical plumes, measured the largest one
2022-04-12	08:58	48.593500	-125.052667	81.46	15	20	detached	diffuse	horizontally curved	slight incline	mid (-15)	fish-whale?
2022-04-12	09:01	48.599167	-125.055000	82.15			detached	diffuse	horizontally curved	slight incline	mid (-14)	fish-whale?
2022-04-12	09:04	48.604500	-125.053333	79.32	9.37	17	detached	dense	vertical	incline	mid (-12)	small plume
2022-04-12	09:05	48.605000	-125.051667	78.4	50	57.25	detached	diffuse	horizontally curved	slight incline	mid (-13)	fish
2022-04-12	09:06	48.605000	-125.048167	74.88	45	60	detached	diffuse	horizontally curved	slight incline	soft (-14)	fish
2022-04-12	09:08	48.602500	-125.042667	71.17	43.65	64	detached	diffuse	horizontally curved	incline	hard (-9)	fish
2022-04-12	09:11	48.598500	-125.035500	67.15	14.51	20	detached	diffuse	horizontal	slight incline	mid (-15)	fish
2022-04-12	09:16	48.591833	-125.023333	64.01	8.34	20	detached	dense	vertical	slight incline	mid (-12)	start a new line at 02:16, horizonal fish go through the vertical dense flare
2022-04-12	09:31	48.575000	-124.988500	51.84	10.01	20	detached	diffuse	horizontal	incline	hard (-4)	fish group-whale?
2022-04-12	09:46	48.561667	-124.959000	49.74	45.73		attached	dense	vertical	slight incline, rugged	mid (-10)	fish group at ~20 m

2022-04-12	10:02	48.553333	-124.941500	61.28	15	40	detached	diffuse	vertical	slight incline	mid (-10)	group of fish
2022-04-12	10:55	48.501447	-124.842500	223	15.53	50	detached	dense	vertical	incline	mid (-17)	plume
2022-04-12	11:52	48.512553	-124.957248	57.8	44.87		attached	dense	vertical	slight incline, rugged	hard (-9)	start to turn to a new line at 3:57
2022-04-12	12:10	48.519000	-125.005833	60	54.2		attached	dense	vertical	slight incline, rugged	hard (-7)	start a new line at 04:10
2022-04-12		48.517150	-124.843650									Abandoned line to transit to sampling stations 0421
2022-04-12	12:20	48.520667	-124.973167	58.29	49.1		attached	dense	vertical	incline	mid (-12)	a group of flares, one after another. Measured the largest one
2022-04-12	12:31	48.519500	-124.944167	66.59	61.23		attached	dense	vertical	slight incline	hard (-9)	two flares
2022-04-12	12:51	48.514333	-124.891000	71.46	51.36		attached	dense	vertical	slight incline	hard (-8)	The flares were continuous and attached, and became detached, then changed to be lower (slightly) detached. The density was lower (slightly) diluted, then, continuously became higher (very) dense.
2022-04-12	12:58	48.512000	-124.872500	136.8	50.77	65.21	detached	dense	vertical	incline	mid (-11)	the following is attached flare
2022-04-12	13:17	48.522500	-124.852500	151.9	66.43		attached	dense	vertical	incline	mid (-17)	return the break in line at 06:13, continuous flare from attached to detached, from lower diluted to higher density, then to lower detached
2022-04-12	13:22	48.528500	-124.863833	129.2	106.26		attached	dense	vertical	incline	mid (-13)	The flares were continuous and attached, and became detached, then changed to be lower (slightly) detached. The density was lower (slightly) diluted, then, continuously became higher (very) dense.
2022-04-12	13:28	48.533833	-124.881500	88.61	70.6		attached	dense	vertical	incline	mid (-10)	The flares were continuous and attached, and became detached, then changed to be lower (slightly) detached. The density was lower (slightly) diluted, then, continuously became higher (very) dense.
2022-04-12	13:31	48.539500	-124.884833	82.43	68.16		attached	dense	vertical	incline	hard (-8)	The flares were continuous and attached, and became detached, then changed to be lower (slightly) detached. The density was lower (slightly) diluted, then, continuously became higher (very) dense.
2022-04-12	14:20	48.597067	-125.003000									end of line
2022-04-12	14:22	48.600567	-125.000033	45	50	45	attached	diffuse	vertical	incline	hard (-6)	Potential small plumes at top of small hill. Possibly some diffuse higher in water column
2022-04-12	14:34	48.593150	-124.007333	52						slight incline	hard (-7)	SOL
2022-04-12	14:36	48.591917	-124.965328	53	51.12	52.66	attached	dense	vertical	slight depression	hard (-7)	
2022-04-12	14:37	48.590032	-124.961320	53	48.04	52.66	attached	dense	vertical	slight depression	hard (-9)	another few small ones just after for next 4 minutes
2022-04-12	14:49	48.577057	-124.932050	55			detached	diffuse	horizontal	slight decline	mid (-15)	possible interference or fish
2022-04-12	15:05	48.559940	-124.898838	65			attached	diffuse	vertical	slight incline	hard (-10)	Several small plumes at seabed, one larger flare extending 10 m
2022-04-12	15:09	48.554400	-124.887342	70	60	70	attached (10 m)	dense	vertical	incline	hard (-9)	Many large plumes stretching from seabed. Good camera site.
2022-04-12	15:15	48.548550	-124.876467	80	30	80	attached	dense, diffuses as it rises	vertical	incline	hard (-8)	Continued features. Very large plume, dense at sea floor, extends to 15m. Good camera site.

2022-04-12	15:20	48.543775	-124.862833	100				dense	horizontal, following slope profile	incline	hard (-11)	Concentration thinning, continued decline. End of gas feature
2022-04-12	15:32	48.536000	-124.848900	150	150	125	detached	dense	horizontal	incline		likely fish
2022-04-12	16:05	48.533850	-124.818133	156								Start of new line. 7
2022-04-12	16:19	48.548343	-124.850930	100	85	100	attached	dense	vertical	incline	hard (-8)	Very dense plume surrounded by smaller features. Larger plumes where it flattens.
2022-04-12	16:22	48.555097	-124.855980	100	15	80	detached	dense	vertical	incline	hard (-7)	Large flare extending through water column, smaller near seabed around it. Good camera site.
2022-04-12	16:25	48.554733	-124.864350	80	50	80	attached	dense at seabed, diffuses through column	horizontal	incline	hard (-7)	higher spread of plumes along slope, some flares extending 30m
2022-04-12	16:27	48.557227	-124.869508	80								End of features
2022-04-12	16:32	48.564087	-124.883615	65	58	65	attached	diffuse	vertical	flat	hard (-9)	Small plumes where seabed flattens